

SKOLKOVO INSTITUTE OF SCIENCE AND TECHNOLOGY

draft version

Jacob Daniel Biamonte, BS, DPhil (Oxon)

**ON THE THEORY OF MODERN QUANTUM
ALGORITHMS**

Specialization 01.01.03 Mathematical Physics

Dissertation submitted for the degree of
Doctor of Physical and Mathematical Sciences

arXiv:2009.10088v1 [quant-ph] 21 Sep 2020

Moscow — 2020

Contents

	Page
Chapter 1. Introduction: Programming Ground States	5
1.1 Computation and the Ising model	9
1.2 Low-energy subspace embedding	15
1.3 Two-body reductions	19
1.4 P- vs. NP problems and physics	23
1.5 Computational phase transitions	24
1.5.1 Thermal states at the SAT phase transition	29
 Chapter 2. Quantum vs Probabilistic Computation	 32
2.1 Defining Mechanics	32
2.1.1 Stochastic time evolution	33
2.1.2 Quantum time evolution	33
2.1.3 Properties in stochastic mechanics	34
2.1.4 Hamiltonian properties in quantum mechanics	35
2.1.5 Observables	36
2.2 Walks on Graphs: quantum vs stochastic	44
2.2.1 Normalized Laplacians	47
2.2.2 Stochastic walk	50
2.2.3 Quantum walk	51
2.2.4 Perron’s theorem	54
2.3 Google page rank—a ground eigenvector problem	59
2.4 Kitaev’s quantum phase estimation algorithm	61
2.5 Finding the ground state	66
 Chapter 3. Tensor Networks and Quantum Circuits	 69
3.1 Clifford gates	69
3.2 Tensor network building blocks	72
3.2.1 Reversible logic	75
3.2.2 Heisenberg picture	77
3.2.3 Stabilizer tensor theory	79

Chapter 4. Variational Search and Optimization	85
4.1 Random vs quantum complexity	86
4.2 Variational quantum computation framework	89
4.3 Variational quantum search	94
4.4 Extending Kitaev's k-controlled U factorization	98
4.5 QAOA vs optimization by adiabatic and quantum annealing	105
4.5.1 Approximating adiabatic evolution	106
4.6 Low-depth quantum circuits	108
4.6.1 A combinatorial quantum circuit area law	108
4.7 Reachability deficits	112
Chapter 5. Variational Quantum Computation	119
5.1 Notions of quantum computational universality	119
5.2 Maximizing projection onto a circuit	121
5.3 Maximizing projection onto the history state	124
5.4 Discussion	128
Chapter 6. Gadget Hamiltonians	130
6.1 Hamiltonian complexity	131
6.2 LOCAL HAMILTONIAN is QMA-complete	132
6.2.1 REAL HAMILTONIAN is QMA-complete	134
6.3 Exact ZZZ-gadget from Z, ZZ	140
6.4 Perturbation theory	142
6.5 Subdivision gadget	146
6.6 YY-gadget	152
Chapter 7. Conclusion and Open Problems	157
List of symbols	160
List of abbreviations	162
Glossary of terms	169
Bibliography	187
List of Figures	190

List of Tables	191
Alphabetical Index	192

Chapter 1. Introduction: Programming Ground States

Early ideas in quantum computation [1–5] lead to the so called, gate model of quantum computation (see the book [6]). We will cover the gate model in detail, starting in § 2. However, our starting point will be in understanding how to embed computational problem instances into the ground state of the Ising model.

To understand contemporary quantum computing applications, we will adopt the view of computation in terms of ground states of physical systems [7; 8]. This will later be used as a foundation to understand the modern class of variational quantum algorithms [9] defined as a model of computation in [10]. The approach taken provides an elegant and practical connection between computer science and physics. On one hand, computational complexity can classify ground state problems. On the other hand, physical systems can be constructed and their ground states can be accessed and used as a computational resource.

The computational properties of ground states are the unifying theme of this monograph and indeed, offer a golden thread connecting the contemporary fundamental underpinnings behind advanced techniques to program quantum enhanced processors, of all types. We want to begin by explaining the core ideas as simply and as plainly as possible. We will then develop these ideas piece-wise as our journey together through these pages commences.

We are concerned with instances of two general problems, where a problem is defined as a *class* in complexity theory. The first is a decision problem, which serves essentially as a theoretical tool to study the limits of computation.

Remark 1. We assume that $\mathbb{N} \stackrel{\text{def}}{=} \mathbb{N} \cup \{0\}$. This sometimes appears in the literature as \mathbb{N}_0 .

Consider then a pseudo Boolean function f . Then f is a map from n -tuples of 0 and 1 to the integers between 0 and some natural number (possibly defined to be $\mathcal{O}(\text{poly } n)$), that is for f pseudo Boolean we have type

$$f: \{0, 1\}^n \rightarrow \mathbb{N}. \tag{1.1}$$

If we consider the class of all such functions, under the strict condition that f can be evaluated for all $y \in \{0, 1\}^n$ in some time not exceeding $\mathcal{O}(\text{poly } n)$, then we arrive at the following decision problem.

Definition 1. (INTEGER DECISION SAT) Consider

$$f: \{0, 1\}^n \rightarrow \mathbb{N}, \quad (1.2)$$

such that $f(y)$ can be evaluated in $\mathcal{O}(\text{poly } n)$ time for all $y \in \{0, 1\}^n$. We want to decide the following:

- (1) if there exists a z such that $f(z) = 0$, or
- (2) if the function $f(z) \geq 1$ for all $z \in \{0, 1\}^n$

where f is promised to be either (1) a YES instance or otherwise (2) a NO instance.

This problem is a standard *decision problem*, the optimization variant is given as

Definition 2. (MIN INTEGER SAT) Given

$$f: \{0, 1\}^n \rightarrow \mathbb{N}, \quad (1.3)$$

such that $f(y)$ can be evaluated in $\mathcal{O}(\text{poly } n)$ time for all $y \in \{0, 1\}^n$. Find

$$\arg \min_{z \in \{0, 1\}^n} f(z) = z', \quad (1.4)$$

where $\min_{z \in \{0, 1\}^n} f(z) = f(z')$.

We will see that INTEGER DECISION SAT relates to physics of actual systems and provides a bridge between the theory of computation and that of physics. In terms of practice, physical systems exist which embed and evolve to approximately solve MIN INTEGER SAT. Function minimization is conceptually easy to understand. It would seem that quantum mechanics provides a richer class of minimization problems, wherein the target function is typically replaced with a Hermitian operator where one is subsequently tasked with determining the ground eigenvalue.

Let us start with an explanatory version of a “quantum” problem, inspired fully by Kitaev’s LOCAL HAMILTONIAN which we will develop and apply to ques-

tions of modern relevance much later in § 5. For now consider the following variant simplified for illustrative purposes.

Definition 3. (DECISION HAMILTONIAN—ignores locality) Let

$$\mathcal{H} = \sum_{l=1}^{\text{poly}(n)} A_l \in \mathcal{L}(\mathbb{C}_2^{\otimes n}) \quad (1.5)$$

be a non-negative Hamiltonian on n qubits. Decide

- (1) if \mathcal{H} has a zero eigenvalue, or
- (2) if all eigenvalues of \mathcal{H} are greater than or equal to some $f(n) > 0$.

$f(n)$ will be determined later.

Accept(ing)ance, or YES instances of DECISION HAMILTONIAN are shown given access to a quantum computer that simulates (1.5) and prepares a quantum state $|\psi\rangle$ (a witness) such that we can calculate the expected value $\langle\psi|\mathcal{H}|\psi\rangle = 0$. While appearing from the outset as artificial, we will develop DECISION HAMILTONIAN in a sequence of steps as a conceptual building block behind powerful tool(s) to probe the power and limitations of quantum enhanced information processing. DECISION HAMILTONIAN is closely related to the more practically encountered variant, which we will study in tandem as follows.

Definition 4. (MIN HAMILTONIAN—ignores locality) Let

$$\mathcal{H} = \sum_{l=1}^{\text{poly}(n)} B_l \in \mathcal{L}(\mathbb{C}_2^{\otimes n}) \quad (1.6)$$

be a non-negative Hamiltonian on n qubits. Determine

$$\min_{\psi \in \mathcal{A}} \langle\psi|\mathcal{H}|\psi\rangle = E^* \quad (1.7)$$

where the domain $\mathcal{A} \subseteq \mathcal{L}(\mathbb{C}_2^{\otimes n})$ is given as a possibly restricted subdomain of $\mathcal{L}(\mathbb{C}_2^{\otimes n})$ and so $E^* \geq E_*$.

We readily establish that

$$0 \leq E_* = \min_{\psi \in \mathcal{L}(\mathbb{C}_2^{\otimes n})} \langle\psi|\mathcal{H}|\psi\rangle \leq E^* = \min_{\psi \in \mathcal{A}} \langle\psi|\mathcal{H}|\psi\rangle. \quad (1.8)$$

Hence, knowledge of E_* provided $\mathcal{A} = \mathcal{L}(\mathbb{C}_2^{\otimes n})$ readily lifts MIN HAMILTONIAN to partition {YES, NO} instances of DECISION HAMILTONIAN. Furthermore, MIN HAMILTONIAN has practical applications as an eigenvalue problem, where similar and restricted forms arise in many areas of engineering and applied science, including determining the ground state energy of electronic structure Hamiltonians [11]. We then consider the following variant of MIN HAMILTONIAN.

Definition 5. (ARGMIN HAMILTONIAN—ignores locality) Let

$$\mathcal{H} = \sum_{l=1}^{\text{poly}(n)} B_l \in \mathcal{L}(\mathbb{C}_2^{\otimes n}) \quad (1.9)$$

be a non-negative Hamiltonian on n qubits. Determine

$$\arg \min_{\psi \subseteq \mathcal{A}} \langle \psi | \mathcal{H} | \psi \rangle = |\psi'\rangle \quad (1.10)$$

where $\mathcal{A} \subseteq \mathcal{L}(\mathbb{C}_2^{\otimes n})$ is given.

Provided the domain \mathcal{A} is appropriately restricted, we will be able to store $|\psi'\rangle$ on a classical computer. In fact, this is often the case. For example, provided that (1.9) represents a binary constrained optimization problem (which we will consider later), then \mathcal{A} can safely be restricted to the domain $\{0, 1\}^n$ so that $|\psi'\rangle$ is readily stored as a bit string. The lack of a tangible description of $|\psi'\rangle$ using a classical computer is one of the foreseen advantages of quantum processors, and a key element of quantum supremacy demonstrations.

While we have presented three rather generic problems, these three problems will be further refined to form the theoretical backbone of Hamiltonian complexity and due in part to their close connection to actual physical processes, we will see that such problems underpin the vast majority of modern quantum programming techniques.

Going forward we will make these problems increasingly more physical in that we will tailor them to apply specifically to restricted settings that are closer to what is available on today's quantum processors. We will also push the limitations of what can be said about the computational complexity of various Hamiltonian energy problems.

The starting place for all of this is to develop a language and the intuition to program ground states. Subsequent chapters will take these ideas in a variety of directions but the starting place begins with one of the most basic, yet most applicable models of statistical mechanics. We will develop techniques to fully control the ground states of Ising Hamiltonians.

1.1 Computation and the Ising model

We will begin with the methodology to program the ground state of a physical system to embed logic functions. This leads directly to the fundamental result establishing that the ground state of the general (tunable or adjustable) Ising model represents a computationally meaningful system: specifically that finding the ground state can be shown to be **NP**-hard in the language of computational complexity. We will build on these results.

Readers should come away with the basic tools needed to embed and sequence logic gates in the ground states of Hamiltonians. They should also be familiar with the idea of a penalty function and the problem of reducing such functions to quadratic form for physical implementation(s). Readers should further become familiar with the problem of three satisfiability (**3-SAT**), its embedding into physical spin systems of spin and its corresponding computational phase transition signature.

This chapter utilizes results from my past work in (2008) and my work with Whitfield, Faccin in (2012), namely [12; 13]. We will consider interacting binary units called *classical spins* and adopt the matrix presentation of Boolean bits in which

$$\text{Logical 0} \mapsto |0\rangle, \quad \text{Logical 1} \mapsto |1\rangle.$$

The concatenation of bits is defined pairwise using Kronecker's tensor (\otimes) where the symbol (\otimes) is often omitted (e.g. $|q\rangle \otimes |r\rangle$ is written equivalently as $|q\rangle |r\rangle$ or $|q,r\rangle$).

Example 1. We can define the vector corresponding to a Boolean switching function f as

$$|f\rangle \stackrel{\text{def}}{=} \sum_{x \in \{0,1\}^n} f(x) |x\rangle. \quad (1.11)$$

For instance, the following is proportional to the Bell state

$$\sqrt{2} |\Phi^+\rangle = \sum_{x_1, x_2} [1 - (x_1 - x_2)^2] |x_1, x_2\rangle = |00\rangle + |11\rangle, \quad (1.12)$$

with $x_1, x_2 \in \{0,1\}$. The Bell state is used in a range of quantum protocols and takes its name after pioneering quantum physicist, John Bell.

There exists a useful method to embed Boolean equations (as well as their pseudo Boolean generalization discussed later) into the low energy configuration of a physical system. To develop these methods, we introduce some machinery.

In this thesis, each spin is considered to be acted on by a matrix in $\text{span}\{\mathbf{1}, Z\}$ over the reals, in other words by a matrix

$$\text{span}\{\mathbf{1}, Z\} = \alpha\mathbf{1} + \beta Z \quad \forall \alpha, \beta \in \mathbb{R}, \quad (1.13)$$

with

$$\mathbf{1} \stackrel{\text{def}}{=} |0\rangle\langle 0| + |1\rangle\langle 1|, \quad Z \stackrel{\text{def}}{=} |0\rangle\langle 0| - |1\rangle\langle 1|. \quad (1.14)$$

We typically assign $\beta = \pm 1/2$, $\alpha = 1/2$ and define orthogonal projectors (1.15) and (1.16).

$$P_1 \stackrel{\text{def}}{=} |1\rangle\langle 1| = \frac{1}{2}(\mathbf{1} - Z) \quad (1.15)$$

$$P_0 \stackrel{\text{def}}{=} |0\rangle\langle 0| = \frac{1}{2}(\mathbf{1} + Z) \quad (1.16)$$

Where equations (1.15) and (1.16) are defined by the relations (1.17) and (1.18).

$$P_0|0\rangle = |0\rangle \quad P_0|1\rangle = 0 \quad (1.17)$$

$$P_1|1\rangle = |1\rangle \quad P_1|0\rangle = 0 \quad (1.18)$$

These equations (1.15), (1.16), (1.17) and (1.18) can be succinctly summarized respectively as (1.19) and (1.20).

$$P_a = \frac{1}{2}(\mathbb{1} + (-1)^a Z) \quad (1.19)$$

$$P_a |b\rangle = \delta_{ab} |b\rangle \quad (1.20)$$

We will emulate logic operations using the lowest eigenstates of operators formed from the real-linear extension taken over

$$\Omega_n \stackrel{\text{def}}{=} \{P_1, P_0\}^{\otimes n} \quad (1.21)$$

for fixed finite n —see Remark 2—in other words we will devise operators in

$$\text{span}\{\Omega_n\}. \quad (1.22)$$

Remark 2 (Notation—span of linear extension). The notation $\{A, B, \dots\}^{\otimes n}$ corresponds to the set of all n -word products of A, B, \dots with tensor (\otimes) as concatenation. The real-linear extension of (1.22) means that we can consider the span of operators P_1, P_0 as well as the span of their composition using the tensor product such as e.g. $\alpha \cdot P_1 \otimes P_0$ acting on two systems with $\alpha \in \mathbb{R}$.

Example 2. We will now establish the following elementary properties.

- (a) For $Z^2 = \mathbb{1}$, Z has eigenvalues ± 1 .
- (b) For $P_a^2 = P_a$, P_a has eigenvalues $0, 1$.
- (c) Consider $\det(Z - \lambda \mathbb{1}) = \lambda^2 - 1 = 0$ and $\det(P - \lambda \mathbb{1}) = \lambda(\lambda - 1) = 0$. By substituting $\lambda \mapsto P_a$ (or Z) and sending scalars c to $c\mathbb{1}$, it follows that P_a and Z satisfy their own characteristic equation.

Consider $(Z - \mathbb{1})Z |j\rangle = 0$ and if $|j\rangle$ is an eigenstate with eigenvalue λ then $\lambda^2 = 1$ and hence $\lambda = \pm 1$, which establishes (a). For the operators from (a) and (b), their eigenvalues and eigenvectors are expressed as $Z |j\rangle = (-1)^j |j\rangle$ and $P_a |j\rangle = j |j\rangle$ for $j = 0, 1$. Similar arguments hold for P_a . Point (c) follows by direct calculation.

The method to program and engineer the ground states of physical systems functions by adding a so called penalty (a.k.a. energy penalty $\geq \Delta$) to undesirable spin configurations. For example, to set a bit to logical zero, we can add a penalty

P_1 . To set a pair of bits to logical 11 ($|11\rangle$), we will add the penalty $P_0 \otimes \mathbb{1} + \mathbb{1} \otimes P_0$ (see Remark 3).

Definition 6. It is common to sometimes adopt the notation as in (1.23).

$$P_a \otimes P_b \otimes \cdots \otimes P_c \stackrel{\text{def}}{=} P_{ab\dots c} \quad (1.23)$$

Remark 3. (Assigning spins to represent specific bit strings). The following operators \mathcal{Q} and \mathcal{Q}' in equations (1.24) and (1.25) will minimize to set k spins to represent the k -long bit string $\omega_1\omega_2\cdots\omega_k$. Note that the over bar is the logical complement (negation), sending Boolean variable x to $\bar{x} = 1 - x$.

$$\mathcal{Q} = \sum_{j=1}^k P_{\bar{\omega}_j} = \sum_{j=1}^k (\mathbb{1} - P_{\omega_j}) \quad (1.24)$$

$$\mathcal{Q}' = \Delta \left(\mathbb{1} - \bigotimes_{j=1}^k P_{\omega_j} \right) \quad (1.25)$$

Table 1 — Contrasting binary, polarity and matrix embeddings of Boolean bits.

Variables	Matrix Embedding
Boolean bit $x_i \in \{0, 1\}$	projector $P_{\bar{x}_i} \stackrel{\text{def}}{=} \bar{x}_i\rangle\langle\bar{x}_i $ with spectrum $\in \{0, 1\}$
Spin variable $s_i \in \{\pm 1\}$	Z matrix $ 0\rangle\langle 0 - 1\rangle\langle 1 $ with spectrum $\in \{\pm 1\}$
Affine transformation relating x_i, s_i $s_i = 1 - 2x_i$	Matrix relation between P_a and Z $P_a = \frac{1}{2}(1 + (-1)^a Z)$

Remark 4. (Locality of an operator). The locality of an operator is the highest number of non-trivial terms in a tensor product describing that operator. For example, the locality of the operator (1.24) is called 1-local, or local or one-body whereas the locality of the operator in (1.25) is k -local.

In (1.24) we project onto the complement of the bits and form a sum over the projectors. Equation (1.25) is given by a tensor product of projectors. Both

of these operators share the same low-energy space. Physical systems implement two-body interactions and so k -body interactions must be emulated. This translates into computational resources.

We will continue explaining penalty functions by developing several examples.

Example 3. (Equality and Inequality Penalties). Two binary variables are equal when they both evaluate to logical 0 (logical 1). Logical equivalence is defined in this way. And similarly for inequivalence.

We wish to construct a non-negative operator $h_{=}$ with the property that

$$\ker\{h_{=}\} = \text{span}\{|x, y\rangle \mid x = y\}$$

is the zero eigenspace and where all other eigenvectors are in an eigenspace $\geq \Delta$. Such an operator is constructed directly from considering a modified truth table for the logical operation. For equality and inequality (right most), the corresponding (energy) truth table is given as follows.

x	y	$x \stackrel{?}{=} y$	$x \stackrel{?}{\neq} y$
$ 0\rangle$	$ 0\rangle$	0	$\geq \Delta$
$ 0\rangle$	$ 1\rangle$	$\geq \Delta$	0
$ 1\rangle$	$ 0\rangle$	$\geq \Delta$	0
$ 1\rangle$	$ 1\rangle$	0	$\geq \Delta$

The penalty functions have an evident expression in terms of the projectors (1.15) and (1.16) as follows:

$$h_{=} \stackrel{\text{def}}{=} \Delta(P_0 \otimes P_1 + P_1 \otimes P_0),$$

$$h_{\neq} \stackrel{\text{def}}{=} \Delta(P_0 \otimes P_0 + P_1 \otimes P_1).$$

Here the defining relation is $h_{=} \stackrel{\text{def}}{=} \Delta - h_{\neq}$. We can check these formula by noting that the tensor product of scalars reduces to the usual product viz.,

$$(P_a \otimes P_b) |q, r\rangle = (P_a |q\rangle) \otimes (P_b |r\rangle) = \delta_{aq} \cdot \delta_{br} |q, r\rangle.$$

Remark 5 (Using \cdot for multiplication by a scalar). Though typically omitted, based on aesthetics we sometimes use \cdot to denote multiplication by a scalar.

The objective is to embed logical operations into the ground states of tunable Ising Hamiltonians. To that end, we must define a family of logical operations that form a universal generating basis from which we can express any logical operation. So far we have only defined penalties that act on two spins. Going further we will develop a penalty to embed the **AND** gate. It is well known that **AND**, **COPY** and **NOT** form a universal basis for Boolean logic. Logic gates and Boolean algebra will be further discussed in Section 1.2.

Example 4. The Logical **AND** operation [12; 13] is constructed similarly to the procedure in Example 3. We want to develop a penalty function such that the zero eigenspace is in

$$\text{span}\{|x, y, z\rangle | z = x \cdot y\}$$

and the orthogonal space

$$\text{span}\{|x, y, z\rangle | z = 1 - x \cdot y\}$$

corresponds to eigenvalues of at least Δ .

From the energy-truth table

x	y	z	$z \stackrel{?}{=} x \cdot y$
0	0	0	0
0	0	1	$\geq \Delta$
0	1	0	0
0	1	1	$\geq \Delta$
1	0	0	0
1	0	1	$\geq \Delta$
1	1	0	$\geq \Delta$
1	1	1	0

we arrive at single penalty for each term $\geq \Delta$ as

$$h_{\wedge} \stackrel{\text{def}}{=} \Delta(P_{001} + P_{011} + P_{101} + P_{110}). \quad (1.26)$$

Expanding and simplifying (1.26) yields

$$h_{\wedge} = \Delta(\mathbb{1} \otimes \mathbb{1} \otimes P_1 + P_1 \otimes P_1 \otimes \mathbb{1} - 2P_1 \otimes P_1 \otimes P_1).$$

To use the AND gate penalty function (1.26) in practice, one can set the input bits using the projectors P_0, P_1 . Alternatively, one could force the output bit to be logical 1 by projecting onto $|0\rangle$

$$\Delta(P_{001} + P_{011} + P_{101} + P_{110}) + \varepsilon \mathbb{1} \otimes \mathbb{1} \otimes P_0 \quad (1.27)$$

where $0 < \varepsilon$.

Now minimization of the penalty function (1.27) would provide input conditions to satisfy the AND function. This approach becomes more interesting when considering a sequence of gates. Hence, penalty functions for a universal set of classical logic gates should be developed. The AND gate by itself is not universal for classical logic: yet AND, together with OR and COPY is. However, the NAND gate is universal provided one can also copy bits.

1.2 Low-energy subspace embedding

Here we will consider embedding switching functions into low-energy subspaces. We will proceed by recalling some basic properties of Boolean algebra.

Definition 7. (A note for mathematicians and computer scientists). We consider the diagonal matrix \mathcal{H} acting on states $|\psi\rangle \in |\{0,1\}^n\rangle$ such that $\mathcal{H}|\psi\rangle = k|\psi\rangle$ where k is a real number. For each such $|\psi\rangle$, the quantity $\langle\psi|\mathcal{H}|\psi\rangle = k$ is called the energy of $|\psi\rangle$ relative to \mathcal{H} . Operators such as \mathcal{H} are called Hamiltonians, or energy functions. We will extend and refine this definition.

Remark 6. The ground state or low-energy subspace of \mathcal{H} from Definition 7 is given by the span of the vectors with minimal k . We have been engineering non-negative Hamiltonians such that their low-energy (zero) eigenspace embeds logical functions.

Definition 8. A Boolean (or switching) function is an n -ary map

$$f: \mathbb{B}^n \rightarrow \mathbb{B} \quad (1.28)$$

where $\mathbb{B} = \{0,1\}$ is the Boolean field and non-negative n is called the **arity** of f . The case $n = 0$ formally defines the constant elements of \mathbb{B} , 0 and 1 (false and true respectively).

Remark 7. The total number of Boolean functions $f: \mathbb{B}^n \rightarrow \mathbb{B}$ for each n is 2^{2^n} .

Example 5. (Majority function). The **majority function** is false when $n/2$ or more input arguments are false and true otherwise. It can be written as

$$M(x_1, \dots, x_n) = \left\lfloor \frac{1}{2} + \frac{1}{n} \left(\sum_{i=1}^n x_i - \frac{1}{2} \right) \right\rfloor, \quad (1.29)$$

where $\lfloor f \rfloor$ is a floor function of f .

Example 6. For $n = 2$ the majority function becomes equivalent to the AND function, which takes bit pairs $x, y \in \mathbb{B}$ to their logical product. The AND of two bits x, y is denoted equivalently as $x \wedge y$, $x \cdot y$, $x \cdot y$, xy and is 1 iff $x = y = 1$ and else 0.

The logical OR function of Boolean variables x, y is written

$$x \vee y = x + y - xy \quad (1.30)$$

The AND, OR, NOT gates have the following respective graphical representations

$$\begin{array}{c} x \\ y \end{array} \left[\text{AND} \right] x \wedge y \quad \begin{array}{c} x \\ y \end{array} \left[\text{OR} \right] x \vee y \quad x \text{---} \oplus \text{---} \neg x$$

where the rightmost gate negates its input bit x , sending it to $1 - x$. Logical negation is written equivalently as $\neg x$, \bar{x} and sometimes x' .

Theorem 1 (see [12]). Any Boolean switching function $f(x_1, x_2, \dots, x_n)$ expressed over the basis $\{\vee, \wedge, \neg\}$ embeds into the low-energy spectrum of a Hermitian operator formed by the linear extension of $\{P_0, P_1, \mathbf{1}\}$ by means of the following maps (1.31) and (1.32).

$$\wedge \longrightarrow + \quad (1.31)$$

$$\vee \longrightarrow \otimes \quad (1.32)$$

For every (positive polarity, a.k.a. non-negated) Boolean variable x_j we apply

$$x_j \longrightarrow P_0^j. \quad (1.33)$$

For negated variable $\neg x_j$ we apply

$$\neg x_j \longrightarrow P_1^j. \quad (1.34)$$

In both cases (1.33) and (1.34), $1 \leq j \leq n$ becomes a spin label index which P^j acts on. In particular, for

$$\mathbf{x} \stackrel{\text{def}}{=} x_1, x_2, \dots, x_n$$

the above mapping induces an operator \mathcal{H} with a zero eigenspace given as (1.35).

$$\text{span}\{|\mathbf{x}\rangle \mid f(\mathbf{x}) = 1, \mathcal{H}|\mathbf{x}\rangle = 0\} \quad (1.35)$$

The only other eigenspace is spanned by eigenvalues at unity (1.36).

$$\text{span}\{|\mathbf{x}\rangle \mid f(\mathbf{x}) = 0, \mathcal{H}|\mathbf{x}\rangle = |\mathbf{x}\rangle\} \quad (1.36)$$

We have been embedding the entire truth table of a function. For which we can always consider a function $y(f(x), x) = 1$ and apply this theorem.

Example 7. Recall the Boolean function from Example 1:

$$1 - (x_1 - x_2)^2. \quad (1.37)$$

We will first express (1.37) over the basis $\{\vee, \wedge, \neg\}$ as $\bar{x}_1\bar{x}_2 \vee x_1x_2$. Under the mapping 1, we arrive at

$$1 - (x_1 - x_2)^2 = \bar{x}_1\bar{x}_2 \vee x_1x_2 \longrightarrow P_0 \otimes P_0 + P_1 \otimes P_1, \quad (1.38)$$

which is identical to the penalty function for equality as given in Example 3.

Definition 9. As is typical in quantum physics, we will often omit identity operators by writing Z_a to mean

$$Z_a \stackrel{\text{def}}{=} \mathbf{1}_1 \otimes \dots \otimes \mathbf{1}_{a-1} \otimes Z_a \otimes \mathbf{1}_{a+1} \otimes \dots \quad (1.39)$$

where the operator Z_a acts on the a^{th} spin. Likewise for pairs of operators with $a \neq b$, $Z_a \otimes Z_b = Z_a Z_b$ and again the identity is omitted.

Here we have developed a method to simulate (in principle) any pseudo Boolean penalty function using Ising Hamiltonians. Physical realizations of classical or quantum annealers and of quantum Ising machines [14–21] are however limited to two-body interactions. Three-body terms (and higher) will be emulated using two-body terms through a construction involving the introduction of slack qubits.

Before considering a method to reduce (or quadratrize) penalty Hamiltonians, let us state the following complexity result.

Theorem 2. (DECISION THREE-BODY PROJECTOR ISING HAMILTONIAN)

Given non-negative

$$\mathcal{H} = \sum_{l=1}^{\text{poly}(n)} P_{abc}^{\alpha\beta\gamma} \quad (1.40)$$

where

$$P_{abc}^{\alpha\beta\gamma} = P_a^\alpha \otimes P_b^\beta \otimes P_c^\gamma \quad (1.41)$$

with $P_x^\kappa = \frac{1}{2}(\mathbf{1} + (-1)^x Z_{(\kappa)})$ acts non-trivially on the bit labeled κ by projecting onto $|x\rangle$. Then the decision problem THREE-BODY PROJECTOR ISING HAMILTONIAN determines if:

- (1) \mathcal{H} has at least one zero eigenvalue or otherwise if
- (2) all eigenvalues of \mathcal{H} are at least unity.

Theorem 2 is the first strong connection between complexity science and physics we will begin to make. The problem is closely related to decision 3-SAT—in fact, there is a bijection between these problems.¹ We will leave the proof of NP-completeness in Theorem 2 to § 1.5.

Theorem 3. (MIN THREE-BODY PROJECTOR ISING HAMILTONIAN is NP-hard)

The minimization of non-negative

$$\min_{x \in \{0,1\}} \langle x | \mathcal{H} | x \rangle = \min_{x \in \{0,1\}} \sum_{l=1}^{\text{poly}(n)} \langle x | P_{abc}^{\alpha\beta\gamma} | x \rangle \quad (1.42)$$

¹Decision 3-SAT canonical and first NP-problem from Cook [22]—Sometimes called the Cook–Levin Theorem as similar results were independently published by Leonid Levin as [Universal search problems]. Problems of Information Transmission (in Russian) **9**(3): 115–116 (1973). Translated into English by Trakhtenbrot [23].

as defined in 2 is NP-hard.

The problem, MIN THREE-BODY PROJECTOR ISING HAMILTONIAN from Theorem 3 is readily reduced to MAX 3-SAT—through a bijection—in which the objective is to violate the fewest clauses.

The proofs of Theorems 2 and 3 will wait until § 1.5. We will first focus on the calculus of reduction of three-body terms to two-body terms. Such techniques are often called, classical gadgets, in relation to the non-perturbative case using gadget Hamiltonians [12; 13; 24]—see § 6.

1.3 Two-body reductions

We study penalty functions as they describe the energy levels of a physical spin system. Spins as stated, are binary units and each physical configuration of spins is assigned a real number representing the energy of the spin configuration. Later on we will study natural physical processes that cause a system to evolve towards the lowest energy configuration. As a first step towards a physical realization, we will consider here the process of embedding higher order ($ZZ \cdots Z$) interactions into two-body interactions by a process that adds ancillary spins [12; 13].

Physical systems with rare exception implement local (one body) and two-body interactions. Two body interactions are terms of the form $J_{ij}Z_iZ_j$. We have so far implemented penalty functions using operators P_0, P_1 . To translate these directly into physical interactions, we have to return to their defining relations and express them in terms of Z operators. In doing such, the following problem illustrates that our penalty function (1.26) requires three-body terms to implement. The penalty function (1.26) must be brought into two-body form [12; 13] by the addition of slack or ancillary spins.

Example 8. Let us express h_\wedge from (1.26) over the basis $\{\mathbf{1}, Z, \otimes\}$. First we remark that transitioning between these two basis will not increase locality. We consider the penalty function over Boolean variables x_1, x_2, x_3 and arrive at a

Pseudo Boolean form truncated past quadratic order	$f = a_0 + a_1x_1 + a_2x_2 + \dots$ $+ a_{12}x_1x_2 + a_{13}x_1x_3 + \dots$ $= a_0 + \sum_i a_ix_i + \sum_{i<j} a_{ij}x_ix_j$
Polarity transform of f	$\tilde{f} = \omega_0 + \omega_1s_1 + \omega_2s_2 + \dots$ $+ \omega_{12}s_1s_2 + \omega_{13}s_1s_3 + \dots$ $= \omega_0 + \sum_i \omega_is_i + \sum_{i<j} \omega_{ij}s_is_j$
Matrix presentation mapping the values of f to the spectrum of a diagonal matrix	$\mathcal{H}_f = a_0\mathbb{1} + a_1P_{\bar{x}_1} + a_2P_{\bar{x}_2} + \dots$ $+ a_{12}P_{\bar{x}_1} \otimes P_{\bar{x}_2} + a_{13}P_{\bar{x}_1} \otimes P_{\bar{x}_3} + \dots$ $= a_0\mathbb{1} + \sum_i a_iP_{\bar{x}_i} + \sum_{i<j} a_{ij}P_{\bar{x}_i} \otimes P_{\bar{x}_j}$
Direct Ising realization of \tilde{f}	$\mathcal{H}_{\tilde{f}} = \omega_0\mathbb{1} + \omega_1Z_1 + \omega_2Z_2 + \dots$ $+ \omega_{12}Z_1Z_2 + \omega_{13}Z_1Z_3 + \dots$ $= \omega_0\mathbb{1} + \sum_i \omega_iZ_i + \sum_{i<j} \omega_{ij}Z_iZ_j$
<p>f and \tilde{f} are related by an affine change of variables $s_i = 1 - 2x_i$ and \mathcal{H}_f and $\mathcal{H}_{\tilde{f}}$ are related as $P_x = \frac{1}{2}(1 + (-1)^x Z)$</p>	

Table 2 — Constructing penalty Hamiltonians from Boolean (or pseudo-Boolean) functions.

penalty function for AND as

$$f_{\wedge} = \Delta(x_3 + x_1x_2 - 2x_1x_2x_3). \quad (1.43)$$

Spin variable s_i and Boolean variable x_i are related by the affine transformation $s_i = 1 - 2x_i$. Substitution of $\frac{1}{2}(1 - s_i)$ into f_{\wedge} changes from Boolean to spin variables, resulting in

$$\frac{\Delta}{4}(2 - s_3 - s_1s_3 - s_2s_3 + s_1s_2s_3). \quad (1.44)$$

To embed this into matrix form, we replace $s_i \mapsto Z_i$ and send multiplication $\cdot \mapsto \otimes$.

We will consider the Hamiltonian applying the logical AND operation, that is a Hamiltonian with the span of the truth table of AND as its ground state. The Boolean function for AND in two-body form can be written

$$f_{\wedge} = a \cdot x_3 + b \cdot x_2x_3 + c \cdot x_1x_2 + d \cdot x_1x_3. \quad (1.45)$$

Hence we arrive at the two-body Hamiltonian for AND

$$h_{\wedge} = a \cdot P_1^3 + b \cdot P_1^2 \otimes P_1^3 + c \cdot P_1^1 \otimes P_1^2 + d \cdot P_1^1 \otimes P_1^3. \quad (1.46)$$

Example 9. (AND penalty). Let us then derive a series of inequalities (equalities) and determine a solution providing non-negative integer values for a, b, c, d such that h_{\wedge} in (1.46) has a zero eigenspace given as

$$\text{span}\{|x_1x_2x_3\rangle \mid x_3 = x_1x_2\}$$

and all other eigenspaces are ≥ 1 . Substituting the values of the truth table into the variables yields the inequalities, one solution is

$$f_{\wedge} = 3x_3 + x_2x_3 - 2x_1x_2 - 2x_1x_3.$$

Example 10. Let us now develop a two-body penalty function that performs the COPY operation. In other words, let us develop the penalty function such that

the low-energy subspace is in

$$\text{span}\{|000\rangle, |111\rangle\}.$$

We will consider three spins and place pairwise equality penalties

$$f_{=} (x_i, x_j) = x_i(1 - x_j) + (1 - x_i)x_j$$

connecting the spins with a triangular interaction graph. Assigning the value $|a\rangle$ to any spin and traversing the triangle minimizes this penalty when all spins take the same value $|a\rangle$. Labeling the spins i, j and k the penalty function reduces as

$$f_{\text{copy}} = 2x_3 + 2x_1 + 2x_2 - 2x_2x_3 - 2x_2x_1 - 2x_3x_1. \quad (1.47)$$

Example 11. It is readily shown that

$$-x_1x_2x_3 = \min_{z \in \mathbb{B}} z(2 - x_1 - x_2 - x_3) \quad (1.48)$$

and that

$$-x_1x_2x_3 = \min_{z \in \mathbb{B}} z(-x_1 + x_2 + x_3) - x_1x_2 - x_1x_3 + x_1, \quad (1.49)$$

hence providing an alternative 2-body to 3-body reduction.

In addition to embedding Boolean logic into the ground state of system of spins, one can consider the following.

Example 12. (Penalty function with constraints). A real valued equality constraint of the form

$$f(x) = c$$

for $x \in \mathbb{R}^n$, $c \in \mathbb{R}$ can be converted to an unconstrained optimization problem using the following penalty function

$$P(x) = A(f(x) - c)^2$$

where $P(x) = 0$ when the constraint is reached; $P(x) > 0$ when the constraint is not reached and $A \in \mathbb{R}$ is a scaling factor. Such problems are readily mapped to the Ising model by considering a Boolean embedding of x .

Example 13. (Number partitioning). Given a set of N positive numbers $S = n_1, \dots, n_N$, is there a partition of this set of numbers into two disjoint subsets R and $S - R$, such that the sum of the elements in both sets is the same?

Let n_i ($i = 1, \dots, N = |S|$) describe the numbers in set S . It can be shown that

$$\mathcal{H} = \left(\sum_i n_i s_i \right)^2 \geq 0 \quad (1.50)$$

vanishes if and only if such a disjoint partition exists. Here s_i is a spin variable $\in \pm 1$.

The following applies to number partitioning (Example 13).

Remark 8. (\mathbb{Z}_2 symmetry). Consider the tunable two-body Ising Hamiltonian acting on n spins as

$$\mathcal{H} = \sum_{i < j} J_{ij} Z_i Z_j \quad (1.51)$$

Using the identity that $XZX = -Z$ or otherwise, for $\tilde{X} = \bigotimes_{l=0}^n X_l$ it can be shown that

$$\left[\tilde{X}, \mathcal{H} \right] = 0 \quad (1.52)$$

and hence one can establish that the definition of $|0\rangle, |1\rangle$ is entirely arbitrary with respect to \mathcal{H} .

1.4 P- vs. NP problems and physics

Let us continue with a more formal definition of efficiency. First we consider the following definition.

Definition 10. (Decision Problem) A decision problem is a problem that can be posed as a YES-NO question of input values.

The following represent YES or NO decision problems.

Example 14. (Primality Testing) Is a given natural number prime?

Example 15. Given two numbers x and y , does x evenly divide y ? The answer is either YES or NO depending upon the values of x and y .

Remark 9. A method for solving a decision problem, given in the form of an algorithm, is called a **decision procedure** for that problem. If the procedure or algorithm terminates in time bounded above by some polynomial in the problem size, then we call the procedure **efficient**.

We will now define \mathbf{P} as the set of **tractable** decision problems: decision problems for which we have polynomial-time algorithms.

Definition 11. The complexity class \mathbf{P} is the set of all decision problems that can be solved with worst-case polynomial time-complexity.

Remark 10. In other words, a problem is in the class \mathbf{P} if

1. it is a decision problem and
2. there exists an algorithm that solves any instance of size n in $\mathcal{O}(n^k)$ time, for some integer k .

Here n is the number of bits needed for encoding the input.

The second class of decision problems that we are concerned with here is called \mathbf{NP} , which stands for **non-deterministic polynomial time**.

The definition of \mathbf{NP} involves the idea of a non-deterministic algorithm. For our purposes, we consider \mathbf{NP} as the class of decision problems where each input can be evaluated in polynomial time. Hence, if we had access to a (apparently fictitious) non-deterministic machine, we might check all inputs simultaneously and decide any \mathbf{NP} problem instance.

While many questions remain in complexity theory, it is still of interest to place physical systems and processes in corresponding classes. For example, a physical process which can be simulated efficiently using a classical computer algorithm would provide a poor candidate to accelerate the solution of \mathbf{NP} problem instances.

1.5 Computational phase transitions

Here in § 1.5 we largely follow [25] and cover some joint work I've recently done with Philathong, Akshay, and Zacharov.

As information is necessarily represented in physical media, the processing, storage and manipulation of information is governed by the laws of physics. Indeed, the theory of computation is intertwined with the laws governing physical processes [3]. Many physical systems and physical processes can be made to represent, and solve computational problem instances. Viewed another way, many variants of naturally occurring processes (such as protein folding) have been shown to represent computationally significant problems, such as **NP**-hard optimization problems. But how long does it take for a physical process to solve problem instances? How can difficult problem instances be generated?

The physical Church-Turing thesis [26; 27] asserts that a universal classical computer can simulate any physical process and vice versa (outside of quantum mechanical processes). It does not propose the algorithm, yet asserts its existence. One might wrongly suspect that undecidable problems can be embedded into physical systems: attempts at this fail, i.e. due to instabilities. What about the **P** vs. **NP** problem? If no physical process existed to solve **NP**-complete problems in polynomial time, then by the physical Church-Turing thesis, no algorithm would exist either. Hence if the laws of physics ruled out such a scenario, this would imply that $\mathbf{P} \neq \mathbf{NP}$.

This distinction between polynomial and exponential resources is a course gaining that computational complexity theory is based around. We do not know if a physical process can be made to solve **NP**-complete problems in polynomial time or not. However, it is asserted that computational phase transitions are a feature of **NP**-complete problems—although specifics of the transition have yet to be formulated (proven) rigorously. We will turn to the theory of computational phase transitions to understand how physics responds to changes in the complexity landscape across the algorithmic phase transition.

This algorithmic phase transition occurs where randomly generated problem instances are thought to be difficult [28–30]. It is observed by the fact that computer algorithms experience a slowdown around this transition point. For example, let us consider the familiar problems of 2- (and 3)-satisfiability (detailed in the next section: the phase transition provably exists for 2-SAT and is only known to be inside a window for 3-SAT). If we let the number of variables be N and uniformly generate M random clauses over these N variables, computer

algorithms appear to slow down at a certain clause to variable ratio (critical clause density of the order parameter $\alpha = M/N$).

What about physical systems that bootstrap physics to naturally solve problems instances? Instances of these problems can be embedded in the lowest energy configuration of physical models [12; 13; 31]. Hence, building such a physical system and cooling (annealing) this system can enable a process which solves such problems [14–21; 32]. For example, a system settling into its low-energy configuration can be programmed such that this low energy configuration represents the solution to 2- (and 3)-SAT instances.

We found that the algorithmic phase transition has a statistical signature in Gibbs' states of problem Hamiltonians generated randomly across the algorithmic phase transition. This was confirmed by exact calculations of 26 binary units (spins) on a mid-scale supercomputer. Physical observation of the effect is hence within reach of near term and possibly even existing physical computing hardware: such as Ising machines [16; 17], annealers [14] and quantum enhanced annealers [33–37].

Since the algorithmic phase transition takes places where randomly generated problem instances are thought to contain difficult instances, this discovery provides a practical benchmark for contemporary physics based processors. The problem of finding hard instances is prominent to such emerging technologies. We purpose a physical experiment to witness the algorithmic phase transition signature and to benchmark contemporary physics based processors.

Propositional satisfiability (SAT) is the problem of determining the satisfiability of sentences in propositional logic. If k is the number of literals in each clause the problem is called k -SAT. Determining the satisfiability of a formula in conjunctive normal form where each clause is limited to at most k literals is NP-complete (Cook [22]);

Definition 12. A decision problem c is NP-complete iff

- (i) c is in NP,
- (ii) every problem in NP is reducible to c in polynomial time.

We recall Theorem 2, and state the following.

Theorem 4. THREE-BODY PROJECTOR ISING HAMILTONIAN is NP-complete.

We will proceed informally and complete a construction proof of Theorem 4. As one recalls from § 1, in NP problems a candidate solution can be checked in polynomial time.

k -satisfiability problems can be reduced—generally called Karp reduction—to 3-satisfiability (3-SAT) when formulas in conjunctive normal form (CNF) are considered with each clause containing at least 3 literals.

Example 16. For an explicit example of turning 3-SAT into a ground state Hamiltonian problem, consider (1.53).

$$f = (x_i \vee \bar{x}_j \vee x_k) \wedge (\bar{x}_g \vee x_r \vee \bar{x}_s) \wedge (\dots) \wedge \dots \quad (1.53)$$

The first clause can be rewritten as an energy penalty viz.,

$$x_i \vee \bar{x}_j \vee x_k \mapsto |0\rangle\langle 0|_i \otimes |1\rangle\langle 1|_j \otimes |0\rangle\langle 0|_k \quad (1.54)$$

and likewise for other clauses.

Remark 11. (The spectrum of Hamiltonian SAT) Given a 3-SAT formula f , it is readily established that the 3-body Ising projector form of f has the following eigenvalue problem.

$$\mathcal{H}_f |x\rangle = f(x) |x\rangle \quad (1.55)$$

where $f(x)$ counts the number of clauses violated by bit string x .

Proof. (THREE-BODY PROJECTOR ISING HAMILTONIAN is NP-complete—Theorem 4) We readily see that every 3-SAT instance can be embedded into an instance of THREE-BODY PROJECTOR ISING HAMILTONIAN. Each candidate solution is evaluated in time proportional to the number of Hamiltonian terms. Moreover, a Yes instance is shown by a witness $|y\rangle$ such that

$$\langle y | \mathcal{H}_f |y\rangle = 0. \quad (1.56)$$

Hence the problem is in NP. We recall the classical result that 3-SAT is Karp reducible (polynomial-time reduction) to general circuit SAT, which is the canonical NP-complete problem. Hence, we establish the completeness result in Theorem 4. \square

Given the clause density defined as $\alpha \stackrel{\text{def}}{=} M/N$ where M is the number of clauses and N is the number of variables, we will generate random SAT instances. As random SAT instances are generated increasing α , a sharp transition occurs. The likely-hood of a random instance being satisfiable goes from near unity to near zero across an increasingly small domain. Crawford and Auton (1993) [28] empirically located the 3-SAT transition at a clause/variable ratio around 4.27.

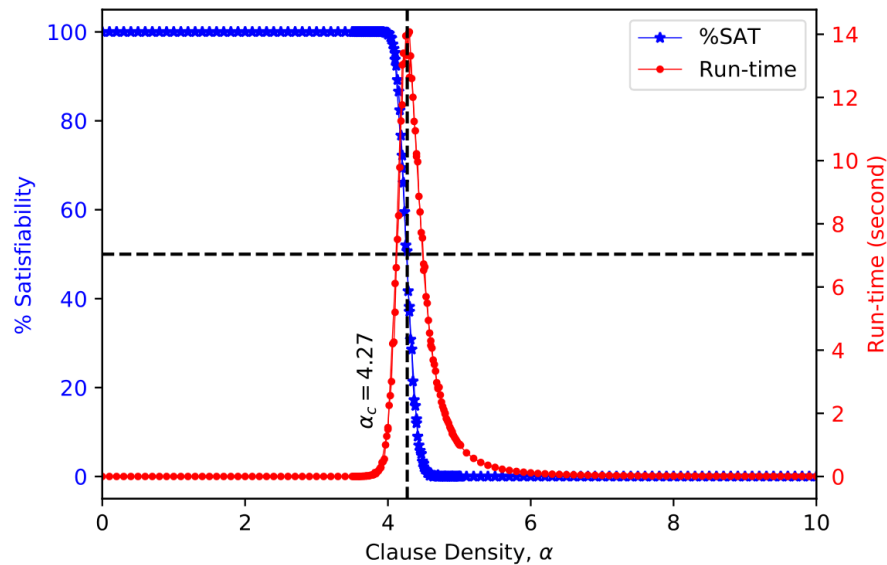


Figure 1.1 — Percent of satisfiable instances (left axis) and run-time (right axis) versus clause density, α . We randomly generated 1,000 3-SAT instances with 300 variables with observed $\alpha_c \approx 4.27$. Figure taken from [25].

Example 17. As a worked example, let us consider a value assignment of x_1, x_2, x_3, x_4 such that $f(x_1, x_2, x_3, x_4) = 1$ and hence (i) show that f in (1.57) is satisfiable.

$$f = (x_1 \vee \bar{x}_3 \vee x_4) \wedge (\bar{x}_2 \vee x_3 \vee \bar{x}_4) \wedge (\bar{x}_1 \vee x_2 \vee x_3) \quad (1.57)$$

From binary search (by hand) we find the assignment $x_1 = 0, x_2 = 0, x_3 = 0$ and x_4 is free. The clause density is 0.75 and the number of nodes in the expansion graph (see Boolean decision diagram) is negligible).

1.5.1 Thermal states at the SAT phase transition

Physical systems at thermal equilibrium are often approximated by a Gibbs state

$$\rho_\beta \stackrel{\text{def}}{=} \frac{e^{-\beta h}}{\langle e^{-\beta h} \rangle} = \frac{1}{\mathcal{Z}} \sum_l e^{-\beta \lambda_l} |l\rangle\langle l| = \frac{1}{\sum_l e^{-\beta \lambda_l}} \sum_l e^{-\beta \lambda_l} |l\rangle\langle l|. \quad (1.58)$$

Where λ_i are the eigenvalues. Note that the computational basis forms the energy basis of the Hamiltonian, hence $|l\rangle\langle l|$ is diagonal. We will soon be concerned with the case that the Hamiltonian $\mathcal{H} = \sum_i C_i$ is a sum over projectors onto 3-SAT clauses and the partition function is $\mathcal{Z} = \sum_l e^{-\beta \lambda_l}$.

Consider the monotonic list,

$$\lambda_0 \leq \lambda_1 \leq \lambda_2 \leq \dots \leq \lambda_r$$

and assume that λ_0 is possibly degenerate. Let φ_0^i be an eigenvector with eigenvalue λ_0 . Let i index all d potentially degenerate eigenvalues satisfying

$$\mathcal{H} |\varphi_0^i\rangle = \lambda_0 |\varphi_0^i\rangle. \quad (1.59)$$

We are interested in the probability of being in the subspace

$$\text{span}\{|\varphi_0^i\rangle \mid \mathcal{H} |\varphi_0^i\rangle = \lambda_0 |\varphi_0^i\rangle\}. \quad (1.60)$$

We let $i = 1$ to d for d the degeneracy count. We are interested in the quantity

$$\begin{aligned} \frac{1}{\mathcal{Z}} \sum_{i=1}^d \langle \varphi_0^i | \left[\sum_l e^{-\beta \lambda_l} |l\rangle\langle l| \right] | \varphi_0^i \rangle &= \\ &= \frac{1}{\mathcal{Z}} \sum_{i,l} \langle \varphi_0^i | l \rangle \langle \varphi_0^i | l \rangle e^{-\beta \lambda_l} = \frac{1}{\mathcal{Z}} \sum_{i=1}^d e^{-\lambda_0 \beta} = \frac{\sum_{i=1}^d e^{-\beta \lambda_0}}{\sum_{l=1}^d e^{-\beta \lambda_l}}. \end{aligned} \quad (1.61)$$

Equation (1.61) can be plotted as an interesting programming exercise.

Proposition 1. (Eigenvalues of thermal states). It can be shown that

$$\rho_\beta = \frac{e^{-\beta \sum_j Z_j}}{\text{tr}\{e^{-\beta \sum_j Z_j}\}} = \bigotimes_j \frac{1}{2} \sum_{b \in \{0,1\}} (1 - (-1)^b \tanh(\beta)) |b\rangle_j \langle b|_j. \quad (1.62)$$

We then derive a formula for the eigenvalues of a state in terms of the Boolean variables in the general bit string $|x_1, x_2, \dots, x_l\rangle$, viz.,

$$\langle x_1, x_2, \dots, x_l | \rho_\beta | x_1, x_2, \dots, x_l \rangle = \prod_{j=1}^l \frac{1}{2} (1 - (-1)^{x_j} \tanh(\beta)). \quad (1.63)$$

If we were to sample ρ_β , the probability of measuring $|x_1, x_2, \dots, x_l\rangle$ is given precisely by (1.63).

We want to investigate the properties of a thermal system, for fixed β playing the role of an inverse temperature. We further want to investigate this across the phase transition. We can intuitively expect that around the phase transition, a thermal system would exhibit a decreased occupancy in its ground state.

Let $|i\rangle$ denote (possibly degenerate) lowest eigenstates of \mathcal{H} . We label these possibly degenerate states by letting i range from 1 up to d . Call λ_{\min} the lowest eigenvalue of \mathcal{H} , then we have (1.65).

We are concerned with the quantity (1.64), giving occupancy in the low-energy subspace for a system at equilibrium for fixed finite inverse temperature β . We call this quantity $p(\lambda_{\min}, \beta)$,

$$p(\lambda_{\min}, \beta) = \frac{1}{\mathcal{Z}} \sum_{i=1}^d \langle i | e^{-\beta \mathcal{H}} | i \rangle \quad (1.64)$$

where

$$\forall i \in \{1, \dots, d\}, \quad \langle i | \mathcal{H} | i \rangle. \quad (1.65)$$

Proposition 2. It can be shown that

$$\lim_{\beta \rightarrow \infty} \frac{1}{\mathcal{Z}} \sum_{i=1}^d \langle i | e^{-\beta \mathcal{H}} | i \rangle \quad (1.66)$$

and hence one can establish that in the zero temperature limit (β is inverse temperature), sampling a thermal system can solve SAT instances with probability one.

Remark 12 (On determining a threshold temperature to reveal the algorithmic phase transition). From Figure 1.2 the ground state occupancy of thermal states can reveal an algorithmic phase transition signature. When the inverse temperature β is relatively small, the easy-hard transition around $\alpha = 4.27$ is missing (Proposition 2 establishes no transition in the zero temperature limit). As pointed out to the author by Vladimir Korepin, a threshold temperature to reveal the algorithmic phase transition appears to be lacking.

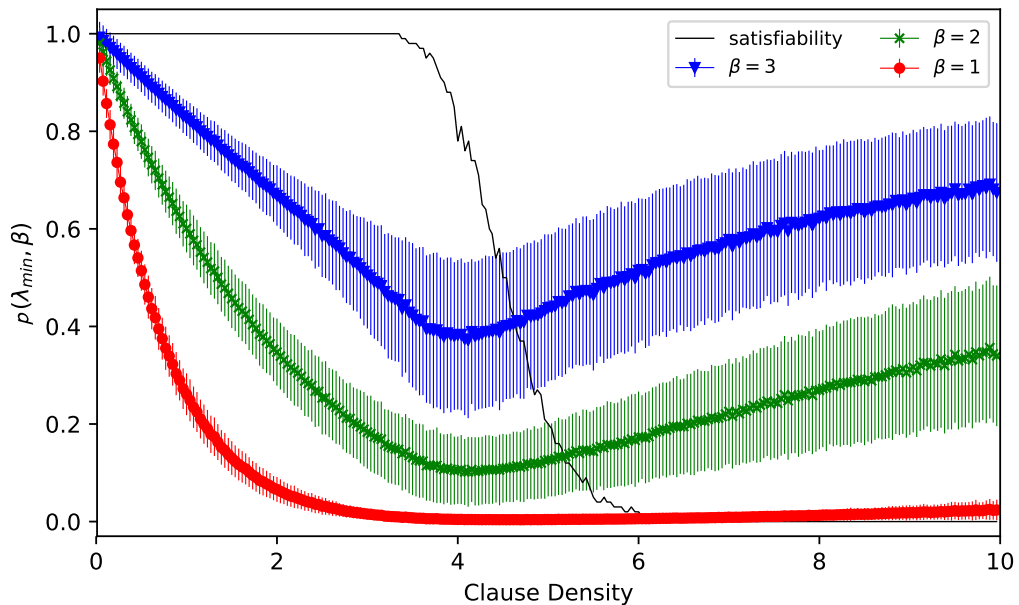


Figure 1.2 — Ground state occupancy of the thermal states corresponding to Hamiltonians embedding 3-SAT instances across the algorithmic phase transition for 26 spins with $\beta = 1, 2, 3$. Figure taken from [25].

Chapter 2. Quantum vs Probabilistic Computation

To understand quantum computation, we will recall and contrast quantum mechanics with stochastic mechanics. Our development partly follows a book coauthored with John Baez [38] as well as other works [39; 40] which among other results were partially reviewed in [41]. Here we offer a more computational focus.

2.1 Defining Mechanics

Understanding quantum computation involves being able to contrast quantum computation from other models. We might then compare standard deterministic bits (c-bits), versus stochastic or probabilistic (p-bits), versus quantum bits (q-bits or qubits). We will begin by mentioning a summary in Table 3.

Our starting place is to describe and contrast stochastic versus quantum mechanics and then point out some of the basic implications the similarities and differences imply when considering walks on graphs.

	bits	probabilistic bits	qubits
state (single unit)	bit $\in \{0,1\}$	real vector $a + b \in \mathbb{R}_+$ $\vec{b} = a\vec{0} + b\vec{1}$ a+b=1	complex vector $\alpha, \beta \in \mathbb{C}$ $\vec{\psi} = \alpha\vec{0} + \beta\vec{1}$ $ \alpha ^2 + \beta ^2 = 1$
state (multi-unit)	bitstring $x \in \{0,1\}^n$	prob.distribution (stochastic vector) $\vec{s} = \{p_i\} \in (0,1)_p$	wavefunction (complex vector) $\vec{\psi} = \{\alpha_x\}_{x \in \{0,1\}^n}$
operations	Boolean logic	stochastic matrices $\sum_{j=1}^S P_{ij} = 1$	unitary matrices $U^\dagger U = \mathbb{1}$
component ops	Boolean gates	tensor product of matrices	tensor product of matrices

Table 3 — Summary of deterministic, probabilistic and quantum computation.

2.1.1 Stochastic time evolution

The stochastic master equation gives the time evolution of a state

$$\frac{d}{dt} |\psi(t)\rangle = -\mathcal{H} |\psi(t)\rangle \quad (2.1)$$

with solution $|\psi(t)\rangle = e^{-t\mathcal{H}} |\psi(0)\rangle$ which can be checked as

$$\frac{d}{dt} e^{-t\mathcal{H}} |\psi(0)\rangle = -\mathcal{H} e^{-t\mathcal{H}} |\psi(0)\rangle = -\mathcal{H} |\psi(t)\rangle. \quad (2.2)$$

2.1.2 Quantum time evolution

The quantum Schrödinger's equation gives the time evolution of a state in quantum mechanics

$$\frac{d}{dt} |\psi(t)\rangle = -i\mathcal{H} |\psi(t)\rangle \quad (2.3)$$

with solution $|\psi(t)\rangle = e^{-it\mathcal{H}} |\psi(0)\rangle$ which can be checked as

$$\frac{d}{dt} e^{-it\mathcal{H}} |\psi(0)\rangle = -i\mathcal{H} e^{-it\mathcal{H}} |\psi(0)\rangle = -i\mathcal{H} |\psi(t)\rangle. \quad (2.4)$$

The operator \mathcal{H} is called the Hamiltonian. Its properties depend whether we are working in a stochastic or quantum system.

Example 18. (Exact Solution of the T.I.S.E.) If $\mathcal{A}^2 = \mathbb{1}$ then

$$e^{-i\theta\mathcal{A}} = \mathbb{1} \cos(\theta) - i\mathcal{A} \sin(\theta). \quad (2.5)$$

Example 19. (Exact Solution of the T.I.S.E.) Let $\mathcal{P}^2 = \mathcal{P}$ then

$$e^{-i\theta\mathcal{P}} = \mathbb{1} + \mathcal{P}(e^{-i\theta} - 1) \quad (2.6)$$

follows by the series expansion

$$e^{\mathcal{A}} = \sum_{k=0}^{k=\infty} \frac{\mathcal{A}^k}{k!}. \quad (2.7)$$

2.1.3 Properties in stochastic mechanics

\mathcal{H} is infinitesimal stochastic for time evolution in stochastic mechanics given by $e^{-t\mathcal{H}}$ to send stochastic states to stochastic states:

1. its columns sum to zero (2.8).
2. its off diagonal entries are real and non-positive (2.9).

$$\sum_i \mathcal{H}_{ij} = 0 \quad (2.8)$$

$$i \neq j \Rightarrow \mathcal{H}_{ij} \leq 0. \quad (2.9)$$

Remark 13. The term *infinitesimal stochastic* was used in [38] while *intensity matrix* more commonly appears in the literature to describe the generator of a one dimensional stochastic semigroup.

Definition 13. A *semigroup* is a unital algebraic structure consisting of a set together with an associative binary \cdot pairing. Hence, a semigroup relaxes the inverse requirement of a group.

Remark 14. In our case, a one dimensional (semi)group has a product structure for non-negative s , such that $U(s) \cdot U(s') = U(s + s')$ where $U(0) = \mathbf{1}$ and U is the s -dependent exponential image of a (infinitesimal stochastic/Hermitian) generator.

2.1.4 Hamiltonian properties in quantum mechanics

\mathcal{H} is self-adjoint (often called Hermitian, $\mathcal{H} = \mathcal{H}^\dagger$) for time evolution given by $e^{-it\mathcal{H}}$ to send quantum states to quantum states, $\mathcal{H} = \mathcal{H}^\dagger$. The eigenvalues of \mathcal{H} take only real values.

The Hamiltonian in quantum mechanics can be written as

$$(\mathcal{H}^\dagger)_{ij} = \overline{\mathcal{H}_{ji}} \quad (2.10)$$

or as

$$\mathcal{H}^\dagger = \sum_l \overline{\lambda_l} (|l\rangle\langle l|)^\dagger = \sum_l \lambda_l |l\rangle\langle l|.$$

A linear map sending quantum states to quantum states is called an isometry (Definition 15). Isometries represent the general collection of deterministic operations on quantum states. A subclass of isometries are unitary maps.

$$\mathcal{U}_t = e^{-it\mathcal{H}} \quad (2.11)$$

Such maps are characterized by

$$\mathcal{U}^\dagger \mathcal{U} = \mathbb{1}. \quad (2.12)$$

A linear map that sends stochastic states to stochastic is the following *stochastic operator*.

$$\mathcal{U}_t = e^{-t\mathcal{H}} \quad (2.13)$$

Such maps are characterized as

$$\sum_i \mathcal{U}_{ij} = 1 \quad (2.14)$$

$$\mathcal{U}_{ij} \geq 0 \quad (2.15)$$

Definition 14. A *bijection* is an invertible one-to-one function between elements of two sets.

Example 20. The COPY operation is bijective. Let $C(x) = (x, x)$ where $C^{-1}(a, b) = \emptyset$ (0) and $C^{-1}(a, a) = a$. Then C^{-1} is a left and right inverse, making C bijective as $C^{-1}(C(x)) = C^{-1}(x, x) = x$.

Definition 15. An *isometry* is a norm preserving bijective map on state(s).

Example 21 (Quantum Isometry). Consider the COPY (C) operation defined on one basis (which then does not violate no-cloning [42]). We have $C(|\psi\rangle) = |\psi\rangle \otimes |\psi\rangle$. Clearly for $|\langle\psi|\psi\rangle|^2 = 1$, $|\psi\rangle \otimes |\psi\rangle$ is normalized. The inverse of C is defined element wise.

2.1.5 Observables

In quantum mechanics an observable is given by a self-adjoint (Hermitian) matrix \mathcal{O} and the expected value of \mathcal{O} relative to quantum state $|\varphi\rangle$ is

$$\langle\varphi|\mathcal{O}|\varphi\rangle = \sum_{ij} \bar{\varphi}_i \mathcal{O}_{ij} \varphi_j, \quad (2.16)$$

where $|\varphi\rangle = \sum_i \varphi_i |i\rangle$.

Remark 15. The L.H.S. of (2.16) is alternatively and equivalently written as $\langle\varphi, \mathcal{O}(\varphi)\rangle$, borrowing functional analysis style notation still common in certain circles.

In stochastic mechanics, an observable \mathcal{O} takes value \mathcal{O}_i for each configuration i and the expected value of \mathcal{O} in the stochastic state φ (equivalently $|\varphi\rangle$) is

$$\mathcal{O}(\varphi) = \sum_i \mathcal{O}_i \varphi_i \quad (2.17)$$

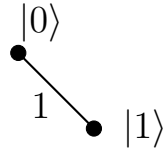
Definition 16. A *simple graph* contains no-self loops (e.g. no single node is both the source and the sink of the same edge).

Remark 16. Some authors alternatively define a *simple graph* to be an un-weighted, undirected graph containing no graph loops or multiple edges.

Definition 17. A *symmetric graph* has only unweighted and undirected edges. Or equivalently, for all nodes a and b in graph G , there is an edge from b to a for each edge from a to b .

Definition 18 (Adjacency matrix). Given a simple and symmetric graph G , we pick a set of *labels* S with cardinality equal to the number of nodes of G . Each ordering of S , induces a basis which lifts naturally to a basis to represent G by an adjacency matrix A .

Let us then develop an extended example for the stochastic case. Let A be the adjacency matrix of the simple, symmetric graph as follows.



A is then Pauli X in this case. To form the graph Laplacian from A we define $D_{ij} = \sum_j A_{ji}$ and $\forall i \neq j D_{ji} = 0$. And so we arrive at (2.18).

$$D = \mathbb{1}, \quad \mathcal{H} = D - A = \mathbb{1} - X. \quad (2.18)$$

From a standard calculation, \mathcal{H} yields the following eigensystem (2.19).

$$\begin{aligned} \lambda_0 = 0 & \quad |\lambda_0\rangle = |+\rangle \\ \lambda_1 = 2 & \quad |\lambda_1\rangle = |-\rangle \end{aligned} \quad (2.19)$$

Let us then assume that the initial state is (2.20).

$$|\varphi(0)\rangle = |0\rangle \quad (2.20)$$

In the eigenbasis (2.20) becomes (2.21).

$$|0\rangle = \frac{1}{\sqrt{2}}(|\lambda_0\rangle + |\lambda_1\rangle) \quad (2.21)$$

and our time dependent propagator in the Laplacian eigenbasis (2.18) is

$$e^{-t\mathcal{H}} = \sum_j e^{-t\lambda_j} |\lambda_j\rangle\langle\lambda_j|. \quad (2.22)$$

The time evolution of a state (2.20) starting at node $|0\rangle$ is given as (2.23).

$$\begin{aligned} e^{-t\mathcal{H}} |0\rangle &= \frac{1}{\sqrt{2}}(e^{-t\lambda_0} |\lambda_0\rangle + e^{-t\lambda_1} |\lambda_1\rangle) \\ &= \frac{1}{2}(1 + e^{-t\lambda_1}) |0\rangle + \frac{1}{2}(1 - e^{-t\lambda_1}) |1\rangle \end{aligned} \quad (2.23)$$

Figure 2.1 illustrates the time dependence of (2.23). The initial state ($|0\rangle$) decays with probability

$$\langle 0|e^{-t\mathcal{H}}|0\rangle = \frac{(1 + e^{-t\lambda_1})}{2},$$

while the probability of measuring state $|1\rangle$ increases with probability

$$\langle 1|e^{-t\mathcal{H}}|1\rangle = \frac{(1 - e^{-t\lambda_1})}{2},$$

for $\lambda_1 = 2$. The long time behavior is given as follows.

$$\lim_{t \rightarrow \infty} |\phi(t)\rangle = \frac{1}{2} |0\rangle + \frac{1}{2} |1\rangle \quad (2.24)$$

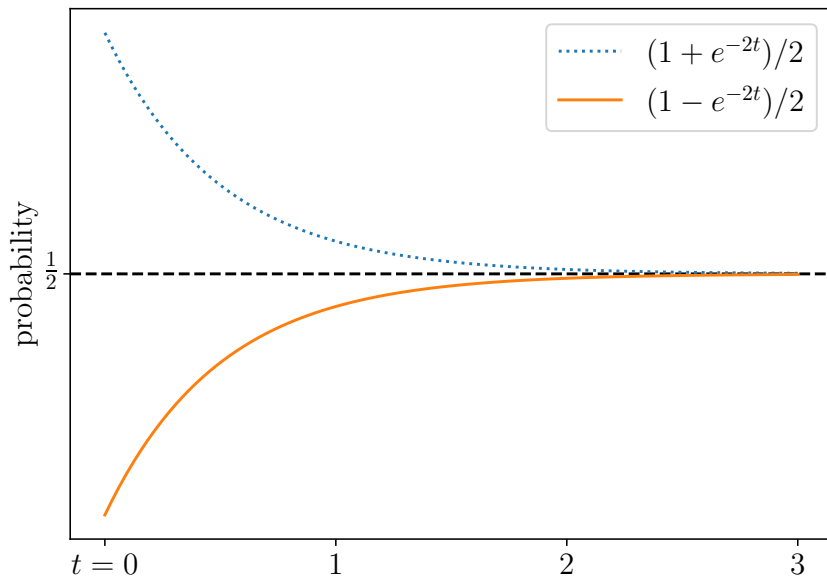


Figure 2.1 — Stochastic probability versus time generated by the graph Laplacian (2.18) with initial state $|0\rangle$. The final state is the equal probabilistic mixture of $|0\rangle$ and $|1\rangle$.

Let us repeat the analysis for the case of a quantum particle on the same graph yet with a complexified form of the generator from (2.18). The time-

dependent quantum particle of a particle walking on this same graph is given as (2.25) with initial state (2.26).

$$e^{-it\mathcal{H}} = \sum_i e^{-it\lambda_i} |\lambda_i\rangle\langle\lambda_i| \quad (2.25)$$

$$|0\rangle = \frac{1}{\sqrt{2}} |\lambda_0\rangle + \frac{1}{\sqrt{2}} |\lambda_1\rangle \quad (2.26)$$

The dynamics readily simplify to the following form (2.27), from which we arrive at the time dependent probability of measuring $|0\rangle$ as (2.28).

$$e^{-it\mathcal{H}} |0\rangle = \frac{1}{\sqrt{2}} |\lambda_0\rangle + \frac{e^{-i2t}}{\sqrt{2}} |\lambda_1\rangle \quad (2.27)$$

$$\begin{aligned} \text{Prob}(|0\rangle) &= \frac{1}{2} \left[\frac{1}{\sqrt{2}}(1 + e^{-i2t}) \right] \left[\frac{1}{\sqrt{2}}(1 + e^{i2t}) \right] \\ &= \frac{1}{4} (2 + e^{-i2t} + e^{i2t}) \\ &= \frac{1 + \cos 2t}{2} \end{aligned} \quad (2.28)$$

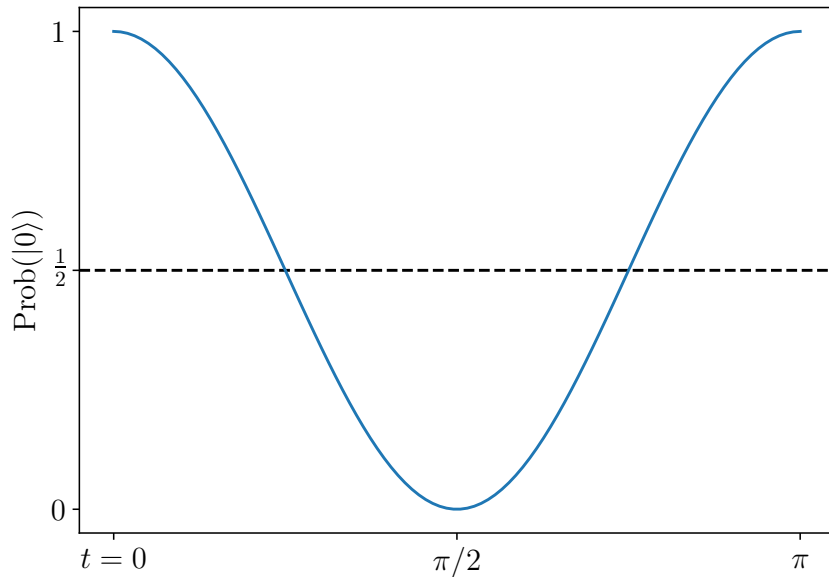


Figure 2.2 — Quantum probability versus time generated by the graph Laplacian (2.18) with initial state $|0\rangle$ exhibits strong oscillations.

Figure 2.2 illustrates that probability for quantum evolution of a closed systems exhibits oscillations. These oscillations are central to the function of a gate model quantum processor.

Example 22 (Local and composite rotation gates). In the gate model of quantum computation, various techniques exist to create quantum logic gates [6]. For example, a Z rotation is evolved as

$$\begin{aligned} e^{-i\theta Z} &= e^{-i\theta}|0\rangle\langle 0| + e^{i\theta}|1\rangle\langle 1| \\ &= e^{-i\theta}(|0\rangle\langle 0| + e^{-2i\theta}) \\ &\sim |0\rangle\langle 0| + e^{i2\theta}|1\rangle\langle 1|. \end{aligned} \tag{2.29}$$

It is left to the reader to consider the following gate generated by non-commuting terms.

$$\mathbf{H} = \frac{1}{\sqrt{2}}(X + Z) \tag{2.30}$$

and to find t s.t. $e^{-it\mathbf{H}} \sim \mathbf{H}$ (up to a unit modulus complex number) realizes the Hadamard gate. The gate can also be created by a product of unitary gates [6].

Remark 17 (Quantum Circuits). We will now begin to utilize an evident and widely used graphical depiction of quantum gates. This will be further developed and connected to the theory of tensor networks in § 3. Here we will adapt an intuitive approach and focus solely on the evident applications at hand.

Definition 19 (Quantum Circuit—Sketch). A *quantum circuit* also called *quantum computational network* is a model for a computation representing a sequence of unitary operators as a sequence of quantum gates on an n -qubit register. The identity gates are given as wires while the gates appear as boxes on the wires in which they act non-trivially upon. Time goes from right to left across the page herein (to match how equations are written).

It is typical to consider a tunable Hamiltonian that will be fully controllable and used to sequence quantum gates. The standard Hamiltonian assumed herein follows in Definition 20.

Definition 20 (Tunable Ising Model with Transverse Field). The tunable Ising model allows the application of any gate formed from the Hamiltonian

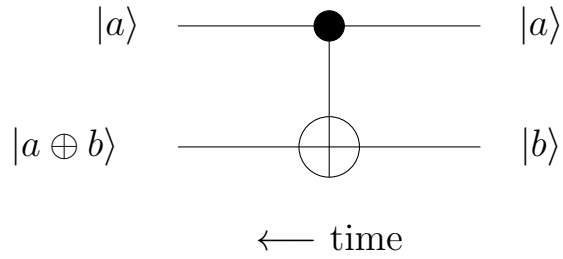
$$\mathcal{H} = \sum_{i,j} J_{ij} Z_i Z_j + \sum_i h_i Z_i + \sum_i \delta_i X_i \quad (2.31)$$

where typically gates are fundamentally assumed to act on one or two qubits at a time. Furthermore, it is typical to consider each gate as being generated by commuting Hamiltonian terms (see Example 22).

Definition 21 (Single Qubit Gate). A single qubit gate is given by the following quantum gate U_t .

$$U_t = e^{-it\mathcal{H}} \longrightarrow \boxed{U_t}$$

As an extended example, let us create a CN gate acting as



$$\begin{aligned} \text{CN} &= (P_1 \otimes X + P_0 \otimes \mathbb{1}) \\ \text{CN}^\dagger &= \text{CN}, \text{CN}^2 = \mathbb{1} \Rightarrow \exists \phi \mid e^{-i\phi \text{CN}} = \text{CN} \\ \text{CN} &= (\mathbb{1} \otimes H) \underbrace{(P_1 \otimes Z + P_0 \otimes \mathbb{1})}_{\text{CN}} (\mathbb{1} \otimes H^\dagger) \end{aligned} \quad (2.32)$$

↓

$$\text{of the form } \alpha Z_1 + \beta Z_2 + \gamma Z_1 Z_2 \text{ as per Definition 20} \quad (2.33)$$

Remark 18. $P_1 \otimes U + P_0 \otimes \mathbb{1}$ is unitary if and only if U is unitary.

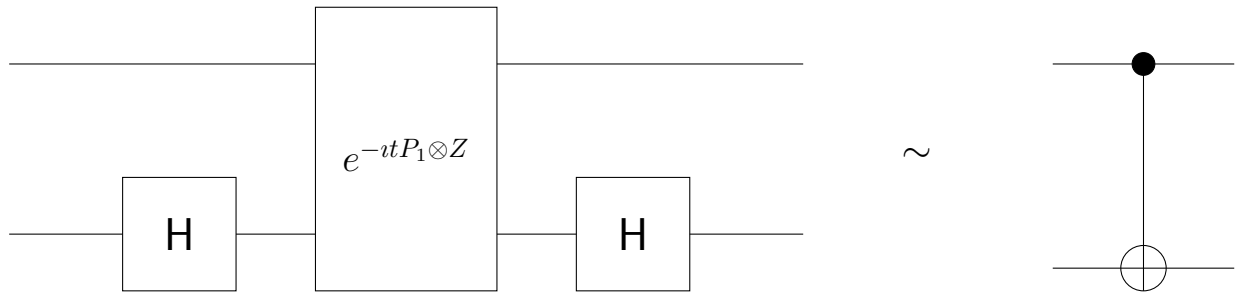
Remark 19. One readily solves for α, β, γ such that (2.33) becomes $P_1 \otimes Z + P_0 \otimes \mathbb{1}$. Here we drop terms proportional to $\mathbb{1}$ since $e^{-i\alpha \mathbb{1}} = e^{-i\alpha} \mathbb{1} \sim \mathbb{1}$ is a global phase (see Definition 22).

Definition 22 (Unit and Scalar Gauge). In quantum theory, a global phase is undetectable. Hence it is common to consider an equivalency class where $|\psi\rangle$ and $e^{i\phi}|\psi\rangle$ are equivalent. This is called working in the *unit gauge*: sometimes we work in the *scalar gauge*, $\mathbb{C}_{/\{0\}}$ (the field \mathbb{C} exclude 0). This amounts to mapping numbers picked up during calculation as

$$\mathbb{C}_{/\{0\}} \rightarrow 1.$$

(See also Definition 38).

Then we arrive at the sequence



Proposition 3. One can find t over the reals such that

$$\text{CN} \sim (\mathbf{1} \otimes H) \cdot (e^{-itP_1 \otimes Z}) \cdot (\mathbf{1} \otimes H^\dagger).$$

Theorem 5 (CNs plus local rotations is universal). CN, together with local unitary rotations is a universal gate set for quantum computation [6].

Remark 20. § 5 makes use of a result by Shi which established the following. A gate comprising the controlled not (a.k.a. Feynman gate) plus any one-qubit gate whose square does not preserve the computational basis is universal for quantum computation [43].

Remark 21. § 6.1 makes use of a result by Bernstein and Vazirani which showed that arbitrary quantum circuits may be simulated using real-valued gates operating on real-valued wave functions [44].

	quantum mechanics	stochastic mechanics
state	vector $\psi \in \mathbb{C}^n$ with $\sum_i \psi_i ^2 = 1$	vector $\psi \in \mathbb{R}^n$ with $\sum_i \psi_i = 1$ and $\psi_i \geq 0$
observable	$n \times n$ matrix \mathcal{O} with $\mathcal{O}^\dagger = \mathcal{O}$ where $(\mathcal{O}^\dagger)_{ij} \stackrel{\text{def}}{=} \overline{\mathcal{O}_{ji}}$	vector $\mathcal{O} \in \mathbb{R}^n$
expected value	$\langle \psi, \mathcal{O}\psi \rangle \stackrel{\text{def}}{=} \sum_{i,j} \overline{\psi_i} \mathcal{O}_{ij} \psi_j$	$\langle \mathcal{O}\psi \rangle \stackrel{\text{def}}{=} \sum_i \mathcal{O}_i \psi_i$
symmetry (linear map sending states to states)	unitary $n \times n$ matrix: $UU^\dagger = U^\dagger U = 1$	stochastic $n \times n$ matrix: $\sum_i U_{ij} = 1, \quad U_{ij} \geq 0$
symmetry generator	self-adjoint $n \times n$ matrix: $\mathcal{H} = \mathcal{H}^\dagger$	infinitesimal stochastic $n \times n$ matrix: $\sum_i \mathcal{H}_{ij} = 0, \quad i \neq j$ $\Rightarrow \mathcal{H}_{ij} \leq 0$
symmetries from symmetry generators	$U(t) = \exp(-it\mathcal{H})$	$U(t) = \exp(-t\mathcal{H})$
equation of motion	$i\frac{d}{dt}\psi(t) = \mathcal{H}\psi(t)$ with solution $\psi(t) = \exp(-it\mathcal{H})\psi(0)$	$\frac{d}{dt}\psi(t) = -\mathcal{H}\psi(t)$ with solution $\psi(t) = \exp(-t\mathcal{H})\psi(0)$

Table 4 — Summary of quantum versus stochastic mechanics reproduced from [38].

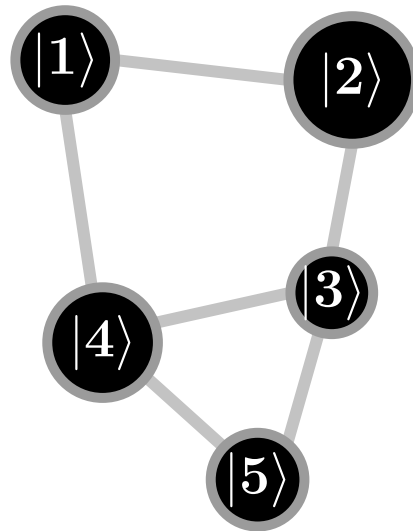


Figure 2.3 — Example of a simple graph, used herein to compare quantum versus stochastic walks.

2.2 Walks on Graphs: quantum vs stochastic

We previously considered as an extended example, showing how a simple graph G can be used to define both stochastic and quantum walks. We will extend our previous example then move towards a more general theory. This segment follows partially a blog post on Azimuth by Tomi Johnson and edited by several of us.¹ The focus of the article was joint work appearing in [39].

As per Definition 16, an example of a simple graph appears in Figure 2.3. To avoid complications, let's stick to simple graphs with a finite number n of nodes. Let's also assume you can get from every node to every other node via some combination of edges i.e. the graph is connected. So finally we note that for the graph in Figure 2.3, there is at most one edge between any two nodes, there are no edges from a node to itself and all edges are undirected.

In this particular example, the graph represents a network of $n = 5$ nodes, where nodes 3 and 4 have degree (number of edges) 3, and nodes 1, 2 and 5 have degree 2.

Definition 23. The *degree of a node* in a network (a.k.a. graph) is the number of connections this node has to other nodes while the *degree distribution* is the prob-

¹Quantum Network Theory (Part 1), Azimuth <https://johncarlosbaez.wordpress.com/2013/08/05/quantum-network-theory-part-1/>.

ability distribution of these degrees over the entire network. Standard concepts in network theory appear in the book [45].

As mentioned in Definition 18, every simple graph defines a matrix A , called the *adjacency matrix*. For a network with n nodes, this matrix is of size $n \times n$, and each element A_{ij} is unity if there is an edge between nodes i and j , and zero otherwise.

Remark 22. We will fix and use the basis defined in accordance with Figure 2.3 throughout this section.

Using the natural ordering per Figure 2.3, the adjacency matrix is

$$\begin{pmatrix} 0 & 1 & 0 & 1 & 0 \\ 1 & 0 & 1 & 0 & 0 \\ 0 & 1 & 0 & 1 & 1 \\ 1 & 0 & 1 & 0 & 1 \\ 0 & 0 & 1 & 1 & 0 \end{pmatrix}$$

By this construction, every adjacency matrix is symmetric (iff $A = A^\top$) and further, because each A is real, it is self-adjoint (iff $A = A^\dagger$). This is an attractive feature as a self-adjoint matrix generates a continuous-time **quantum walk**. Informally, a quantum walk is an evolution arising from a quantum walker moving on a network.

The state of a quantum walk is represented by a size n complex column vector ψ (written equivalently $|\psi\rangle$). Each element $\langle i|\psi\rangle$, is the so-called amplitude associated with node i and the probability of the walker being found on that node (if measured) is the modulus of the amplitude squared $|\langle i|\psi\rangle|^2$. Here i is the standard basis vector with a single non-zero i -th entry equal to unity, and $\langle u, v\rangle = u^\dagger v$ remains the usual inner vector product.

A quantum walk evolves in time according to the Schrödinger's equation (2.60) under some Hamiltonian, \mathcal{H} . If the initial state is $\psi(0)$ then the solution to the T.I.S.E. is again written as

$$\psi(t) = \exp(-it\mathcal{H})\psi(0).$$

Remark 23. Recall that the probabilities $\{|\langle i|\psi(t)\rangle|^2\}_i$ are guaranteed to be correctly normalized when the Hamiltonian \mathcal{H} is self-adjoint.

There are several common matrices defined by graphs. Perhaps the most familiar is the graph Laplacian. The Laplacian \mathcal{L} is the $n \times n$ matrix $\mathcal{L} = D - A$, where the degree matrix D is an $n \times n$ diagonal matrix with elements given by the degrees

$$D_{ii} = \sum_j A_{ij}$$

For the graph drawn in Figure 2.3, the degree matrix and Laplacian are:

$$\begin{pmatrix} 2 & 0 & 0 & 0 & 0 \\ 0 & 2 & 0 & 0 & 0 \\ 0 & 0 & 3 & 0 & 0 \\ 0 & 0 & 0 & 3 & 0 \\ 0 & 0 & 0 & 0 & 2 \end{pmatrix} \quad \text{and} \quad \begin{pmatrix} 2 & -1 & 0 & -1 & 0 \\ -1 & 2 & -1 & 0 & 0 \\ 0 & -1 & 3 & -1 & -1 \\ -1 & 0 & -1 & 3 & -1 \\ 0 & 0 & -1 & -1 & 2 \end{pmatrix}$$

The Laplacian is self-adjoint and generates a quantum walk. Recall from § 2.1.3 this matrix also has another property; it is infinitesimal stochastic. Recall that this means that its off diagonal elements are non-positive and its columns sum to zero. This is interesting because an infinitesimal stochastic matrix generates a continuous-time stochastic walk. Such walks have been studied extensively in the literature, including work by myself and others, partially reviewed in [41] and appearing as research in [39; 46] as well as [47; 48] which considered time-symmetry breaking in quantum walks.

Recall that a stochastic walk is an evolution arising from a stochastic walker moving on a network. A state of a stochastic walk is represented by a size n non-negative column vector ψ . Each element $\langle i|\psi\rangle$ of this vector is the probability of the walker being found on node i . A stochastic walk evolves in time according to the master equation

$$\frac{d}{dt}\psi(t) = -\mathcal{L}\psi(t). \quad (2.34)$$

where H is called the stochastic Hamiltonian. If the initial state is $\psi(0)$ then the solution is written as

$$\psi(t) = \exp(-t\mathcal{L})\psi(0).$$

The probabilities $\{\langle i|\psi(t)\rangle\}_i$ are guaranteed to be non-negative and correctly normalized when the stochastic Hamiltonian \mathcal{L} is infinitesimal stochastic.

2.2.1 Normalized Laplacians

To analyze the important uniform escape model we need to go beyond the class of generators that produce both quantum and stochastic walks. Further, we have to determine a related quantum walk. We'll see below that both tasks are achieved by considering the normalized Laplacians: one generating the uniform escape stochastic walk and the other a related quantum walk.

The two normalized Laplacians (studied in e.g. [39] as well as many other places) are as follows.

Definition 24 (Asymmetric Normalized Laplacian). The asymmetric normalized Laplacian is given as

$$S = \mathcal{L}D^{-1}$$

which generates the uniform escape stochastic walk by S .

Definition 25 (Symmetric Normalized Laplacian). The symmetric normalized Laplacian is given as

$$Q = D^{-1/2}\mathcal{L}D^{-1/2}$$

which generates a unitary quantum walk Q . Proposition 4 and 5 will illuminate exactly why this choice was made: so as to exploit a relationship between eigenvectors between asymmetric and symmetric normalized Laplacians.

For the graph drawn in Figure 2.3, the asymmetric normalized Laplacian S is given as (2.35).

$$\begin{pmatrix} 1 & -1/2 & 0 & -1/3 & 0 \\ -1/2 & 1 & -1/3 & 0 & 0 \\ 0 & -1/2 & 1 & -1/3 & -1/2 \\ -1/2 & 0 & -1/3 & 1 & -1/2 \\ 0 & 0 & -1/3 & -1/3 & 1 \end{pmatrix} \quad (2.35)$$

Remark 24. The identical diagonal elements indicate that the total rates of leaving each node are identical, and the equality within each column of the other non-zero elements indicates that the walker is equally likely to hop to any node connected to its current node. This is, after all, how the uniform escape model takes its name.

For the same graph drawn in Figure 2.3, the symmetric normalized Laplacian Q is given as (2.36).

$$\begin{pmatrix} 1 & -1/2 & 0 & -1/\sqrt{6} & 0 \\ -1/2 & 1 & -1/\sqrt{6} & 0 & 0 \\ 0 & -1/\sqrt{6} & 1 & -1/3 & -1/\sqrt{6} \\ -1/\sqrt{6} & 0 & -1/3 & 1 & -1/\sqrt{6} \\ 0 & 0 & -1/\sqrt{6} & -1/\sqrt{6} & 1 \end{pmatrix} \quad (2.36)$$

The diagonal elements being identical in the quantum case indicates that all the nodes are of equal energy. Walks not obeying this are said to exhibit *disorder*.

Returning to the graph from Figure 2.3, we have consequently defined two matrices: one S that generates a stochastic walk, and one Q that generates a quantum walk. The natural question to ask is whether these walks are related. This question was studied extensively in [39]. Before considering aspects of this relationship, consider the following definition.

Definition 26 (Similar Matrices). Two $n \times n$ matrices (A and B) are called *similar* if there exists an invertible $n \times n$ matrix P such that

$$B = P^{-1}AP. \quad (2.37)$$

Underpinning a relationship between the quantum and stochastic generators is the property that:

Proposition 4 (Spectral Similarity of Generators). S and Q are similar by the transformation (2.38).

$$S = D^{1/2}QD^{-1/2} \quad (2.38)$$

From Proposition 4 we deduce the following.

Proposition 5. Consider,

$$\begin{aligned} Q|\phi_k\rangle &= \varepsilon_k|\phi_k\rangle, \\ (D^{1/2}QD^{-1/2})(D^{1/2}|\phi_k\rangle) &= \varepsilon_k(D^{1/2}|\phi_k\rangle), \\ S|\pi_k\rangle &= \varepsilon_k|\pi_k\rangle. \end{aligned} \tag{2.39}$$

Hence, any eigenvector $|\phi_k\rangle$ of Q associated to eigenvalue ε_k implies that $|\pi_k\rangle \propto D^{1/2}|\phi_k\rangle$ is an eigenvector of S associated to the same eigenvalue.

One also establishes the converse. Any eigenvector $|\pi_k\rangle$ of S implies an eigenvector $|\phi_k\rangle \propto D^{-1/2}|\pi_k\rangle$ of Q associated to the same eigenvalue ε_k . And because Q is self-adjoint, the symmetric normalized Laplacian can be decomposed as

$$Q = \sum_k \varepsilon_k \Phi_k,$$

where ε_k is real and $\Phi_k = |\phi_k\rangle\langle\phi_k|$ are orthogonal. Multiplying from the left by $D^{1/2}$ and the right by $D^{-1/2}$ results in a similar decomposition for S

$$S = \sum_k \varepsilon_k \Pi_k,$$

with orthogonal projectors $\Pi_k = D^{1/2}\Phi_k D^{-1/2}$.

We now have all the ingredients necessary to study the walks generated by the normalized Laplacians and the relationship between them.

Definition 27 (Summary see Figure 2.4). G is a simple graph that specifies:

1. A the adjacency matrix (generator of a quantum walk).
2. D the diagonal matrix of the degrees.
3. \mathcal{L} the symmetric Laplacian (generator of stochastic and quantum walks), which when normalized by D returns both:
 - 3.1 S the generator of the uniform escape stochastic walk and
 - 3.2 Q the quantum walk generator to which \mathcal{L} is similar.

2.2.2 Stochastic walk

The uniform escape stochastic walk generated by S has a practically useful stationary state. A stationary state of a stochastic walk is stationary (invariant) with respect to changes in parameter playing the role of time. From the master equation $\frac{d}{dt} |\psi(t)\rangle = -S |\psi(t)\rangle$ the stationary state must be an eigenvector $|\pi_0^i\rangle$ of S with eigenvalue $\varepsilon_0 = 0$. A pair of theorems hold:

Theorem 6 (Uniqueness of the Stationary State). There always exists a unique (up to multiplication by a positive number) positive eigenvector $|\pi_0\rangle$ (abbreviated as $|\pi\rangle$) of S with eigenvalue $\varepsilon_0 = 0$, i.e., a unique stationary state $|\pi\rangle$.

Theorem 7. Irregardless of the initial state $|\psi(0)\rangle$, the stationary state $|\pi\rangle$ is obtained in the long-time limit: $\lim_{t \rightarrow \infty} |\psi(t)\rangle = |\pi\rangle$.

Definition 28 (All 1's Vector). Let boldface $|+\rangle = \sum |i\rangle$ denote the unnormalized all ones vector, where non-boldface $\sqrt{2}|+\rangle = |0\rangle + |1\rangle$ is the familiar eigenstate of the X operator.

To determine this unique stationary state (Theorem 6), consider the Laplacian \mathcal{L} , which is both infinitesimal stochastic and symmetric. Among other things, this means the rows of \mathcal{L} sum to zero

$$\sum_j \mathcal{L}_{ij} = 0$$

which means the all ones vector $|+\rangle$ is an eigenvector of \mathcal{L} with zero eigenvalue

$$\mathcal{L}|+\rangle = 0$$

Inserting the identity $\mathbb{1} = D^{-1}D$ into this equation we recover that $D|+\rangle$ is a zero eigenvector of S

$$\mathcal{L}|+\rangle = (\mathcal{L}D^{-1})(D|+\rangle) = S(D|+\rangle) = 0$$

Therefore one must normalize $|+\rangle$ to recover the long-time stationary state of the walk, viz.,

$$|\pi\rangle = \frac{D}{\sum_i D_{ii}} |+\rangle.$$

Proposition 6 (Long-Time Probability). For each element $\langle i|\pi\rangle$ of this state, the long-time probability of finding a walker at node i , is proportional to the degree D_{ii} of node i .

Remark 25. We can validate Proposition 6 for the graph from Figure 2.3, where $|\pi\rangle$ is as follows.

$$\begin{pmatrix} 1/6 \\ 1/6 \\ 1/4 \\ 1/4 \\ 1/6 \end{pmatrix}$$

This hence implies that the long-time probability $1/6$ for nodes 1, 2 and 5, and $1/4$ for nodes 3 and 4.

2.2.3 Quantum walk

Let us now consider the quantum walk generated by Q . Little remains known about quantum walks on networks of arbitrary geometry. We recover below the analytical results [39] obtained by exploiting the similarity of S and Q .

In contrast to stochastic walks, for a quantum walk every eigenvector $|\phi_i^k\rangle$ of Q is a stationary state of the quantum walk. The stationary state $|\phi_0\rangle$ is of particular interest, both physically and mathematically. Physically, since eigenvectors of the Q correspond to states of well-defined energy equal to the associated eigenvalue, $|\phi_0\rangle$ is the state of lowest energy $\varepsilon_0 = 0$, hence the name ground state.

Mathematically, the relationship between eigenvectors implied by the similarity of S and Q means

$$|\phi_0\rangle \propto D^{-1/2} |\pi\rangle \propto D^{1/2} |+\rangle. \quad (2.40)$$

Therefore, for a system in its ground state, the probability of being measured to be at node i is given by

$$|\langle i|\phi_0\rangle|^2 \propto |\langle i|D^{1/2}\rangle|^2 = D_{ii}. \quad (2.41)$$

The probability (2.41) shows a proportionality with a nodes degree and is therefore exactly the same as $\langle i|\pi\rangle$, the probability in the stationary state $|\pi\rangle$ of the stochastic walk (Proposition 6). A zero energy quantum walk Q leads to exactly the same distribution of the walker over the nodes as in the long-time limit of the uniform escape stochastic walk S [39].

Hence, the work [39] determined that the standard notion of degree distribution plays a role in quantum walks. But what if the walker starts in some other initial state? We therefore must ask if there is some quantum walk analogue of the unique long-time state of a stochastic walk?

In fact, the quantum walk in general does not converge to a stationary state. But there is a probability distribution that can be thought to characterize the quantum walk in the same way as the long-time state characterizes the stochastic walk. It's the long-time average probability vector P .

Provided a complete lack of knowledge as to the time that had passed since the beginning of a quantum walk, the best estimate for the probability of measuring the walker to be at node i would be the long-time average probability (2.42).

$$\langle i|P\rangle = \lim_{T \rightarrow \infty} \frac{1}{T} \int_0^T |\psi_i(t)|^2 dt \quad (2.42)$$

Equation 2.42 will be simplified. We begin by inserting the decomposition $Q = \sum_k \varepsilon_k \Phi_k$ into $|\psi(t)\rangle = e^{-iQt} |\psi(0)\rangle$ to get $|\psi(t)\rangle = \sum_k e^{-i\varepsilon_k t} \Phi_k |\psi(0)\rangle$ and thus,

$$\langle i|P\rangle = \lim_{T \rightarrow \infty} \frac{1}{T} \int_0^T \left| \sum_k e^{-i\varepsilon_k t} \langle i|\Phi_k \psi(0)\rangle \right|^2 dt.$$

Due to the integral over all time the interferences between terms corresponding to different eigenvalues average to zero, leaving

$$\langle i|P\rangle = \sum_k |\langle i|\Phi_k \psi(0)\rangle|^2. \quad (2.43)$$

The long-time average probability (2.43) is then the sum of terms contributed by the projections of the initial state onto each eigenspace.

Hence we arrive at a distribution (2.43) that characterizes a quantum walk for a general initial state. Our approach of better understanding the long-time average probability is through the term $|\langle i|\Phi_0\psi(0)\rangle|^2$ associated with the zero energy eigenspace, since we have subsequently characterized this space.

For example, we know the zero energy eigenspace is one-dimensional and spanned by the eigenvector ϕ_0 . This means that the projector is just the usual outer product

$$\Phi_0 = |\phi_0\rangle\langle\phi_0|, \quad (2.44)$$

where we have normalized $|\phi_0\rangle$ according to the inner product $\langle\phi_0|\phi_0\rangle = 1$. The zero eigenspace contribution to the long-time average probability then breaks into the product of two probabilities, as

$$\begin{aligned} |\langle i|\Phi_0\psi(0)\rangle|^2 &= |\langle i|\phi_0\rangle\langle\phi_0|\psi(0)\rangle|^2 = |\langle i|\phi_0\rangle|^2|\langle\phi_0|\psi(0)\rangle|^2 = \\ &= \langle i|\pi\rangle|\langle\phi_0|\psi(0)\rangle|^2. \end{aligned} \quad (2.45)$$

The first probability $\langle i|\pi\rangle$ in the product (2.45) corresponds to finding a quantum state in the zero energy eigenspace at node i (as we found above). The second probability $|\langle\phi_0|\psi(0)\rangle|^2$ from (2.45) relates to being in this eigenspace to begin with (which for the one dimensional zero energy eigenspace means just the inner product with the ground state).

This turns out to be enough to say something interesting about the long-time average probability for all states. Sketching the results from [39], we have illustrated how we can break the long-time probability vector P into a sum of two normalized probability vectors

$$P = (1 - \eta) |\pi\rangle + \eta |\Omega\rangle, \quad (2.46)$$

the first $|\pi\rangle$ is the degree dependent stochastic stationary state associated with the zero energy eigenspace and the second is associated with the higher energy eigenspaces $|\Omega\rangle$, with

$$\langle i|\Omega\rangle = \frac{\sum_{k \neq 0} |\langle i|\Phi_k\psi(0)\rangle|^2}{\eta}. \quad (2.47)$$

The weight of each term in (2.46) is governed by the parameter

$$\eta = 1 - |\langle \phi_0 | \psi(0) \rangle|^2.$$

One could consider (2.46) as unity minus the probability of the walker being in the zero energy eigenspace, or equivalently the probability of the walker being outside the zero energy eigenspace. So even though we don't know anything about $|\Omega\rangle$ we know its importance is controlled by a parameter η that governs how close the long-time average distribution P of the quantum walk is to the corresponding stochastic stationary distribution $|\pi\rangle$. Can we say anything physical about when η is big or small?

As the eigenvalues of Q have a physical interpretation in terms of energy, the answer is yes. The quantity η is the probability of being outside the zero energy state. Call the next lowest eigenvalue $\Delta = \min_{k \neq 0} \varepsilon_k$ the energy gap. If the quantum walk is not in the zero energy eigenspace then it must be in an eigenspace of energy greater or equal to Δ . Therefore the expected energy E of the quantum walker must bound η , $E \geq \eta\Delta$. A quantum walk as such with low energy is hence similar to a stochastic walk in the long-time limit (we already knew this exactly in the zero energy limit).

2.2.4 Perron's theorem

As we have seen in our previous extended example, stochastic systems evolve to their low eigenvalue eigenstates. As we have cared to contrast quantum versus stochastic evolution by comparison of dynamics subject to the same generator, it is worth mentioning the following. So called stoquastic Hamiltonian's are often considered in complexity theory as examples having elements of quantum mechanics and classical theory of stochastic matrices [49–52]. Indeed, stoquastic Hamiltonians, those for which all off-diagonal matrix elements in the standard basis are real and non-positive (see Definition 29, commonly describe physical systems.

Remark 26. This subsegment follows partially a blog post on Azimuth written by the author and edited by John Baez.² The focus of the post resulted in the book [38] and influenced other studies including [39].

Definition 29 (Stoquastic Hamiltonian). Hamiltonians where all the off-diagonal elements in the standard basis are real and non-positive (or alternatively, exclusively non-negative) are called *stoquastic*.

More formally:

Definition 30 (Stoquastic Hamiltonian). Hamiltonian,

$$\mathcal{H} = \sum_i \mathcal{H}_i \quad (2.48)$$

is stoquastic if in some local basis \mathcal{B} the terms \mathcal{H}_i all have matrix entries that are zero or negative,

$$\langle \psi | \mathcal{H} | \phi \rangle \leq 0 \quad \forall \psi, \phi \in \mathcal{B} \mid \psi = \phi. \quad (2.49)$$

Here we will establish some of the core elements to recover several known results about stoquastic Hamiltonians and the comparison of quantum versus stochastic walks on graphs, generated by stoquastic Hamiltonians. To begin with, we note that a simple graph can consist of many separate graphs, called components.

Definition 31 (Connected Simple Graph). A simple graph is connected if it is nonempty and there is a path of edges connecting any vertex to any other.

In quantum mechanics it's good to think about observables that have positive expected values:

$$\langle \psi | \mathcal{O} | \psi \rangle > 0 \quad (2.50)$$

for every quantum state $\psi \in \mathbb{C}^n$. These are called *positive definite*. But in stochastic mechanics it's good to think about matrices that are positive in a more naive sense:

²Network Theory (Part 20), Azimuth <https://johncarlosbaez.wordpress.com/2012/08/06/network-theory-part-20/>.

Definition 32. An $n \times n$ real matrix T is positive if all its entries are positive:

$$T_{ij} > 0 \tag{2.51}$$

for all $1 \leq i, j \leq n$.

Definition 33. A vector $\psi \in \mathbb{R}^n$ is positive if all its components are positive:

$$\psi_i > 0 \tag{2.52}$$

for all $1 \leq i \leq n$.

Remark 27 (Nonnegative). One will also define nonnegative matrices and vectors in the same way, replacing > 0 by ≥ 0 . A good example of a nonnegative vector is a stochastic state.

In 1907, Perron proved the following fundamental result about positive matrices.

Theorem 8 (Perron's Theorem). Given a positive square matrix T , there is a positive real number r , called the Perron–Frobenius eigenvalue of T , such that r is an eigenvalue of T and any other eigenvalue λ of T has $|\lambda| < r$. Moreover, there is a positive vector $\psi \in \mathbb{R}^n$ with $T\psi = r\psi$. Any other vector with this property is a scalar multiple of ψ . Furthermore, any nonnegative vector that is an eigenvector of T must be a scalar multiple of ψ .

Remark 28. Hence, if T is positive, it has a unique eigenvalue with the largest absolute value. This eigenvalue is positive. Up to a constant factor, it has a unique eigenvector. We can choose this eigenvector to be positive. And then, up to a constant factor, it's the only nonnegative eigenvector of T .

Definition 34 (Strongly Connected Graph). A directed graph is *strongly connected* if there is a directed path of edges going from any vertex to any other vertex.

Definition 35 (Irreducible Matrix). A nonnegative square matrix T is irreducible if its graph G_T is strongly connected.

Theorem 9 (Perron–Frobenius Theorem). Given an irreducible nonnegative square matrix T , there is a positive real number r , called the *Perron–Frobenius eigenvalue* of T , such that r is an eigenvalue of T and any other eigenvalue λ of T has $|\lambda| \leq r$. Moreover, there is a positive vector $\psi \in \mathbb{R}^n$ with $T\psi = r\psi$. Any other vector with this property is a scalar multiple of ψ . Furthermore, any nonnegative vector that is an eigenvector of T must be a scalar multiple of ψ .

Example 23. The only conclusion of Theorem 9 that is weaker than Theorem 8 is that there may be other eigenvalues with $|\lambda| = r$. For example, the Pauli- X matrix is irreducible and nonnegative. Its Perron–Frobenius eigenvalue is 1, but it also has -1 as an eigenvalue. In general, Perron–Frobenius theory says quite a lot about the other eigenvalues on the circle $|\lambda| = r$.

Definition 36 (Dirichlet Operator). \mathcal{L} is a *Dirichlet operator* if it's both self-adjoint and infinitesimal stochastic

With these theorems (9 and 8), we arrive at several consequences.

Proposition 7. Let \mathcal{L} be an irreducible Dirichlet operator with n eigenstates. In stochastic mechanics, there is only one valid state that is an eigenvector of \mathcal{L} : the unique so-called *Perron–Frobenius state*. The other $n - 1$ eigenvectors are forbidden states of a stochastic system: the stochastic system is either in the Perron–Frobenius state, or in a superposition of at least two eigenvectors. In quantum mechanics, all n eigenstates of \mathcal{L} are valid states.

Irreducible Dirichlet operators

To establish Proposition 7, we note first that, the matrix H is rarely non-negative: its off-diagonal entries will always be nonnegative while its diagonal entries can be negative. This can be fixed by a simple *energy shift* as,

$$T = H + c\mathbb{1} \tag{2.53}$$

where $c > 0$ is chosen from H .

Remark 29. This matrix T from (2.53) has

1. the same eigenvectors as H ,
2. off-diagonal matrix entries which are the same as those of H , so T_{ij} is nonzero for $i \neq j$ exactly when the graph we started with has an edge from i to j .

So, for $i \neq j$, the graph G_T will have a directed edge going from i to j precisely when our original graph had an edge from i to j . And that means that if our original graph was connected, G_T will be strongly connected. Thus, by definition, T is irreducible.

Since T is nonnegative and irreducible, the Perron–Frobenius theorem implies the following.

Proposition 8. Suppose H is the Dirichlet operator coming from a connected finite simple graph with edges labelled by positive numbers. Then the eigenvalues of H are real. Let λ be the largest eigenvalue. Then there is a positive vector $\psi \in \mathbb{R}^n$ with $H\psi = \lambda\psi$. Any other vector with this property is a scalar multiple of ψ . Furthermore, any nonnegative vector that is an eigenvector of H must be a scalar multiple of ψ .

Proof. The eigenvalues of H are real since H is self-adjoint. Notice that if r is the Perron–Frobenius eigenvalue of $T = H + c\mathbb{1}$ and

$$T\psi = r\psi \tag{2.54}$$

then

$$H\psi = (r - c)\psi \tag{2.55}$$

By the Perron–Frobenius theorem the number r is positive, and it has the largest absolute value of any eigenvalue of T . Thanks to the subtraction, the eigenvalue $r - c$ may not have the largest absolute value of any eigenvalue of H . It is, however, the largest eigenvalue of H , so we take this as our λ . The rest follows from the Perron–Frobenius theorem. \square

Definition 37. A Dirichlet operator is irreducible if it comes from a connected finite simple graph with edges labelled by positive numbers.

Proof of the following is left to the reader.

Theorem 10. Suppose H is an irreducible Dirichlet operator. Then H has zero as its largest real eigenvalue. There is a positive vector $\psi \in \mathbb{R}^n$ with $H\psi = 0$. Any other vector with this property is a scalar multiple of ψ . Furthermore, any nonnegative vector that is an eigenvector of H must be a scalar multiple of ψ .

2.3 Google page rank—a ground eigenvector problem

Evidently nodes in a complex network have different roles and their influence on system dynamics varies widely depending on their topological characteristics. (this is particularly relevant in walks that break time reversal symmetry, as introduced in [47] and experimentally probed in [48] and characterized in [53]).

One of the simpler (and widely applied) characteristics in network analysis [54] is the degree centrality, defined as the number of edges incident on that node. Many real world networks have been found to follow a widely heterogeneous distribution of degree values [54].

Despite the complexity of the linking pattern, the degree distribution of a network directly (and in some regimes dominantly) affects the associated dynamics. In fact, it can be shown that the probability of finding a memoryless random walker at a given node of a symmetric network in the stationary low-energy state, is just proportional to the degree of such a node [55].

We will now summarize our findings to explain Figure 2.4.

In [39] together with coauthors, we consider the relationship between the stochastic and the quantum version of such processes, with the ultimate goal of shedding light on the meaning of degree centrality in the case of quantum networks.

We considered a stochastic evolution governed by the Laplacian matrix $\mathcal{L}_S = \mathcal{L}D^{-1}$, the stochastic generator that characterizes classical random walk dynamics and leads to an occupation probability proportional to node degree.

In the quantum version, a Hermitian generator is required and we proposed the symmetric Laplacian matrix $\mathcal{L}_Q = D^{-\frac{1}{2}}\mathcal{L}D^{-\frac{1}{2}}$, generating a valid quantum walk that, however, does not lead to a stationary state, making difficult a direct comparison between classical and quantum versions of the dynamics. A common and useful workaround to this issue was to average the occupation probability over time, as in (2.43).

The generators of the two dynamics are spectral similar (see Figure 2.4) and hence share the same eigenvalues, while the eigenvectors are related by the transformation $|\phi_i^C\rangle = D^{-\frac{1}{2}}|\phi_i^Q\rangle$. As a consequence, if the system is in the ground state the average probability to find the walker on a node will be the same as in

the classic case, which will depend solely on the degree of each node. For the cases in which the system is not in the ground state, it is possible to define a quantity

$$\varepsilon = 1 - \left\langle \phi_0^Q \left| \rho_0 \right| \phi_0^Q \right\rangle,$$

describing how far from the classical case the probability distribution of the quantum walker will be. In the case of uniformly distributed initial state ρ_0 , this provides a measure for the heterogeneity of the degree distribution of a quantum network [39].

Remark 30 (Directed Networks). Many networks of practical significance are not symmetric, but directed. How can these networks be encoded into quantum systems when considering the constraint that Hamiltonians must be Hermitian? (One approach is to consider directing transport by breaking time-reversal symmetry [47]).

The non-symmetric adjacency matrix representing the directed connectivity of the World Wide Web, a.k.a. the Google matrix G , satisfies the Perron-Frobenius theorem [38] and hence there is a maximal eigenvalue corresponding to an eigenvector of positive entries $G|p\rangle = |p\rangle$. The eigenvector $|p\rangle$ corresponds to the limiting distribution of occupation probabilities of a random web surfer—it represents a unique attractor for the dynamics independently of the initial state. The vector $|p\rangle$ is known as the Page-Rank. A dumping factor is often included in the computation to assure the Perron-Frobenius theorem is satisfied.

Several recent studies embed G into a quantum system and consider quantum versions of Google’s Page-Rank [56–58]. The work [59] relied on an adiabatic quantum algorithm to compute the Page-Rank of a given directed network, whereas Burillo et al. [60] rely on a mixture of unitary and dissipative evolution to define a ranking that converges faster than classical PageRank.

The page-ranking vector $|p\rangle$ is an eigenvector of $\mathbb{1} - G$ corresponding to the zero eigenvalue (the lowest). This fact leads to a definition of a Hermitian operator which can play the role of a Hamiltonian, defined as:

$$\mathcal{H} = (\mathbb{1} - G)^\dagger (\mathbb{1} - G), \tag{2.56}$$

though non-local (if G is k -local then h is k^2 -local), its ground state represents the target Page-Rank which could be found by adiabatic quantum annealing into the ground state. Using a quantum computer to accelerate the calculation of various network properties has been considered widely, see e.g. the survey [41].

2.4 Kitaev's quantum phase estimation algorithm

Quantum algorithms have a long and rich history, with many seminal developments. Early milestones include the Deutsch-Jozsa algorithm [61], the Bernstein–Vazirani algorithm [62], Simon's algorithm [63] as well as others [64].

The *quantum phase estimation algorithm* (a.k.a. *quantum eigenvalue estimation algorithm*), estimates the eigenvalue of an eigenvector of a unitary operator. Loosely speaking, given a U and a quantum state $|\psi\rangle$ such that $U|\psi\rangle = e^{i\lambda}|\psi\rangle$, the algorithm estimates λ with high probability within additive error ε , using $\mathcal{O}(1/\varepsilon)$ controlled- U gates. Phase estimation is a central component (subroutine) to many other quantum algorithms, such as Shor's algorithm [6]. This algorithm has appeared in my own research, including [11; 65–67].

Let

$$\mathcal{H} \in \mathcal{L}(\mathbb{C}_2^{\otimes d}) \quad \Phi \in \mathbb{C}_2^{\otimes d} \quad (2.57)$$

with

$$\mathcal{H} = \mathcal{H}^\dagger \quad \mathcal{H}\varphi_i = \lambda_i\varphi_i \quad (2.58)$$

so \mathcal{H} is a finite dimensional Hamiltonian, then

$$\Phi = \sum_i e^{-i\lambda_i} \langle \varphi_i | \phi \rangle |\varphi_i\rangle \quad (2.59)$$

is a solution to Schrödinger's equation

$$i\frac{d}{dt}\Phi = \mathcal{H}\Phi. \quad (2.60)$$

In general, eigenvectors evolve under the T.I.S.E. as

$$\varphi_i(t) = e^{-it\lambda_i}\varphi_i(0). \quad (2.61)$$

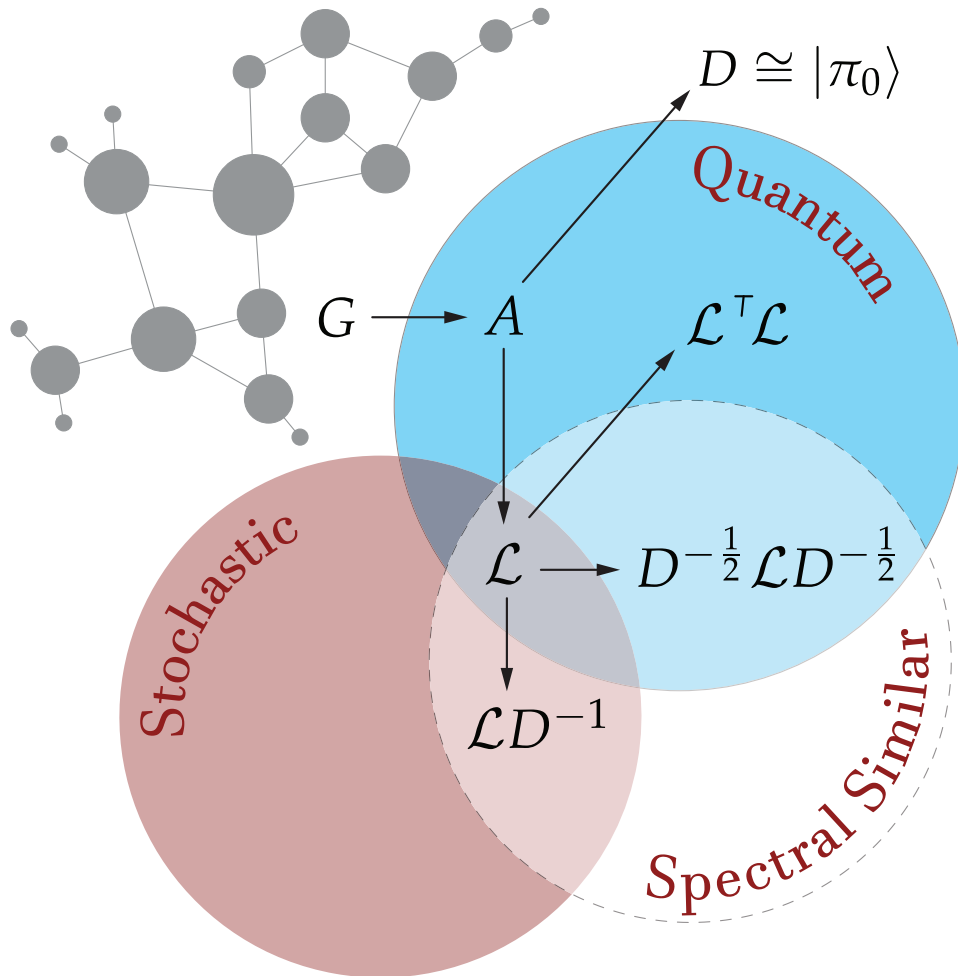


Figure 2.4 — Known mappings between quantum and stochastic generators. Here $G = (V, E)$ is a graph with adjacency matrix A , D is a diagonal matrix of node degrees. This yields the graph Laplacian $\mathcal{L} = D - A$, and hence, the stochastic walk generator $\mathcal{L}_S = \mathcal{L}D^{-1}$, from this a similarity transform results in $\mathcal{L}_Q = D^{-\frac{1}{2}} \mathcal{L} D^{-\frac{1}{2}}$, which generates a valid quantum walk and exhibits several interesting connections to the classical case. The mapping $\mathcal{L} \rightarrow \mathcal{L}^\top \mathcal{L}$ preserves the lowest 0 energy ground state, opening the door for adiabatic quantum annealing which solves computational problems by evolving a system into its ground state. (Figure from [41] which was modified from [39]).

Definition 38. (The global phase) We say a global phase is not detectable as $|\langle \phi | \varphi \rangle|^2$ is invariant under $\varphi \mapsto e^{-i\alpha} \varphi$, $\psi \mapsto e^{-i\alpha} \psi \forall \alpha, \beta \in \mathbb{R}$. Some authors will write for $\varphi \in \mathbb{C}_2^{\otimes d}$ and for $c \in \mathbb{C}/\{0\}$, $c\varphi \sim \varphi$ (spoken, “is reducible to” or hence “equivalent”) and call this a *ray in Hilbert space*. Mathematically this is a pairing $\mathbb{C}/\{0\} \times \mathbb{C}_2^{\otimes d}$ which induces an equivalence $\mathbb{C}/\{0\} \times \mathbb{C}_2^{\otimes d} \sim \mathbb{C}_2^{\otimes d}$ as

$$\frac{|\langle c\phi | d\varphi \rangle|^2}{\langle c\phi | c\phi \rangle \langle d\varphi | d\varphi \rangle} = \frac{\langle c\phi | d\varphi \rangle \langle d\varphi | c\phi \rangle}{\langle c\phi | c\phi \rangle \langle d\varphi | d\varphi \rangle} = |\langle \phi | \varphi \rangle|^2 \quad (2.62)$$

for unit vectors φ and ϕ where $\langle c\phi | c\phi \rangle = \bar{c}c$. Here we work in the unit normalized gauge, fixing probability such that $\langle \varphi | \varphi \rangle = 1$ which is indeed invariant under $\varphi \mapsto e^{-i\alpha} \varphi$. We will write $e^{-i\alpha} \varphi \sim \varphi$. (See also Definition 22).

Proposition 9. Equation (2.59) satisfies (2.60).

We indeed can't measure a global phase, but we can measure a relative one. Consider the Hamiltonian (2.63) (see also [65]).

$$\mathcal{H} \rightarrow |1\rangle\langle 1| \otimes \mathcal{H} \quad \text{or} \quad \mathcal{H} \rightarrow P_1 \otimes \mathcal{H} \quad (2.63)$$

Hence from (2.63) one partitions an enlarged (double) eigenspace, into a zero subspace

$$\ker\{|1\rangle\langle 1| \otimes \mathcal{H}\} = \text{span}\{|0\rangle \otimes |q\rangle\} \quad (2.64)$$

and the eigenspace of the original \mathcal{H} is the same with eigenvectors \otimes -concatenated by $|1\rangle$

$$(|1\rangle\langle 1| \otimes \mathcal{H}) |1\rangle \otimes |\varphi_i\rangle = \lambda_i |1\rangle \otimes |\varphi_i\rangle \quad (2.65)$$

We consider the T.I.S.E.

$$e^{-it|1\rangle\langle 1| \otimes \mathcal{H}} \underbrace{\left(\frac{1}{\sqrt{2}} (|0\rangle + |1\rangle) \otimes |\varphi_i\rangle \right)}_{\text{initial state}} \quad (2.66)$$

by linearity

$$\begin{aligned} &= \frac{1}{\sqrt{2}} (|0, \varphi_i\rangle + e^{-i\lambda_i t} |1, \varphi_i\rangle) \\ &= \frac{1}{\sqrt{2}} (|0\rangle + e^{-i\lambda_i t} |1\rangle) |\varphi_i\rangle \end{aligned} \quad (2.67)$$

We change to the X -basis with the Hadamard gate $H = \frac{1}{\sqrt{2}}(X + Z)$ and then measure in Z .

$$\frac{1}{\sqrt{2}}H(|0\rangle + e^{-i\lambda_it} |1\rangle) = \frac{1}{2}(|0\rangle - e^{-i\lambda_it} |1\rangle) + \frac{1}{2}(|1\rangle + e^{-i\lambda_it} |0\rangle) \quad (2.68)$$

The probabilities for measuring $|0\rangle$ and $|1\rangle$, respectively are (see Figure 2.5)

$$\begin{aligned} \text{Prob}(|0\rangle\langle 0|) &= \frac{1}{4}(1 + e^{-i\lambda_it})(1 + e^{i\lambda_it}) \\ &= \frac{1}{4}(1 + e^{-i\lambda_it} + e^{i\lambda_it} + 1) \\ &= \frac{1}{2}(1 + \cos(\lambda_it)) \end{aligned} \quad (2.69)$$

and

$$\text{Prob}(|1\rangle\langle 1|) = \frac{1}{2}(1 - \cos(\lambda_it)). \quad (2.70)$$

By sampling from the original wavefunction and measuring $\langle 0|$ we can recover λ_i —see also Figure 2.5. The described procedure was the quantum phase estimation algorithm [7] related to how it appeared in [65].

From phase estimation we can obtain the eigenvalue of a given eigenvector. The following questions now follow

1. How do we simulate \mathcal{H} using elementary gates?
2. How do we prepare $|\psi_i\rangle$?

For the first question, consider $\mathcal{H} = A + B$ with $[A, B] \neq 0$. It can be shown that it is possible to approximate the evolution of \mathcal{H} . Let us recall the following.

Definition 39. (Lie Product Formula). For Hermitian matrices \mathcal{A} and \mathcal{B} ,

$$e^{\mathcal{A}+\mathcal{B}} = \lim_{k \rightarrow \infty} \left(e^{\mathcal{A}/k} e^{\mathcal{B}/k} \right)^k. \quad (2.71)$$

Definition 40 (Suzuki–Trotter Expansion). The second order operator Taylor expansion establishes that

$$e^{(\mathcal{A}+\mathcal{B})\delta} = e^{\delta\mathcal{A}} e^{\delta\mathcal{B}} + O(\delta^2). \quad (2.72)$$

Similarly to the product formula, It is often typical that one of the terms \mathcal{A} or \mathcal{B} is considered as a diagonal operator in the standard computational Z basis. And that the non-diagonal second term is typically 1- or 2-body.

We will first simulate \mathcal{A} . Let \mathcal{A} be diagonal in $\mathcal{L}(\mathbb{C}_2^{\otimes d})$. This term could embed e.g. the 3-SAT problem and hence may contain 3-body interactions. To develop an example to simulate 3-body interactions consider

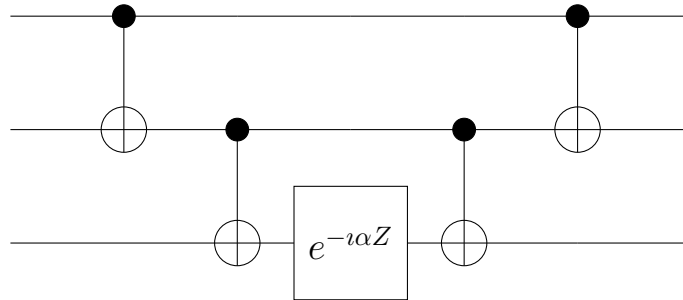
$$\alpha Z \otimes Z \otimes Z. \quad (2.73)$$

Proposition 10. The basis vector $|a,b,c\rangle$ for $a,b,c \in \mathbb{B}$ evolves under the propagator $e^{-it\alpha Z_1 Z_2 Z_3}$ as

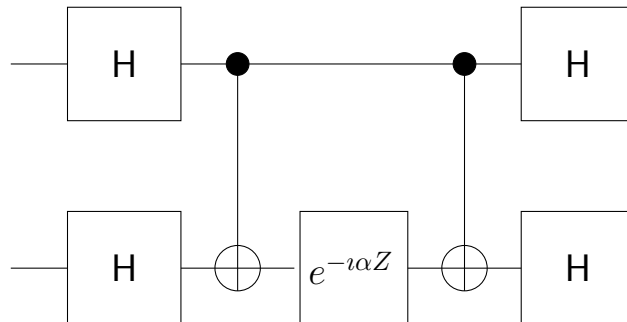
$$e^{i\alpha(-1)^{a \odot b \odot c}} |a,b,c\rangle \quad (2.74)$$

where \odot denotes the operation of negated exclusive OR, called logical equivalence ($a \odot b \odot c = 1 \oplus a \oplus b \oplus c$).

Proposition 11. The following circuit simulates the 3-body interaction (2.73) as $e^{-it\alpha Z_1 Z_2 Z_3}$.



Now we will focus on simulating \mathcal{B} , which we will assume is a sum over 2-body terms. For example terms such as $X_i X_j$. In a circuit this would be implemented as



We have hence implemented the evolution for a 2-body term in the X basis. In general we note that $\alpha X_i X_j = \alpha(HZ_i H) \otimes (HZ_j H)$ and since we used $Z_i Z_j$

interactions to realize the CN gate, we would typically implement X_1X_2 terms without the need for CN gates.

Remark 31. Readers might complain that we realized a ZZ interaction using two CN gates. This method does scale up to realize many-body interactions and it is sometimes the case that direct access to the Hamiltonian (presumably to realize a controlled- Z gate) is not always possible.

Proposition 12. It can be shown that,

$$e^{-it\sum J_{ij}X_iX_j} = H^{\otimes n} e^{-it\sum J_{ij}Z_iZ_j} H^{\otimes n} \quad (2.75)$$

for H the Hadamard gate. Likewise, Z terms are typically enough to be transformed into other Hamiltonians using local rotations, see for instance work on simulating electronic structure Hamiltonians [11].

2.5 Finding the ground state

As we introduced early in § 1, the ground state problem was considered here in several forms.

1. Stochastic systems as described here, evolve to their lowest-eigenvalue state(s).
2. Page-rank is a ground state sampling problem, which (as explained) can be performed on a quantum processor (such as an adiabatic processor or ground state computer).
3. Phase-estimation can be used to determine eigenvalues of operators on a quantum processor.

To prepare a candidate lowest-energy state $|\psi\rangle$ on a quantum processor, a classical iterative optimization method can be used (as explored next in § 4). If $|\psi\rangle$ is the ground state of the Hamiltonian then we consider the following optimization problem (a variational upper bound).

$$\min_{\varphi} \langle \varphi | \mathcal{H} | \varphi \rangle \geq \langle \psi | \mathcal{H} | \psi \rangle \quad (2.76)$$

Note that a solution to this optimization problem corresponds to a ground state of the Hamiltonian \mathcal{H} . Several approaches will be presented to solve optimization problems given in the form (2.76).

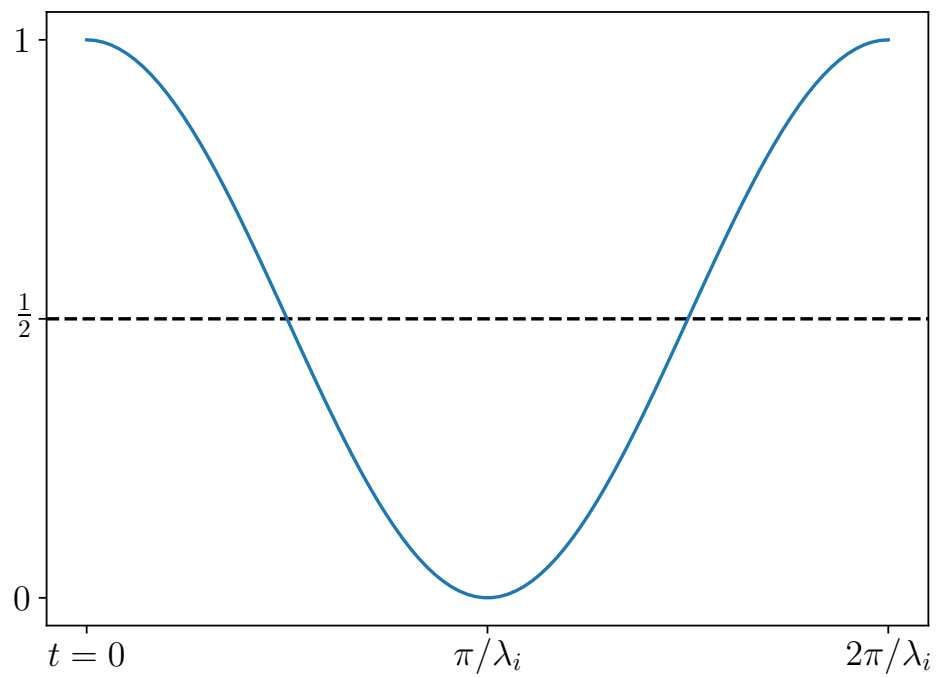


Figure 2.5 — A plot of $\frac{1}{2} + \frac{1}{2} \cos \lambda_i t$. The plane wave $\cos \lambda_i t$ has angular frequency λ_i with period $\frac{2\pi}{\lambda_i}$.

Chapter 3. Tensor Networks and Quantum Circuits

Tensor networks in physics are often traced back to a 1971 paper by Penrose [68] but actually date back further, appearing in various forms in the work of Cayley. Such network diagrams appear in digital circuit theory, and form the foundations of quantum computing—starting with the work of Feynman and others in the 1980’s [4] and further extended by Deutsch in his ‘quantum computational network model’ [5].

Most of the modern interest in tensor networks stems from their use in numerical algorithms employing tensor contraction. There are many reviews and surveys devoted to tensor network algorithms—see [69–83], as well as, *Tensor Networks in a Nutshell*, which I wrote with Ville Bergholm [84] as well as my book, *Quantum Tensor Networks: a pathway to modern diagrammatic reasoning* [85].

The Feynman gate is a (if not the) central building block for quantum information processing tasks. It has been used extensively in diagrammatic reasoning in categorical quantum mechanics [86; 87]. Let’s recall the building blocks used in the tensor network construction of the Feynman gate. Here we will review and introduce tensor networks by considering this gate.

As related to diagrammatic reasoning in quantum theory [86; 87], an algebraic theory of logic gates [88] was cast into the setting of tensor network states—and used at the crossroads of condensed matter theory and quantum computation [89–91]. We adapted these and other tools [86; 87] and discovered efficient tensor network descriptions of finite Abelian lattice gauge theories [92]. These tools also lead to the discovery of a wide class of efficiently contractable tensor networks, representing counting problems [93]. The methods (in part) trace some of their roots back to categorical quantum mechanics in work [86; 87] surrounding the so called, ZX-calculus (stabilizer tensor networks).

3.1 Clifford gates

Definition 41. The collection of Clifford gates is generated with the following.

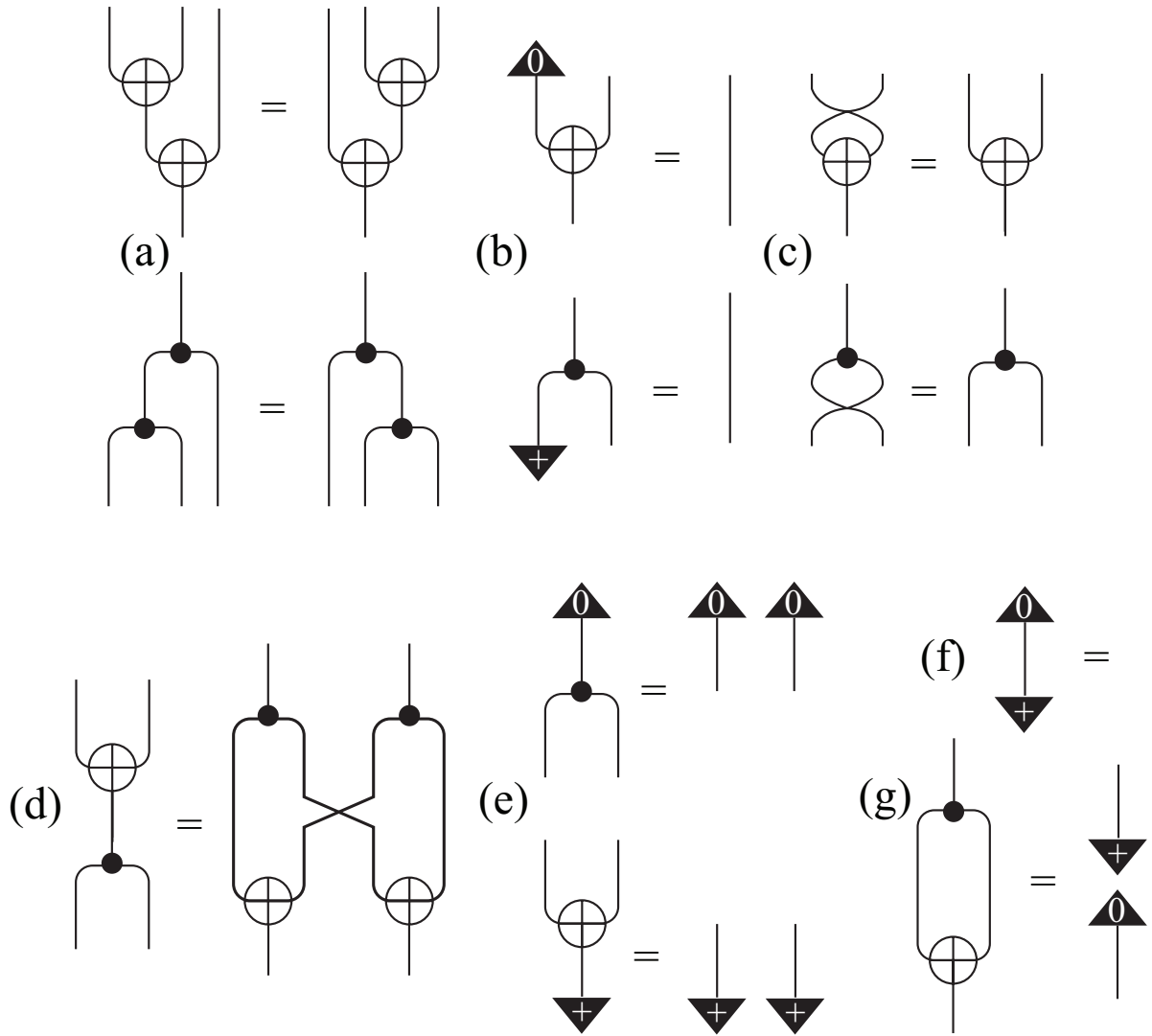


Figure 3.1 — Lafont’s 2003 model of circuits included the bialgebra (d) and Hopf (g) relations between the building blocks needed to form a controlled-NOT gate—see also ZX calculus [87]. [Redrawn from [88] as it appeared in [89]]. [(a) associativity; (b) gate unit laws; (c) symmetry; (e) copy laws; (f) unit scalar given as a blank on the page.]

- (a) The controlled-NOT gate, CN.
- (b) The Hadamard gate $H = \frac{1}{\sqrt{2}}(X + Z)$.
- (c) The phase gate $P = |0\rangle\langle 0| + i|1\rangle\langle 1|$.
- (d) The Pauli gates generating the Pauli algebra on a single qubits with 16 elements.

The gates (a-d) are presented graphically in Figure 3.2.

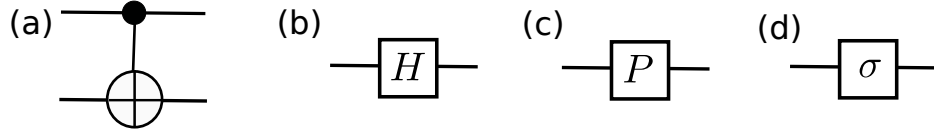


Figure 3.2 — Clifford generators drawn as quantum gates.

Remark 32 (Single qubit Clifford group). The standard properties of single qubit gates follow.

- (i) $HXH = Z$ and $HZH = X$
- (ii) $PXP^\dagger = Y$ and $PYP^\dagger = Z = P^2$

These gates above generate the single qubit Clifford group.

Remark 33 (Properties of Clifford circuits). We now list elementary properties of Clifford circuits.

- (i) Clifford circuits generate the Clifford group.
- (ii) Let P_n be the collection of 4^n n -letter words with \otimes as concatenation generated from the alphabet

$$\{\pm\mathbb{1}, \pm X, \pm Y, \pm Z, \pm i\mathbb{1}, \pm iX, \pm iY, \pm iZ\}. \quad (3.1)$$

All operators g in the Clifford group acts as an involution when P_n is conjugated by g , that is

$$gP_n g^\dagger = P_n. \quad (3.2)$$

- (iii) Note, alternative notation to write P_1 could be

$$P_1 = \{\pm\mathbb{1}, \pm i\}\{\mathbb{1}, X, Y, Z\}. \quad (3.3)$$

- (iv) Defining properties of the Pauli matrices:

$$X^2 = Y^2 = Z^2 = \mathbb{1} = -iXYZ. \quad (3.4)$$

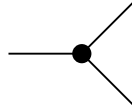
3.2 Tensor network building blocks

A universal model of computation can be expressed in terms of networks (i.e. circuits built from gates) [6; 90]. The first gate to consider copies binary inputs (0 and 1) like this

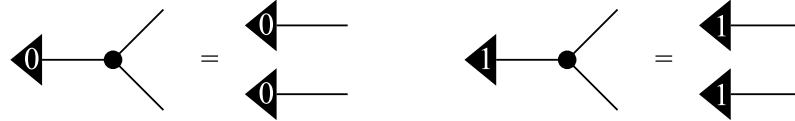
$$0 \rightarrow 0,0 \quad (3.5a)$$

$$1 \rightarrow 1,1 \quad (3.5b)$$

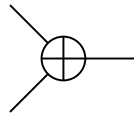
In the diagrammatic tensor network language, the COPY-gate is



and graphically, equation (3.5a) and (3.5b) become



The next gate performs the exclusive OR operation (XOR). Given two binary inputs (say a and b), the output ($a \oplus b = a + b - 2ab$) is 1 iff exactly a single input is 1 (that is, addition modulo 2). The gate is drawn as



The XOR gate allows one to realize any linear Boolean function. Let f be a function from n -long bit strings $x_1x_2 \dots x_n$ to single bits $\in \{0,1\}$. Then $f(x_1, x_2, \dots, x_n)$ is linear over \oplus if it can be written as

$$f = c_1x_1 \oplus c_2x_2 \oplus \dots \oplus c_{n-1}x_{n-1} \oplus c_nx_n \quad (3.6)$$

where $\mathbf{c} \stackrel{\text{def}}{=} (c_1, c_2, \dots, c_{n-1}, c_n)$ is any n -long Boolean string. Hence, there are 2^n linear Boolean functions and note that negation is not allowed. When negation is allowed a constant $c_0 \oplus f$ is added (mod 2) to equation 3.6 and for $c_0 = 1$,

the function is called affine. In other words, negation is equivalent to allowing constant 1 as

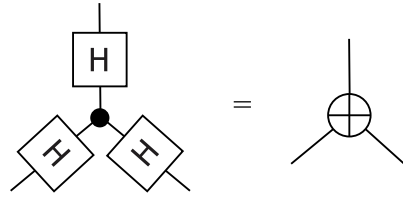


$$(3.7)$$

which sends Boolean variable x to $1 - x$. Using the polarity representation of f ,

$$\hat{f}(\mathbf{x}) = (-1)^{f(\mathbf{x})} \quad (3.8)$$

we note that linear Boolean functions index the columns of the n -fold tensor product of 2×2 Hadamard matrices (that is, $H^{\otimes n}$ where the i - j th entry of each 2×2 is $\sqrt{2}H_{ij} \stackrel{\text{def}}{=} (-1)^{i \cdot j}$). Importantly (where equality is up to a scalar),



$$(3.9)$$

up to isometry as there could be an omitted scale factor depending on conventions [87]. By equation 3.9 one can think of XOR as being a copy operation in another basis. We send binary 0 to $|+\rangle \stackrel{\text{def}}{=} (1,0)^\top$ and 1 to $|-\rangle \stackrel{\text{def}}{=} (0,1)^\top$ where \top is transpose. Then XOR acts as a copy operation:

$$|+\rangle \rightarrow |+,+\rangle \quad (3.10a)$$

$$|-\rangle \rightarrow |-, -\rangle \quad (3.10b)$$

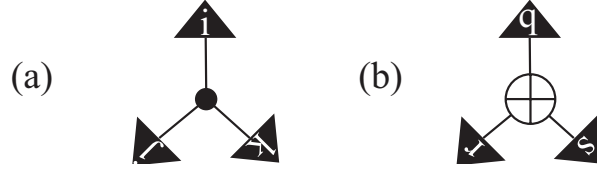
using $H^2 = \mathbb{1}$, $|+\rangle \stackrel{\text{def}}{=} H|0\rangle$ and $|-\rangle \stackrel{\text{def}}{=} H|1\rangle$.

Concatenating the COPY- and XOR gates yields the logically reversible Feynman gate [6; 85; 87])



$$(3.11)$$

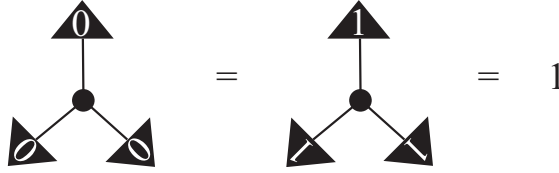
A simplistic methodology to connect quantum circuits with indexed tensor networks starts with the definition of two tensors, in terms of components.



In (a) we have

$$\delta^i_{jk} = 1 - (i + j + k) + ij + ik + jk \quad (3.12)$$

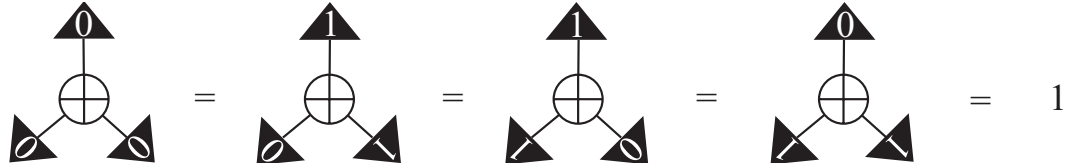
where the indicies (i, j and k) take values $\in \{0,1\}$. In other words, the following contractions evaluate to unity.



Likewise for (b) we have

$$\oplus^q_{rs} = 1 - (q + r + s) + 2(qr + qs + sr) - 4qrs \quad (3.13)$$

where the following contractions evaluate to unity (the XOR tensor is fully symmetric, hence the three rightmost contractions are identical by wire permutation).



Then the Feynman gate (CN) is given as the following tensor contraction¹

$$\sum_m \delta^{ij}_{m \oplus_{qr}} = \text{CN}^{ij}_{qr} \quad (3.14)$$

where we raised an index on δ . All quantum circuits can be broken into their building blocks and thought of as indexed tensor contractions in this way.

¹Equation (3.14) expands to $1 - (i + j + q + r) + ij + iq + jq + ir + jr + 2(qr - iqr - jqr)$.

3.2.1 Reversible logic

A reversible computer is built using gates that implement bijective functions. Quantum gates are unitary: hence reversible classical gates are a subclass. Let us recall the critical implication of reversible logic.

We will consider n -long bit strings in lexicographic order indexed by natural numbers i . So $y_0 = 00 \cdots 0$, $y_2 = 00 \cdots 10$ etc. We will further consider inputs as being uniformly distributed over the y 's and define the change in Shannon's entropy between a circuit's input and output (implementing g) as

$$\Delta S \stackrel{\text{def}}{=} \sum_i P\{g(y_i)\} \ln_2 P\{g(y_i)\} - \sum_i P(y_i) \ln_2 P(y_i) \quad (3.15)$$

where the probability $P\{y_i\} = 2^{-n}, \forall i$ for the uniform distribution. Equation (3.15) vanishes identically iff g is a reversible function.

For g non-reversible (a.k.a. a non-injective surjective function), there exists at least one pair y_i, y_j such that $g(y_j) = g(y_i)$ and hence, information is lost as the input can not be uniquely recovered from the output (so the Shannon entropy of the output distribution is strictly $< n$) and hence, (3.15) is non-vanishing. The vanishing of (3.15) is a central implication of reversible computation, and provides an abstract argument related to Landauer's principle.

Universal classical computation can be realized with reversible logic gates. However, using the Feynman gate is not enough since it only can be used to implement linear functions. An additional reversible gate must be added, such as the Toffoli or Fredkin gate(s).

Stabilizer tensor networks

Stabilizer circuits use gates from the normalizer of the n qubit Pauli group—generated by the Clifford gates [94]. The gates include: (i) the single qubit Pauli gates X, Y and Z ; (ii) the Feynman gate; (iii) the Hadamard gate; (iv) the phase gate $P = |0\rangle\langle 0| + i|1\rangle\langle 1|$.

Theorem 11 (Minimal Stabilizer Tensor Generators [95]). The following generating tensors are sufficient to simulate any stabilizer quantum circuit:

- (a) a vector $|t\rangle \stackrel{\text{def}}{=} |0\rangle + \imath|1\rangle$,
- (b) the Hadamard gate and
- (c) the XOR- and COPY tensors and
- (d) a covector $\langle +| \stackrel{\text{def}}{=} \langle 0| + \langle 1|$.

Proof. We will establish this by recovering the Clifford gates (i-iv). By linearity, the copy tensor induces a product between vector pairs, producing a third vector where the coefficients of the input vector pair are multiplied. This allows us to recover from (a) the family $|t^k\rangle \stackrel{\text{def}}{=} |0\rangle + \imath^k|1\rangle$ for integer k as, for instance,

(3.16)

which recovers the vector $\sqrt{2}|+\rangle$ from (3.10a). Then from (d) we can recover a cup (or cap) allowing one to raise/lower indicies (3.17.a), and importantly, (3.17.b) illustrates that

(3.17)

$|t^k\rangle \stackrel{\text{def}}{=} |0\rangle + \imath^k|1\rangle$ lifts to a unitary operator where the Clifford gate P is recovered for $k = 1$ —thereby establishing (iv). Considering (3.17.a) above, we have t^4 which turns into the identity operator. The L.H.S. of this equation (3.17.a) then corresponds to a Bell state or costate depending on your convention. From equation (3.17.b) above, we create a map corresponding to k^k . For $k = 2$ we recover the standard Pauli Z matrix, then $HZH = X$ and $PXP^3 = Y$. So we recover the Pauli gates (i). The Feynman gate was constructed in (3.11) establishing (ii) and the Hadamard gate (iii) was assumed. □

Definition 42. The cross on wire



denotes the Z gate.

Before continuing on, we note that various other identities can be derived for stabilizer tensors, such as the following.²

3.2.2 Heisenberg picture

We consider the following unitary operator as

$$U_t = e^{-it\mathcal{H}}, \quad U_t U_t^\dagger = \mathbb{1} \quad (3.18)$$

with $\mathcal{H}^\dagger = \mathcal{H}$. The time evolution of a quantum state $|\varphi_0\rangle$ is

$$|\varphi_t\rangle = e^{-it\mathcal{H}} |\varphi_0\rangle, \quad \forall t \langle \varphi_t | \varphi_t \rangle = 1. \quad (3.19)$$

This is called *Schrödinger's picture*.

A second time evolution formalism is called *Heisenberg's picture*. Suppose we have a quantum system in state $|\psi\rangle$, we apply U ($UU^\dagger = \mathbb{1}$)

$$UN |\varphi\rangle = UNU^\dagger U |\psi\rangle \quad (3.20)$$

Then the evolution of operator N is given by

$$N \rightarrow UNU^\dagger \quad (3.21)$$

1. We want to follow the evolution of a number of N 's to reconstruct the evolution of $|\psi\rangle$.
2. Evolution in (3.21) is linear so we will follow a complete basis of $n \times n$ matrices.

²Showing that $Z_i |\psi\rangle = Z_j |\psi\rangle$ for all i, j for $|\psi\rangle$ a GHZ-state.

We call P the Pauli group. As mentioned before it contains $4 \cdot 4^n$ elements. These elements are tensor products of $X, Y, Z, \mathbb{1}$ and with prefactors $\pm 1, \pm i$. There's a multiplicative group homomorphism

$$MN \rightarrow UMNU^\dagger = (UMU^\dagger)(UNU^\dagger)$$

so we can follow just a generating set of the group. A good one for the Pauli group is $\{X_1, \dots, X_n, Z_1, \dots, Z_n\}$.

The set of operators that leave P fixed under conjugation form the normalizer called the Clifford group C . This group C is much smaller than the unitary group on n -qubits, $\mathfrak{U}(2^n)$, yet contains many operations of interest. Some gates in C are the Hadamard gate

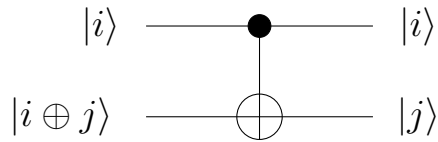
$$H = \frac{1}{\sqrt{2}}(X + Z)$$

the phase gate

$$P = |0\rangle\langle 0| + i|1\rangle\langle 1|, \tag{3.22}$$

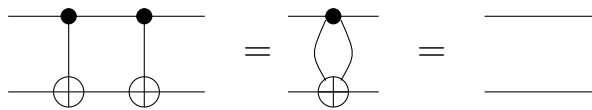
and the CN gate

$$\text{CN} |ij\rangle = |i, i \oplus j\rangle$$

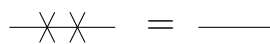


We will derive basic circuit identities and state them graphically, as is common [6] in quantum circuits. Here we will adopt a tensor network approach and state identities that are also tensor symmetries [85].

Proposition 13 ($\text{CN}^2 = \mathbb{1}$). This is given graphically as follows. (See also e.g. bialgebra law in [87]).



Proposition 14 ($Z^2 = \mathbb{1}$). This identity is given graphically as follows.



3.2.3 Stabilizer tensor theory

Here we will build towards establishing Theorem 12. U stabilizes a quantum state $|\varphi\rangle$ iff $U|\varphi\rangle = (+1)|\varphi\rangle$. Stabilizers of $|\varphi\rangle$ form a group. Stabilizers states in terms of n commuting and different operators S from the Pauli algebra. The operators that generate this group are

$$\{\mathbb{1}, X, Y, Z, \pm i, \otimes\}$$

Example 24 (Single qubit stabilizers).

X	$ +\rangle = \frac{ 0\rangle+ 1\rangle}{\sqrt{2}}$
Y	$ y^+\rangle = \frac{ 0\rangle+i 1\rangle}{\sqrt{2}}$
Z	$ 0\rangle$
$-X$	$ -\rangle = \frac{ 0\rangle- 1\rangle}{\sqrt{2}}$
$-Y$	$ y^-\rangle = \frac{ 0\rangle-i 1\rangle}{\sqrt{2}}$
$-Z$	$ 1\rangle$

Example 25. The Bell state is a stabilizer state.

$$\sqrt{2}|\Phi^+\rangle = \sum_{a,b} (a \oplus \neg b) |a,b\rangle = |00\rangle + |11\rangle \quad (3.23)$$

The group that corresponds to this state is

$$S = \{\mathbb{1} \otimes \mathbb{1}, X \otimes X, -Y \otimes Y, Z \otimes Z\} \quad (3.24)$$

This group is of order 2^n and is indeed abelian.

Before stating the proving the main theorem of this segment (Theorem 12), we will state some helpful graphical identities.

Remark 34. The COPY-tensor has stabilizer generators $X_i X_j X_k$, $Z_i Z_j$ for $i, j, k = 1, 2, 3$ a qubit index. For example,

$$Z_i Z_j (|000\rangle + |111\rangle) = |000\rangle + |111\rangle. \quad (3.25)$$

The following will present these identities graphically (Proposition 15).

Proposition 15 (Stabilizers of COPY). The following are the Pauli stabilizers of COPY.

Proposition 16 (Gate-COPY). The following identity (gate-COPY) is derived.

We will now state the main theorem of this segment.

Theorem 12 (Graphical Proof Gottesman–Knill Theorem). There exists an efficient graphical rewrite proof (by bounding the number of rewrites) of the Gottesman–Knill theorem. Derive the gate identities in paper [94] and prove the main theorem using the methods from this segment.

Theorem 12 is proven by using the graphical tensor calculus to derive the gate identities in paper [94]. We will establish this piece-wise, by working example.

Remark 35. To prove the theorem (12), we need to understand how

$$\{Z_1, \dots, Z_n, X_1, \dots, X_n\} \quad (3.26)$$

evolve under conjugation by H , P , CN . To simulate the evolution of, (3.26) there are $2n$ tensor contractions. Each can be done graphically. We can establish the following (The negative one above an arrow $\xrightarrow{-1}$ means that the mapping has an inverse).

$$H: Z \xrightarrow{-1} X, \quad H: X \xrightarrow{-1} Z \quad (3.27)$$

$$P: X \xrightarrow{-1} Y, Z \xrightarrow{-1} Z \quad (3.28)$$

$$\begin{aligned}
\text{CN: } X \otimes \mathbb{1} &\xrightarrow{-1} X \otimes X \\
\mathbb{1} \otimes X &\xrightarrow{-1} \mathbb{1} \otimes X \\
Z \otimes \mathbb{1} &\xrightarrow{-1} Z \otimes \mathbb{1} \\
\mathbb{1} \otimes Z &\xrightarrow{-1} \mathbb{1} \otimes Z
\end{aligned} \tag{3.29}$$

$$\begin{aligned}
XYX &= -X \\
YZY^\dagger &= -Z
\end{aligned} \tag{3.30}$$

Proposition 17 (Computational and \pm -Basis Change). This relationship (3.27) is given graphically as follows.

$$-\boxed{\text{H}}-\times-\boxed{\text{H}}- = -\oplus-$$

Proposition 18. From $H^2 = \mathbb{1}$ and Proposition 17 we recover the R.H.S. of (3.27).

$$-\boxed{\text{H}}-\oplus-\boxed{\text{H}}- = -\boxed{\text{H}}-\boxed{\text{H}}-\times-\boxed{\text{H}}-\boxed{\text{H}}- = -\frac{Z}{\times}-$$

Remark 36. The other identities follow accordingly and are encapsulated as part(s) of the following examples.

Proposition 19 (Stabilizers Transform Covariantly—see e.g. [85]). Let N be a stabilizer of state $|o\rangle$. Then MNM^\dagger is a stabilizer of the state $(M|o\rangle)$.

The following Lemma is used as Lemma 15 in § 5. It is stated below as Lemma 1 as it is relevant to Proposition 19.

Lemma 1 (Clifford Normalizer). Let \mathcal{C} be the set of all Clifford circuits on n qubits, and let \mathcal{P} be the set of all elements of the Pauli group on n qubits. Let $C \in \mathcal{C}$ and $P \in \mathcal{P}$ then it can be shown that

$$CPC^\dagger \in \mathcal{P}$$

or in other words

$$C(\sigma_\alpha^a \sigma_\beta^b \cdots \sigma_\gamma^c)C^\dagger = \sigma_{\alpha'}^{a'} \sigma_{\beta'}^{b'} \cdots \sigma_{\gamma'}^{c'}$$

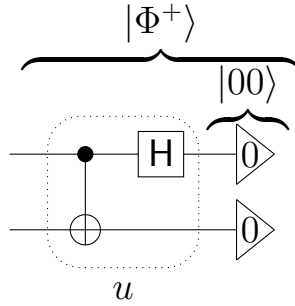
and so Clifford circuits act by conjugation on tensor products of Pauli operators to produce tensor products of Pauli operators.

To apply Lemma 1, essentially, we are interested in Heisenberg evolution of X_i and Z_j for i, j ranging over all qubit labels. Hence, we arrive at the following. Denote by σ some Pauli observable evolving under a Clifford circuit U . Then

$$U : \sigma \rightarrow \sigma' = U\sigma U^\dagger = \sigma' U U^\dagger \quad (3.31)$$

where from Lemma 1, σ' is a Pauli string. To prove Theorem 12, this is exactly our strategy. We consider the circuit $U\sigma U^\dagger$. Then we determine (by graphical rewrites) $\sigma U^\dagger = U^\dagger \sigma'$. We show that this is always possible with the considered Clifford generators. Hence, graphical rewrites exist to prove Theorem 12.

We will now consider an extended example related to Bell state stabilizers which will illustrate the building blocks needed to prove Theorem 12. Let us now verify by tensor contraction that $X_1 X_2, -Y_1 Y_2, Z_1 Z_2$ are indeed stabilizers. The following circuit produces the Bell state $|\Phi^+\rangle$.



Such that

$$|\Phi^+\rangle = \frac{|00\rangle + |11\rangle}{\sqrt{2}} = u |00\rangle. \quad (3.32)$$

We begin by application of Proposition 19. First, consider stabilizers of the initial state, as follows.

$$Z_1 Z_2 |00\rangle = |00\rangle \quad (3.33)$$

$$Z \otimes \mathbb{1} |00\rangle = |00\rangle \quad (3.34)$$

$$\mathbb{1} \otimes Z |00\rangle = |00\rangle \quad (3.35)$$

Hence, the stabilizers of $|00\rangle$ form the Abelian group (3.36).

$$\{\mathbf{1}, Z_1, Z_2, Z_1 Z_2\} \quad (3.36)$$

Acting on the initial state $|00\rangle$ with u yields:

$$\begin{aligned} u|00\rangle &= |\Phi^+\rangle, \\ N|\Phi^+\rangle &= |\Phi^+\rangle. \end{aligned} \quad (3.37)$$

From Proposition 19 we know that

$$\begin{aligned} N|00\rangle &= |00\rangle, \\ u|00\rangle &= uN|00\rangle = uNu^\dagger u|00\rangle = uNu^\dagger |\Phi^+\rangle, \\ N &\rightarrow uNu^\dagger. \end{aligned} \quad (3.38)$$

Hence, Proposition 19 asserts that if (3.36) is a stabilizer of the initial state, then (3.39) is a stabilizer of the final state $u|00\rangle$

$$\{\mathbf{1}, uZ_1u^\dagger, uZ_2u^\dagger, uZ_1Z_2u^\dagger\} \quad (3.39)$$

Recall Lemma 1. We then must determine e.g. $Z_1Z_2u^\dagger = u^\dagger\sigma'$. This is done graphically as follows.

$$\begin{aligned} Z \otimes Z |\Phi^+\rangle : & \begin{array}{c} \text{---} \times \text{---} \bullet \text{---} \boxed{\text{H}} \text{---} \triangleright 0 \\ \text{---} \times \text{---} \oplus \text{---} \rightarrow \text{---} \triangleright 0 \end{array} = \\ & \begin{array}{c} \times \bullet \text{---} \boxed{\text{H}} \text{---} \triangleright 0 \\ \oplus \times \text{---} \triangleright 0 \end{array} = \begin{array}{c} \bullet \text{---} \boxed{\text{H}} \text{---} \triangleright 0 \\ \oplus \text{---} \triangleright 0 \end{array} \end{aligned}$$

Which simply shows that $Z \otimes Z$ is a stabilizer of $|\Phi^+\rangle$, as expected. Consider then evolution of Z_1 . We arrive at the following rewrites.

$$\begin{array}{c} \bullet \text{---} \boxed{\text{H}} \times \boxed{\text{H}} \bullet \\ \oplus \text{---} \text{---} \oplus \end{array} = \begin{array}{c} \bullet \oplus \bullet \\ \oplus \oplus \end{array} = \begin{array}{c} \bullet \bullet \oplus \\ \oplus \oplus \end{array} =$$

Which arrives graphically at $X \otimes X$ being a stabilizer of $|\Phi^+\rangle$. From this, Theorem 12 follows directly as the required graphical rewrites have all been established.

Chapter 4. Variational Search and Optimization

The topic of real-world Noisy Intermediate Scale Quantum Technology (NISQ) processors is exploding in interest. As NISQ processors operate in the presence of noise and systematic fabrication errors, novel methodologies to program and control NISQ processors are now emerging. Situated between a quantum simulator and a gate-model based device, a leading methodology, known as variational quantum algorithms, utilizes a classical-to-quantum feedback loop to control and tune a quantum system to produce desired output(s) [9; 96]. Interesting recent findings include the discovery of barren plateaus [97] and (the author together with coauthors) of reachability deficits [98], a recent connection between variational algorithms and contextuality has been made in [99], and novel findings relating barren plateaus to circuit depth appeared in [100].

As variational quantum algorithms rely on minimization of some cost function, an important finding shows how to evaluate the gradients of said cost function exactly [101; 102]. In addition, less general, though equally interesting work includes studying level-1 QAOA [103] and recent findings related to circuit-parameter concentrations between instance solutions [104].

Variational quantum algorithms seek to reduce quantum state preparation requirements while necessitating measurements of individual qubits in the computational basis [9; 96]. A sought reduction in coherence time is mediated through an iterative classical-to-quantum feedback and optimization process. Systematic errors which map to deterministic yet unknown control parameters—such as time-variability in the application of specific Hamiltonians or poor pulse timing—can have less impact on variational algorithms, as states are prepared iteratively and varied over to minimize objective function(s).

In the contemporary noisy intermediate-scale quantum (NISQ) enhanced technology setting [105], variational quantum algorithms are used to prepare quantum state(s) for one of three purposes.

- (i) In the case of variational quantum approximate optimization (QAOA [96]), a state is prepared by alternating a Hamiltonian representing a penalty function (such as the NP-hard Ising embedding of 3-SAT) with a Hamiltonian representing local tunneling terms. The state is measured

- and the resulting bit string minimizes the penalty function. The minimization process is iterated by updating Hamiltonian application times.
- (ii) In the case of variational eigenvalue minimization (VQE [9]), the state is repeatedly prepared and measured to obtain a set of expected values which is individually calculated and collectively minimized. (applications of VQE include [106; 107])
 - (iii) In the case of generative quantum enhanced machine learning [108], a quantum circuit is tuned subject to a given training dataset which is hence used to represent (non-linear) probability distributions such as $p(x) = |\psi(x)|^2/\mathcal{Z}$ or $p(x) = e^{-\mathcal{H}(x)}/\mathcal{Z}$ where $p(x)$ is the expected value of sampling bit string x , ψ is a wave function, \mathcal{H} is a Hamiltonian and \mathcal{Z} is a normalization factor.

In the present chapter, we will present a general framework that is expressive enough to describe any known variational algorithm. We will however zoom in and focus on variational search and optimization, leaving a more detailed study of universal variational quantum computation [10] to Chapter 5. We begin with the idea of an approximate or random algorithm.

4.1 Random vs quantum complexity

One-sided vs two-sided error: The answer returned by a *deterministic algorithm* is always expected to be correct. That is not the case for random algorithms, including Monte Carlo algorithms.

Definition 43 (One-Sided Error). For *decision problems*, random algorithms are generally classified as either

1. NO- (a.k.a. false-) biased or
2. YES- (a.k.a. true-) biased,

subject to the following.

1. A false-biased algorithm is always correct when it returns false.
2. A true-biased algorithm is always correct when it returns true.

Definition 44 (Two-Sided Error). Probabilistic (a.k.a. random) algorithms that have no bias are said to have *two-sided errors*. The answer provided by the

algorithm (true or false; YES or NO) will be incorrect, or correct, with some bounded probability.

Example 26 (Randomized Primality Testing). The Solovay–Strassen primality test is used to determine whether a given number is prime and functions as follows.

1. The algorithm always returns *true* for prime number inputs.
2. For composite inputs, the algorithm always returns *false* with probability at least $\frac{1}{2}$ and *true* with probability less than $\frac{1}{2}$.

Thus, *false* answers are certain to be correct, whereas *true* answers remain uncertain—this is said to be a $\frac{1}{2}$ -correct *false-biased algorithm*.

Informally, a problem is in BPP if there is a corresponding algorithm with the following properties:

1. the algorithm has access to *coin flips* to make random decisions,
2. the algorithm is guaranteed to run in polynomial time (in the input size),
3. on any given run of the algorithm, it has a probability of at most $\frac{1}{3}$ of giving the wrong answer, whether the answer is YES or NO.

Definition 45. (bounded-error probabilistic polynomial time). BPP is the class of decision problems solvable in polynomial time with an error probability bounded away from $\frac{1}{3}$ for all instances.

More formally as a language (decision) problem.

Definition 46. A language \mathcal{L} is in BPP if and only if there exists a computational machine \mathcal{M} that runs for polynomial time on all inputs and

1. $\forall x \in \mathcal{L}$, \mathcal{M} outputs 1 with probability greater than or equal to $\frac{2}{3}$,
2. $\forall x \notin \mathcal{L}$, \mathcal{M} outputs 1 with probability less than or equal to $\frac{1}{3}$.

Remark 37. BPP contains P, the class of problems solvable in polynomial time with a deterministic machine, since a deterministic machine is a special case of a probabilistic machine.

In practice, an error probability of $\frac{1}{3}$ in Definition 46 might not be acceptable. The choice of $\frac{1}{3}$ in Definition 46 is however, arbitrary. The probability can take any constant between 0 and $\frac{1}{2}$ (exclusive) and the set BPP will be unchanged.

Furthermore, the probability does not even have to be constant: the same class of problems is defined by

1. allowing error as high as $\frac{1}{2} - n^c$ or
2. or requiring error as small as 2^{-n^c} ,

where c is any positive constant, and n is the length of input.

Hence, there is a probability of error, but if the algorithm is run many times, the chance that the majority of the runs are wrong drops off exponentially as a consequence of the **Chernoff bound**. This makes it possible to create a highly accurate algorithm by merely running the algorithm several times and taking a *majority vote*.

Example 27. If we instead defined BPP with the restriction that the algorithm can be wrong with probability at most 2^{-100} , this would result in the same class of problems.

We now arrive at BQP [7], the quantum analogue of the complexity class BPP.

Definition 47. Bounded-error quantum polynomial time (BQP) is the class of decision problems solvable by a quantum computer in polynomial time, with an error probability of at most $\frac{1}{3}$ for all instances.

A decision problem is a member of BQP if there exists a quantum algorithm that solves the decision problem with *high probability* and is guaranteed to run in polynomial time in the size of the input. A run of the algorithm will correctly solve the decision problem with a probability of at least $\frac{2}{3}$. More formally, BQP is the languages associated with certain bounded-error uniform families of quantum circuits [6].

Definition 48. A language \mathcal{L} is in BQP if and only if there exists a polynomial-time uniform family of quantum circuits $\{Q_n : n \in \mathbb{N}\}$, such that $\forall n \in \mathbb{N}$, Q_n takes n qubits as input and outputs 1 bit:

1. $\forall x \in \mathcal{L}, \Pr(Q_{|x|}(x) = 1) \geq \frac{2}{3}$,
2. $\forall x \notin \mathcal{L}, \Pr(Q_{|x|}(x) = 0) \geq \frac{2}{3}$.

Remark 38. Similarly to other **bounded error** probabilistic classes such as BPP, the choice of $\frac{1}{3}$ in Definition 48 is arbitrary. We can run the algorithm a constant number of times and take a majority vote to achieve any desired probability of correctness less than 1, using the aforementioned Chernoff bound. The complexity

class is unchanged by allowing error as high as $\frac{1}{2} - n^{-c}$ on the one hand, or requiring error as small as 2^{-n^c} on the other hand, where c is any positive constant, and n is the length of input.

Definition 49. PSPACE is the set of all decision problems that can be solved using a polynomial amount of computational space.

The exact relationship of BQP to P, NP, and PSPACE remains unknown. However:

Remark 39. Known class relationships include (see Figure 4.1):

$$P \subseteq BPP \subseteq BQP \subseteq PSPACE$$

Hence, the class of problems that can be efficiently solved by quantum computers includes all problems that can be efficiently solved by deterministic classical computers. It however does include problems that cannot be solved by classical computers with polynomial space resources (regardless of the time taken to solve each instance). The suspected class relationships are given in Figure 4.1.

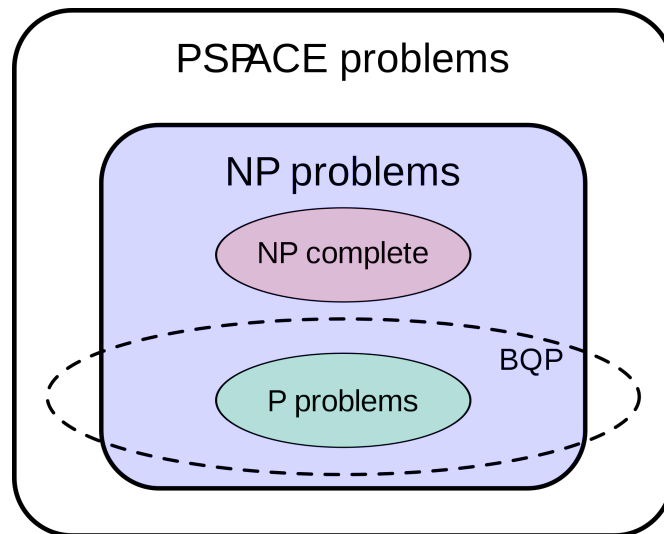


Figure 4.1 — The suspected relationship of BQP to other classes [6].

4.2 Variational quantum computation framework

Definition 50 (Variational Statespace). The variational statespace of a p -parameterized n -qubit state preparation process is the union of $|\psi(\boldsymbol{\theta})\rangle$ over real

assignments of $\boldsymbol{\theta}$,

$$\bigcup_{\boldsymbol{\theta} \in \mathbb{R}^{\times p}} \{|\psi(\boldsymbol{\theta})\rangle\} \subseteq \mathbb{C}_2^{\otimes n}. \quad (4.1)$$

Variational statespace examples include preparing $|\psi(\boldsymbol{\theta})\rangle$ by either:

(1.i) A quantum circuit with e.g. $\boldsymbol{\theta} \in [0, 2\pi]^{\times p}$ tunable parameters as

$$|\psi(\boldsymbol{\theta})\rangle = \prod_{l=1}^L U_l |0\rangle^{\otimes n}, \quad (4.2)$$

where U_l is adjusted by θ_l for $l = 1$ to p .

(1.ii) By tuning accessible time-dependent, piece-wise continuous and appropriately bounded parameters (function $\theta_k(t)$ corresponding to Hermitian $A^{(k)}$) as

$$|\psi\rangle = \mathcal{T}\{e^{-i\sum \theta_k(t)A^{(k)}}\} |0\rangle^{\otimes n}, \quad (4.3)$$

where \mathcal{T} time orders the sequence and superscript k indexes the k th operator $A^{(k)}$.

Definition 51 (Variational Sequence). A variational sequence specifies parameters to prepare a state in a variational statespace. It can be given by defining a specific sequence of gates or by specifying control parameter values.

Contrasting (1.i) and (1.ii) above suggests an interesting connection between variational algorithms and optimal quantum control. Indeed, we will provide an objective function that can be efficiently calculated given access to a suitable quantum processor. Minimization of this objective function produces a close 2-norm approximation to the output of a given quantum circuit. The variational sequence minimizing the objective function is given precisely in the form (1.i Eq. 4.2). Finding a shorter sequence to accomplish this same task (4.2) by finding a variational sequence in the form (4.3) can be stated as optimization of a suitable objective function. The definition of such a *universal* objective function, is a contribution of this work.

Definition 52 (Objective Function). We consider an objective function as the expected value of an operator expressed with real coefficients $\mathcal{J}_{\alpha\beta\cdots\gamma}^{ab\cdots c}$ in the Pauli basis as,

$$\mathcal{H} = \sum \mathcal{J}_{\alpha\beta\cdots\gamma}^{ab\cdots c} \cdot \sigma_\alpha^a \sigma_\beta^b \cdots \sigma_\gamma^c \quad (4.4)$$

where Greek letters index Pauli matrices, Roman letters index qubits and the sum is over a subset of the 4^n elements in the basis, where the tensor (\otimes) is omitted.

We are concerned primarily with Hamiltonians where $\mathcal{J}_{\alpha\beta\cdots\gamma}^{ab\cdots c}$ is given and known to be non-vanishing for at most some $\text{poly}(n)$ terms. This wide class includes Hamiltonians representing electronic structure [109]. More generally, such Hamiltonians are of bounded cardinality.

Definition 53 (Objective Function Cardinality). The number of terms in the Pauli basis $\{\mathbb{1}, X, Y, Z\}^{\otimes n}$ needed to express an objective function.

Definition 54 (Bounded Objective Function). A family of objective functions is *efficiently computable* when uniformly generated by calculating the expected value of an operator with $\text{poly}(n)$ bounded cardinality over

$$\Omega \subset \{\mathbb{1}, X, Y, Z\}^{\otimes n}. \quad (4.5)$$

We will now use the Cartesian tensor (\times) as states need not be proximally interacting and can be sequenced and independently prepared at different times.

Definition 55 (Poly-Computable Objective Function). An objective function

$$f: |\phi\rangle^{\times \mathcal{O}(\text{poly}(n))} \rightarrow \mathbb{R}_+ \quad (4.6)$$

is called poly-computable provided $\text{poly}(n)$ independent physical copies of $|\phi\rangle$ can be efficiently prepared to evaluate a bounded objective function.

Efficiently computable objective function examples include:

- (2.i) Calculating the expected value of Hamiltonian's in the Pauli basis known to have bounded cardinality.
- (2.ii) Calculating the expected value of the $\mathcal{O}(\ln n)$ generated ring without inverses with \mathcal{H} of bounded cardinality

$$\{\mathcal{H}, \cdot, +, \mathbb{R}\} \quad (4.7)$$

which includes the divergence $\mathbb{E}^2 = \langle \mathcal{H}^2 \rangle - \langle \mathcal{H} \rangle^2$ that vanishes if and only if the prepared state is an eigenstate of the Hamiltonian \mathcal{H} .

Acceptance (as follows) must be shown by providing a solution to the optimisation problem defined by the objective function.

Definition 56 (Accepting a Quantum State). An objective function f *accepts* $|\phi\rangle$ when given $\mathcal{O}(\text{poly } n)$ copies of $|\phi\rangle$,

$$f(|\phi\rangle^{\times \mathcal{O}(\text{poly}(n))}) = f(|\phi\rangle, |\phi\rangle, \dots, |\phi\rangle) < \Delta \quad (4.8)$$

evaluates strictly less than a chosen real parameter $\Delta > 0$.

Remark 40. Appropriately bounded objective functions (Hamiltonians) from Chapter 1 are readily seen to represent Poly-computable objective functions. For example, consider some penalty function described by the following Hamiltonian of bounded cardinality

$$\mathcal{H} = \sum_{i < j} J_{ij} Z_i Z_j + \sum_i h_i Z_i. \quad (4.9)$$

Assume further that this Hamiltonian embeds some objective function $f(\mathbf{x})$. Then the quantum state $|\mathbf{x}\rangle$ will minimize (4.9). This is shown by measuring (4.9) in the Z basis and recovering \mathbf{x} and calculating $f(\mathbf{x})$ classically from the description of \mathcal{H} .

The following theorem (13) applies rather generally to variational quantum algorithms that minimise energy by adjusting a variational state to cause an objective function to accept. Herein acceptance will imply the preparation of a quantum state, which begs to establish the following.

Theorem 13 (Energy to Overlap Variational Stability Lemma—[10]). Let non-negative $\mathcal{H} = \mathcal{H}^\dagger \in \mathcal{L}(\mathbb{C}_d)$ have spectral gap Δ and non-degenerate ground eigenvector $|\psi\rangle$ of eigenvalue 0. Consider then a unit vector $|\phi\rangle \in \mathbb{C}_d$ such that

$$\langle \phi | \mathcal{H} | \phi \rangle < \Delta \quad (4.10)$$

it follows that

$$1 - \frac{\langle \phi | \mathcal{H} | \phi \rangle}{\Delta} \leq |\langle \phi | \psi \rangle|^2 \leq 1 - \frac{\langle \phi | \mathcal{H} | \phi \rangle}{\text{Tr}\{\mathcal{H}\}}. \quad (4.11)$$

Proof. (Theorem 13). Let $\{|\psi_x\rangle\}_{x=0}^{d-1}$ be the eigenbasis of \mathcal{H} . The integer variable x monotonically orders this basis by corresponding eigenvalue

$$\lambda_0 = 0 \leq \lambda_1 = \Delta \leq \dots . \quad (4.12)$$

Consider $|\phi\rangle = \sum c_x |\psi_x\rangle$ and $P(x) = |c_x|^2$ with $c_x = \langle \psi_x | \phi \rangle$. Then

$$\langle \phi | \mathcal{H} | \phi \rangle = \sum_{-0} P(x) \lambda(x) = \sum_{-0} P(x) \lambda(x) \quad (4.13)$$

Consider $1 = \langle \phi | \phi \rangle = \sum P(x) = P(0) + \sum_{-0} P(x)$. So $1 - P(0) \geq P(x) \quad \forall x \neq 0$. Hence

$$\sum_{-0} P(x) \lambda(x) \leq (1 - P(0)) \sum_{-0} \lambda(x) \quad (4.14)$$

From $\lambda(0) = 0$ we have that

$$(1 - P(0)) \sum \lambda(x) = (1 - P(0)) \cdot \text{Tr}\{\mathcal{H}\} = (1 - |\langle \psi_0 | \phi \rangle|^2) \cdot \text{Tr}\{\mathcal{H}\} \quad (4.15)$$

from which the upper bound follows.

For the lower bound, starting from the assumption $\langle \phi | \mathcal{H} | \phi \rangle < \Delta$ we consider a function of the integers $\tilde{\lambda}(x) \cdot \Delta = \lambda(x) \quad \forall x > 0$. Then

$$\langle \phi | \mathcal{H} | \phi \rangle = \sum_{-0} P(x) \lambda(x) = \sum_{-0} P(x) \lambda(x) = \Delta \cdot \sum_{-0} P(x) \tilde{\lambda}(x) \quad (4.16)$$

hence $\sum_{-0} P(x) \tilde{\lambda}(x) < 1$ as $\tilde{\lambda}(x) \geq 1, \forall x \geq 0$. We then have that

$$\sum_{-0} P(x) \leq \sum_{-0} P(x) \tilde{\lambda}(x) < 1 \quad (4.17)$$

and so $1 - \sum_{-0} P(x) \tilde{\lambda}(x) \geq 0$. Hence,

$$1 = \langle \phi | \phi \rangle = P(0) + \sum_{-0} P(x) \leq P(0) + \sum_{-0} P(x) \tilde{\lambda}(x) \quad (4.18)$$

We establish that

$$1 \leq P(0) + \sum_{-0} \frac{P(x) \lambda(x)}{\Delta} = |\langle \psi_0 | \phi \rangle|^2 + \frac{\langle \phi | \mathcal{H} | \phi \rangle}{\Delta} \quad (4.19)$$

which leads directly to the desired lower bound. \square

4.3 Variational quantum search

Here we will consider a two-level variant of the alternating operator ansatz following [110]. The procedure can be readily adapted to 3-SAT (as first developed in [96]). Quantum search has been studied in the variational framework in several recent studies, including [111].

Definition 57. In this section, we let

1. n be the number of qubits and
2. $N = 2^n$ be the size of the search space,
3. where we are searching for a particular bitstring $\boldsymbol{\omega} = \omega_1, \omega_2, \omega_3, \dots, \omega_n$.

Remark 41 (Defining QAOA Hamiltonians). As in [96] and elsewhere, QAOA works by sequencing a pair of operators. One driver (defined in the X -basis typically) and the other defined as the classical penalty function we seek to minimize.

To specify the quantum algorithm, as in [110] we consider a pair of rank-1 projectors (4.20).

$$P_{\boldsymbol{\omega}} = |\boldsymbol{\omega}\rangle\langle\boldsymbol{\omega}| \quad (4.20)$$

$$P_{+} = |+\rangle\langle+|^{\otimes n} = |\mathbf{s}\rangle\langle\mathbf{s}| \quad (4.21)$$

where

$$|\mathbf{s}\rangle = \frac{1}{\sqrt{N}} \sum_{\mathbf{x} \in \{0,1\}^n} |\mathbf{x}\rangle. \quad (4.22)$$

To find $|\boldsymbol{\omega}\rangle$, we consider a split-operator variational ansatz, formed by sequencing a pair of operators (see Remark 41). These operators prepare a state $|\varphi(\boldsymbol{\alpha}, \boldsymbol{\beta})\rangle$, with vectors $\boldsymbol{\alpha} = \alpha_1, \alpha_2, \dots, \alpha_p$ and $\boldsymbol{\beta} = \beta_1, \beta_2, \dots, \beta_p$. We seek to minimize the orthogonal complement of the subspace for the searched string (4.23).

$$P_{\boldsymbol{\omega}^{\perp}} = \mathbb{1} - P_{\boldsymbol{\omega}} \quad (4.23)$$

Remark 42. We sometimes call (4.21) the driver Hamiltonian or diffusion operator.

The state is varied to minimize this orthogonal component (4.24).

$$\min_{\boldsymbol{\alpha}, \boldsymbol{\beta}} \langle \varphi(\boldsymbol{\alpha}, \boldsymbol{\beta}) | P_{\omega^\perp} | \varphi(\boldsymbol{\alpha}, \boldsymbol{\beta}) \rangle \geq \min_{|\phi\rangle} \langle \phi | P_{\omega^\perp} | \phi \rangle \quad (4.24)$$

To prepare the state we develop the sequence (4.25).

$$|\varphi(\boldsymbol{\alpha}, \boldsymbol{\beta})\rangle = \mathcal{K}(\beta_p) \mathcal{V}(\alpha_p) \cdots \mathcal{K}(\beta_1) \mathcal{V}(\alpha_1) |s\rangle \quad (4.25)$$

Where the operators are defined as (4.26) and (4.27).

$$\mathcal{V}(\alpha) \stackrel{\text{def}}{=} e^{i\alpha P_\omega} \quad (4.26)$$

$$\mathcal{K}(\beta) \stackrel{\text{def}}{=} e^{i\beta P_+} \quad (4.27)$$

The length of the sequence is $2p$, for integer p . We consider now the following problems on which the variational algorithm will work.

Example 28 (Standard Oracle, Variational Diffusion). Using a computer program, one can find p angles $\boldsymbol{\beta} = (\beta_1, \dots, \beta_p)$ and fixing $\boldsymbol{\alpha} = (\alpha_1 = \pi, \dots, \alpha_p = \pi)$ to minimize (4.24) via the sequence (4.25), given the operators (4.26) and (4.27).

In this problem (Example 28) we have fixed the standard black-box oracle of Grover's algorithm and the algorithm optimizes to find the angles in the diffusion operator. We will also consider a restricted variational problem where all the diffusion operators must apply the same variational angle.

Example 29 (Standard Oracle, Restricted Variational Diffusion). As in Example 28, using a computer program one can find p angles $\boldsymbol{\beta} = (\beta, \dots, \beta)$ and choosing $\boldsymbol{\alpha} = (\alpha_1 = \pi, \dots, \alpha_p = \pi)$.

A third problem to which we will apply the variational algorithm is considering both the oracle and the diffusion angles as variational parameters. We consider in this case a phase matching condition, meaning that angles are restricted to be equal.

Example 30 (Restricted Variational Oracle and Diffusion). As Example 28 we will use a computer program to find $2p$ angles $(\boldsymbol{\alpha}, \boldsymbol{\beta}) = (\alpha_1, \dots, \alpha_p, \beta_1, \dots, \beta_p)$ with the restriction $\boldsymbol{\beta} = \boldsymbol{\alpha} = \alpha_1, \alpha_2, \dots, \alpha_p$ and $\alpha_1 = \alpha_2 = \dots = \alpha_p$.

Finally we consider variations of the oracle angles of the oracle and the diffusion operator separately.

Example 31 (Variational Oracle and Diffusion). As problem 28 we will use a computer program to find $2p$ angles $(\boldsymbol{\alpha}, \boldsymbol{\beta}) = (\alpha_1, \dots, \alpha_p, \beta_1, \dots, \beta_p)$.

Remark 43. We also call this last variation (Example 31) a two-level split operator ansatz. Note that the angles obtained in (4.24) only minimize the selected cost function for a particular number of qubits. Once the number of qubits change, the angles obtained in the minimization do not necessarily give the highest probability to find the searched item. Also it's important to note that these angles are independent of $\boldsymbol{\omega}$, if we fix the number of qubits in the problem and run the algorithm with a particular set of angles, then these angles give the same probability no matter the $\boldsymbol{\omega}$ we are looking for. As stated earlier our objective is to see if variational algorithms are able to recover Grover's algorithm, for this we need a way of comparing both algorithms.

Example 32. To compare these variational algorithms with Grover's algorithm, consider the two-level split-operator ansatz case for $p = 1$. Here we recover Grover's operators as the optimal solution for finding a particular string. To prove this, first note that there is only one pair of angles (α, β) , so we consider (4.26) and (4.27) directly. Since $|\boldsymbol{\omega}\rangle\langle\boldsymbol{\omega}|$ is a projector we can expand (4.26).

$$\begin{aligned} \mathcal{V}(\alpha) &= e^{i\alpha|\boldsymbol{\omega}\rangle\langle\boldsymbol{\omega}|} = \mathbb{1} + (e^{i\alpha} - 1)|\boldsymbol{\omega}\rangle\langle\boldsymbol{\omega}| \\ &= \mathbb{1} - (e^{i\tilde{\alpha}} + 1)|\boldsymbol{\omega}\rangle\langle\boldsymbol{\omega}| \end{aligned} \quad (4.28)$$

Where in the last step we have defined $\tilde{\alpha} = \alpha - \pi$. Now we expand the unitary for the driver Hamiltonian (4.29).

$$\begin{aligned} \mathcal{K}(\beta) &= e^{i\beta|\mathbf{s}\rangle\langle\mathbf{s}|} \\ &= H^{\otimes n}(\mathbb{1} + (e^{i\beta} - 1)|\mathbf{0}\rangle\langle\mathbf{0}|)H^{\otimes n} \\ &\sim H^{\otimes n}(-\mathbb{1} + (e^{i\tilde{\beta}} + 1)|\mathbf{0}\rangle\langle\mathbf{0}|)H^{\otimes n} \\ &= (e^{i\tilde{\beta}} + 1)|\mathbf{s}\rangle\langle\mathbf{s}| - \mathbb{1} \end{aligned} \quad (4.29)$$

Where \sim relates the equivalence class of operators indiscernible by a global phase, H is the Hadamard gate and $\tilde{\beta} = \beta - \pi$. Notice that for $\tilde{\alpha} = \tilde{\beta} = 0$ Grover's oracle and diffusion operators are recovered.

Example 33. To see that the variational search includes Grover's operators for the case $p > 1$, let us impose $\alpha_1 = \alpha_2 = \dots = \alpha_p$ and $\beta_1 = \beta_2 = \dots = \beta_p$. In Figure 4.2 and Figure 4.3 the circuits for the oracle and the diffusion operator respectively are shown. If i pairs of operators (4.26) and (4.27) are applied to the initial state $|\mathbf{s}\rangle$ as in (4.25), then we write the prepared state as (4.30).

$$|\varphi_i\rangle = A_i \frac{1}{\sqrt{N-1}} \sum_{x \neq \omega} |x\rangle + B_i |\omega\rangle \quad (4.30)$$

$$A_{i+1} = \left(1 - \frac{2}{N}\right) A_i - 2 \frac{\sqrt{N-1}}{N} B_i \quad (4.31)$$

$$B_{i+1} = 2 \frac{\sqrt{N-1}}{N} A_i - \left(1 - \frac{2}{N}\right) B_i \quad (4.32)$$

We can relate the amplitudes of one step with the amplitudes of the next step with a recursion such as those that appear in (4.31) and (4.32); we express the effect of the operators for the variational search over the state as a matrix (4.33).

$$\begin{pmatrix} 1 + \frac{a(N-1)}{N} & -a(b+1) \frac{\sqrt{N-1}}{N} \\ -a \frac{\sqrt{N-1}}{N} & (b+1) \left(1 + \frac{a}{N}\right) \end{pmatrix} \quad (4.33)$$

Here $a = e^{i\alpha} - 1$ and $b = e^{i\beta} - 1$. Notice that for $a = b = -2$ the same relation between amplitudes at different steps in (4.31) and (4.32) up to a global phase in the definition of the Grover operators is obtained. Thus, the variational search space includes Grover's original algorithm. From this matrix it is also possible to see that if the target state is changed, then the angles found through the variational algorithm will give the same probabilities.

Remark 44 (Comparison with Grover). Grover's search is provably optimal in the large size limit. The success probability of Grover's algorithm goes from unity for two-qubits, decreases for three- and four-qubits and returns near unity for five-qubits then oscillates ever-so-close to unity, reaching unity in the infinite

qubit limit. The variational approach employed here found an experimentally discernible improvement of 5.77% and 3.95% for three- and four-qubits respectively as shown in Figure 4.4 [110].

Realization of diffusion and oracle circuits (Figures 4.2 and 4.3). Oracle and diffusion operators can be rewritten via n -body control gates as

$$\mathcal{V}(\alpha) = \bigotimes_{i=1}^n X_i^{1-\omega_i} \left(\mathbb{1}_{2^{n-1}} \oplus e^{i\alpha} \right) \bigotimes_{i=1}^n X_i^{1-\omega_i} \quad (4.34)$$

and

$$\mathcal{K}(\beta) = H^{\otimes n} X^{\otimes n} \left(\mathbb{1}_{2^{n-1}} \oplus e^{i\beta} \right) X^{\otimes n} H^{\otimes n} \quad (4.35)$$

and therefore can be realized using $O(n^2)$ basic gates [112]. Here operator $\mathbb{1}_{2^{n-1}}$ is the $(2^n - 1) \times (2^n - 1)$ identity matrix. (See also the gate realizations in [113] which can be readily bootstrapped to realize the circuits in Figures 4.2 and 4.3).

4.4 Extending Kitaev's k -controlled U factorization

We have employed k -controlled gates when considering QAOA (see Figure 4.2 and 4.3). A classical problem of importance is how to realize these gates as a sequence of two-body gates. Here we were inspired by work appearing in the book [7] and with some small but notable improvements present a competitive method to realize such gates. We quantify the scaling of the method exactly.

Remark 45. The decomposition of arbitrary n -qubit gates into universal gate sets has been studied extensively [112; 114]. Here we develop just a decomposition for k -controlled unitary gates. Our method is inspired by a Toffoli and related factorization(s) appearing in the book [7]—see Figure 4.5.

Remark 46. The results of the method are competitive with the best contemporary findings. See for example the results in [115] which argue that a Toffoli gate requires a total of five two-qubit gates.

We will begin by recalling some basic facts about the Pauli group which will later will be used to define a new factorization for k -controlled X gates.

N	$100 \times (P_{\text{variational}} - P_{\text{Grover}})/P_{\text{Grover}}$	step p_{max}	angle
2^3	5.77%	2	2.12^{rad}
2^4	3.95%	3	2.19^{rad}
2^5	0.08%	4	2.76^{rad}
2^6	0.34%	6	2.60^{rad}

Table 5 — Percentage increase between the highest probability for finding the solution after measurement obtained in Grover and the two-level variational ansatz [110]. Percent given as a function of $N = 2^n$ where n is the number of qubits and at step p_{max} on which the probability of finding the solution string is maximum. The same table is obtained for the two-level split-operator ansatz with one angle or with $2p$ angles. Both the diffusion and oracle use the same angle. (Table originally from [110]).

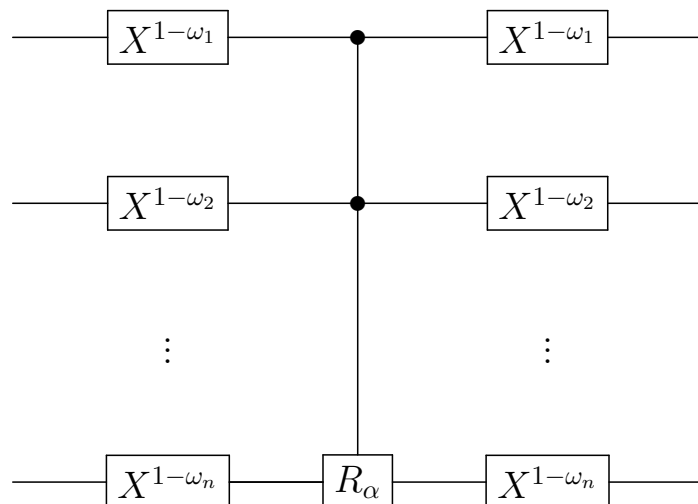


Figure 4.2 — Oracle circuit used in Grover search and its variational incarnation.

Remark 47 (Pauli group algebra). The complete properties of the Hermitian Pauli (group-) algebra can be derived from the following identity:

$$\sigma_i \sigma_j = \mathbb{1} \delta_{ij} + \imath \varepsilon^{ijk} \sigma_k \quad (4.36)$$

Where σ_i corresponds to an element in the Pauli group algebra. In particular it is easy to see that for $i \neq j$

$$\{\sigma_i, \sigma_j\} = 0, \quad (4.37)$$

where $\{\cdot, \cdot\}$ is the anti-commutator.

Definition 58 (Group commutator). Consider unitaries $U, K \in \mathcal{L}(A)$. Then the group commutators of U and K is defined as

$$[U, K] = UKU^\dagger K^\dagger. \quad (4.38)$$

Lemma 2. For $i \neq j$ and $t \in \mathbb{R}$

$$\sigma_i e^{-\imath t \sigma_j} \sigma_i = e^{\imath t \sigma_j}. \quad (4.39)$$

Proof. Consider that

$$\sigma_i e^{-\imath t \sigma_j} \sigma_i = \cos(t) \mathbb{1} - \imath \sin(t) \sigma_i \sigma_j \sigma_i. \quad (4.40)$$

Using the anti-commutator property of (4.37), we establish that $\sigma_i \sigma_j \sigma_i = -\sigma_j$. Hence,

$$\sigma_i e^{-\imath t \sigma_j} \sigma_i = \cos(t) \mathbb{1} + \imath \sin(t) \sigma_j = e^{\imath t \sigma_j}. \quad (4.41)$$

□

Lemma 3. For $i \neq j$ and using (4.39)

$$[\sigma_i, e^{-\imath t \sigma_j}] = \sigma_i e^{-\imath t \sigma_j} \sigma_i e^{\imath t \sigma_j} = e^{\imath 2t \sigma_j}. \quad (4.42)$$

Proof. From Lemma 2, we establish that

$$\sigma_i e^{-\imath t \sigma_j} \sigma_i e^{\imath t \sigma_j} = e^{\imath t \sigma_j} e^{\imath t \sigma_j} = e^{\imath 2t \sigma_j}. \quad (4.43)$$

□

Now that we have established the necessary facts of the Pauli group algebra, we define the notation that we will use for the decomposition.

Definition 59 (Controlled gates). Denote by U_j^i the gate U acting on qubit j and controlled by qubit i . Specifically let X be the NOT gate and V be its square-root. Then X_j^i is the CN gate and V_j^i is the controlled- V gate (it is also true that $V_j^i = \sqrt{X_j^i}$). We will denote qubit with label j to initially be in state $|j\rangle$. If the control qubits are given by indices i_1, \dots, i_k and the target qubit is j , then we denote this gate as $U_j^{i_1 i_2 \dots i_k}$.

Remark 48 (Unwanted phase factor). One needs to keep in mind that $X, V \notin \mathbf{SU}(2)$. Indeed, $\det X = -1$, $\det V = i$. Exponentials as $e^{it\sigma_i}$ all belong to $\mathbf{SU}(2)$ and cannot emulate X or its roots without adding an extra multiplier. For this reason, there will be trailing phase multipliers in what follows. Kitaev's gate choice also had this feature [7].

Before fully defining our decomposition, we start by showing a specific case, the Toffoli gate (Figure 4.5) and the k -controlled X gate (Figure 4.7).

Lemma 4 (Toffoli gate). The Toffoli gate, or using notation of Definition 59, the gate $X_b^{a_1 a_2}$, has a factorization into four control gates as

$$X_b^{a_1 a_2} = V_b^{a_1} Z_b^{a_2} (V^\dagger)_b^{a_1} Z_b^{a_2}. \quad (4.44)$$

The circuit for the decomposition of the Toffoli gate is shown in Figure 4.5. Note that from the previous decomposition, we can also give a factorization for the gate $Z_b^{a_1 a_2}$ by multiplying from and left and right by a Hadamard gate acting on qubit b as

$$Z_b^{a_1 a_2} = \sqrt{Z}_b^{a_1} X_b^{a_2} (\sqrt{Z}^\dagger)_b^{a_1} X_b^{a_2}. \quad (4.45)$$

Proof. All gates in the factorization act in part on the same qubit b . We just need to check the resulting operator over qubit b given the different combinations for $a_1, a_2 \in \{0,1\}^2$. It is clear that for $a_1, a_2 \in \{00,01,10\}$ the result is an identity operation on qubit b . To prove that $VZV^\dagger Z = X$, consider Lemma 3. The result follows by replacing $\sigma_i = Z$, $\sigma_i = X$ and $t = \pi/4$. \square

Lemma 5. For a k -controlled $X_b^{a_1, a_2, \dots, a_k}$ gate, we have the following decomposition. Assume first that k is even, thus $k = 2q$ with q a natural number. Then consider the following factorization (4.46).

$$X_b^{a_1 \dots a_{2q}} = V_b^{a_1 \dots a_q} Z_b^{a_{q+1} \dots a_{2q}} (V^\dagger)_b^{a_1 \dots a_q} Z_b^{a_{q+1} \dots a_{2q}} \quad (4.46)$$

If k is odd, then $k = 2q + 1$. In this case we consider the following factorization (4.47).

$$X_b^{a_1 \dots a_{2q+1}} = V_b^{a_1 \dots a_q} Z_b^{a_{q+1} \dots a_{2q+1}} (V^\dagger)_b^{a_1 \dots a_q} Z_b^{a_{q+1} \dots a_{2q+1}} \quad (4.47)$$

The circuits for 3- and k -controlled X gate are shown in Figures 4.6 and 4.7.

Proof. The proof follows in the same way as in Lemma 4 but considering all possible bitstrings $a_1 \dots a_k \in \{0,1\}^k$. \square

Now we show the decomposition proposed for general k -controlled rotations in the X and Z axis (up to of course a controlled phase factor ι). Note that having defined a decomposition for this rotations, we can define a general decomposition for any k -controlled unitary.

Lemma 6. For a k -controlled X rotation acting on qubit b , $R_x(\theta)_b^{a_1, a_2, \dots, a_k}$, a factorization for k even follows as (4.48) where $k = 2q$.

$$R_x(\theta)_b^{a_1 \dots a_{2q}} = R_x(\theta/2)_b^{a_1 \dots a_q} Z_b^{a_{q+1} \dots a_{2q}} R_x(-\theta/2)_b^{a_1 \dots a_q} Z_b^{a_{q+1} \dots a_{2q}} \quad (4.48)$$

For the k odd case we have the following (4.49).

$$R_x(\theta)_b^{a_1 \dots a_{2q+1}} = R_x(\theta/2)_b^{a_1 \dots a_q} Z_b^{a_{q+1} \dots a_{2q+1}} R_x(-\theta/2)_b^{a_1 \dots a_q} Z_b^{a_{q+1} \dots a_{2q+1}} \quad (4.49)$$

Proof. As in Lemma 5, we check for all possible bitstrings $a_1 \dots a_k \in \{0,1\}^k$. The important case is when $a_1 \dots a_k = 111 \dots 1$. Lemma 3 proves that

$$R_x(\theta) = R_x(\theta/2) Z R_x(-\theta/2) Z$$

which verifies the given decomposition. \square

Remark 49. From these decompositions (4.48) and (4.49), we can also obtain similar results for $R_z(\phi)_b^{a_1, a_2, \dots, a_k}$.

Lemma 7. The number of 2-controlled gates needed to implement a k -controlled X gate is given by the function $g(k)$ such that $g(1) = 1$ and defined recursively (4.50) or equivalently (4.51).

$$g(k) = \begin{cases} 4g(k/2) & k \text{ even} \\ 2g(\lfloor k/2 \rfloor) + 2g(\lfloor k/2 \rfloor + 1) & k \text{ odd} \end{cases} \quad (4.50)$$

$$g(k) = 2g(\lfloor k/2 \rfloor) + 2g(\lceil k/2 \rceil) \quad (4.51)$$

Proof. We just need to prove this by induction. For the initial condition we have that the 2-controlled gates are counted correctly. Assume the property holds for $1, 2, \dots, k-1$ and let us prove it for k . We want to prove that $g(k)$ counts the number of 2-controlled gates needed to implement the k -controlled X gate. By Lemma 6 we arrive at the decomposition for k even (4.48) where $k = 2q$.

$$R_x(\theta)_b^{a_1 \dots a_{2q}} = R_x(\theta/2)_b^{a_1 \dots a_q} Z_b^{a_{q+1} \dots a_{2q}} R_x(-\theta/2)_b^{a_1 \dots a_q} Z_b^{a_{q+1} \dots a_{2q}} \quad (4.52)$$

For k odd, we arrive at the following (4.49).

$$R_x(\theta)_b^{a_1 \dots a_{2q+1}} = R_x(\theta/2)_b^{a_1 \dots a_q} Z_b^{a_{q+1} \dots a_{2q+1}} R_x(-\theta/2)_b^{a_1 \dots a_q} Z_b^{a_{q+1} \dots a_{2q+1}} \quad (4.53)$$

For k even, $g(k) = 4g(k/2)$. Comparing with the decomposition from Lemma 6, we see that it counts correctly two-body gates. The same reasoning applies for k odd. \square

Lemma 8 (Solution of recursion (4.51)). The solution for the recurrence of $g(k)$, defined in (4.50) has the form

$$f(k) = 3k2^{\lfloor \log_2 k \rfloor} - 2^{1+2\lfloor \log_2 k \rfloor}. \quad (4.54)$$

Proof. Note that if $k = 2^p$ then $g(k) = f(k) = k^2$. Now we show that when $2^p \leq k \leq 2^{p+1}$ we have $g(k) = f(k) = 3k2^p - 2^{1+2p}$.

To prove this for g , we proceed again by strong induction. The base case is trivial. Assume then that k is even. Then,

$$g(k) = 4g(k/2) = 4[3k2^{p-1} - 2^{1+2(p-1)}] = 3k2^p - 2^{1+2p}. \quad (4.55)$$

When k is odd, we have

$$\begin{aligned} g(k) &= 2g(\lfloor k/2 \rfloor) + 2g(\lfloor k/2 \rfloor + 1) \\ &= [3(k-1)2^{p-1} - 2^{2p}] + [3(k+1)2^{p-1} - 2^{2p}] = 3k2^p - 2^{1+2p}. \end{aligned} \quad (4.56)$$

Which establishes the property for g . When $2^p \leq k \leq 2^{p+1}$, then

$$f(k) = 3k2^p - 2^{1+2p}$$

and thus $g(k) = f(k)$. □

Lemma 9 (Lower bound for scaling of g). The function $g(k)$ defined as in (4.50) has an asymptotic lower bound that scales as $\Omega(k^2)$.

Proof. Let $g(k)$ be defined as (4.50). We proceed by strong induction. Note first that $1^2 \leq g(1)$ and $2^2 \leq g(2)$. Assume that the property holds for $g(k-1), g(k-2), \dots, g(1)$. Consider the cases k even and k odd separately. For k even:

$$g(k) = 4g(k/2) \geq 4(k/2)^2 = k^2. \quad (4.57)$$

For k odd:

$$g(k) \geq 2(\lfloor k/2 \rfloor)^2 + 2(\lfloor k/2 \rfloor + 1)^2 \geq 2(\lfloor k/2 \rfloor)^2 + k^2 \geq k^2. \quad (4.58)$$

Since for every $k > 0$, $g(k) \geq k^2$ we conclude $g(k) = \Omega(k^2)$. □

Lemma 10 (Upper bound for scaling of g). The function $g(k)$ defined as in (4.50) has an asymptotic upper bound that scales as $\mathcal{O}(k^2)$.

Proof. We use the solution of the recursion $f(k) = 3k2^{\lfloor \log_2 k \rfloor} - 2^{1+2\lfloor \log_2 k \rfloor}$ to bound the scaling for the number of gates. Notice that

$$f(k) = 3k2^{\lfloor \log_2 k \rfloor} - 2^{1+2\lfloor \log_2 k \rfloor} \leq 3k2^{\log_2 k} - 2^{1+2(\log_2 k - 1)} = \frac{5}{2}k^2. \quad (4.59)$$

Thus $f(k) = \mathcal{O}(k^2)$. □

4.5 QAOA vs optimization by adiabatic and quantum annealing

Here we will briefly discuss another form of optimization, known now as quantum annealing and closely related to adiabatic quantum optimization. Several variational algorithms were inspired by algorithms that have their roots in the adiabatic model of quantum computation.

Remark 50. We must recall that the complete dynamics of a physical system is given by the Schrödinger equation

$$i\hbar \frac{d}{dt} |\psi(t)\rangle = \mathcal{H}(t) |\psi(t)\rangle, \quad (4.60)$$

where $\mathcal{H}(t)$ is the Hamiltonian of the system and $|\psi(t)\rangle$ is the state of the system at time t . The evolution of the Hamiltonian induces the unitary operator $U(t)$. In the case of a time independent Hamiltonian, the unitary evolution can be expressed as $U(t) = \exp\{-it\mathcal{H}\}$ for time-independent \mathcal{H} .

Informally, the adiabatic theorem states that when the ground state of a system evolves under a time-dependent Hamiltonian which is varied slowly enough, the system tends to remain in its lowest energy state. In other words, starting in an easy to prepare ground state of Hamiltonian \mathcal{H}_0 , we slowly transform \mathcal{H}_0 to some final Hamiltonian \mathcal{H}_f . In doing so, provided the adiabatic theorem is satisfied, ensure that we evolve to the ground state of \mathcal{H}_f . Here \mathcal{H}_f can embed a problem instance, solved by e.g. finding the ground state.

Remark 51. In the framework of adiabatic quantum computation, the quantum mechanical system is

1. Described by the Hamiltonian \mathcal{H}_0 at time $t = 0$.
2. Then the system is slowly evolved into the final Hamiltonian \mathcal{H}_f .
3. We set the final Hamiltonian \mathcal{H}_f such that finding the ground state of \mathcal{H}_f is equivalent to a minimization problem of a function

$$f : \{0,1\}^n \rightarrow \mathbb{R}. \quad (4.61)$$

As is typical, the step (3.) above is used to give an explicit form of the final Hamiltonian as

$$\mathcal{H}_f = \sum_{z \in \{0,1\}^n} f(z) |z\rangle \langle z|, \quad (4.62)$$

for a binary string z . The choice of the initial Hamiltonian \mathcal{H}_0 is independent of the solution of the problem and will be such that it is not diagonal in the computational basis. One example is to choose \mathcal{H}_0 to be diagonal in the Hadamard basis,

$$\mathcal{H}_0 = \sum_{z \in \{0,1\}^n} h(z) |\hat{z}\rangle \langle \hat{z}|, \quad (4.63)$$

where $|\hat{z}\rangle$ are the state of $|z\rangle$ in Hadamard basis and $h(0^n) = 0$ and $h(z) \geq 1$ for all $z \neq 0^n$. The time dependent Hamiltonian $\mathcal{H}(s)$ can be defined as

$$\mathcal{H}(s) = (1 - s)\mathcal{H}_0 + s\mathcal{H}_f, \quad s \in [0,1]. \quad (4.64)$$

When s varies from $0 \rightarrow 1$ the Hamiltonian changes from $\mathcal{H}_0 \rightarrow \mathcal{H}_f$. By the adiabatic theorem, the initial ground state, $|\psi_0\rangle$ is mapped to the global minimum of the function f .

4.5.1 Approximating adiabatic evolution

Remark 52. The state preparation takes inspiration from the quantum adiabatic algorithm, where a system is initialized in an easy to prepare ground state of a local Hamiltonian $\mathcal{H}_x = \sum_i \sigma_x^{(i)}$, the driver Hamiltonian, which is then slowly transformed to the problem Hamiltonian, \mathcal{V} [116]. As we will see, Trotterization of this procedure gives a long QAOA sequence.

Remark 53. One can discretize the continuous time evolution of \mathcal{H}_s from (4.64) by a quantum circuit [117].

Remark 54. The approximation is established in two steps following [117].

1. Discretize the evolution from \mathcal{H}_0 to \mathcal{H}_f by a finite sequence of Hamiltonians $\mathcal{H}'_1, \mathcal{H}'_2, \dots$ that gives rise to the same overall behavior.

2. Show how at any instant the combined Hamiltonian $\mathcal{H}'_j = (1-s)\mathcal{H}_0 + s\mathcal{H}_f$ is approximated by interleaving two simple unitary transformations.

Remark 55 (ℓ_2 induced operator norm). To express the error of our approximation, we use the ℓ_2 induced operator norm $\|\circ\|_2$:

$$\|M\|_2 \stackrel{\text{def}}{=} \max_{\|x\|_2=1} \|Mx\|_2.$$

Remark 56. The next lemma compares two Hamiltonians $\mathcal{H}(t)$ and $\mathcal{H}'(t)$ and their respective unitary transformations $U(T)$ and $U'(T)$.

Lemma 11 (Approximation Error [117]). Let $\mathcal{H}(t)$ and $\mathcal{H}'(t)$ be two time-dependent Hamiltonians for $0 \leq t \leq T$, and let $U(T)$ and $U'(T)$ be the respective unitary evolutions that they induce. If the difference between the Hamiltonians is limited by $\|\mathcal{H}(t) - \mathcal{H}'(t)\| \leq \delta$ for every t , then the distance between the induced transformations is bounded by $\|U(T) - U'(T)\| \leq \sqrt{2T\delta}$.

Proof. (Lemma 11 [117]). Let $\psi(t)$ and $\psi'(t)$ be the two state trajectories of the two Hamiltonians \mathcal{H} and \mathcal{H}' with initially $\psi(0) = \psi'(0)$. Then, for the inner product between the two states (with initially $\langle \psi'(0) | \psi(0) \rangle = 1$), we have

$$\frac{d}{dt} \langle \psi'(t) | \psi(t) \rangle = -i \langle \psi'(t) | (\mathcal{H}(t) - \mathcal{H}'(t)) | \psi(t) \rangle.$$

Because at any moment t we have $\|\psi(t)\| = \|\psi'(t)\| = 1$ and $\|\mathcal{H}(t) - \mathcal{H}'(t)\| \leq \delta$, we see that at $t = T$ the lower bound $|\langle \psi'(T) | \psi(T) \rangle| \geq 1 - T\delta$ holds. This confirms that for every vector ψ we have $\|U(T)|\psi\rangle - U'(T)|\psi\rangle\| \leq \sqrt{2T\delta}$. \square

Remark 57. Lemma 11 tells us how we might deviate from the ideal Hamiltonian $\mathcal{H}(t) \stackrel{\text{def}}{=} (1 - \frac{t}{T})\mathcal{H}_0 + \frac{t}{T}\mathcal{H}_f$, without introducing too much error to the induced evolution.

An approximation of the evolution, $\mathcal{H}_0 \rightarrow \mathcal{H}_f$ is given by a sequence of Hamiltonians,

$$\mathcal{H}'_1, \mathcal{H}'_2, \dots, \mathcal{H}'_r, \dots \quad (4.65)$$

where

$$\mathcal{H}'_r = (1 - r\Delta s)\mathcal{H}_0 + r\Delta s\mathcal{H}_f \quad (4.66)$$

and the parameter s is slightly varied from 0 to 1. In the limit of $\Delta s \rightarrow 0$, the sequence becomes infinite. The unitary evolution then becomes

$$U'(s = 1) = \cdots \exp\{-i\mathcal{H}'_r\} \cdots \exp\{-i\mathcal{H}'_1\} = \cdots U'_r \cdots U'_1 \quad (4.67)$$

A second approximation, using the Campbell-Baker-Hausdorff theorem gives,

$$\begin{aligned} U'_r &= \exp\{-i(1 - r\Delta s)\mathcal{H}_0\} \cdot \exp\{-ir\Delta s\mathcal{H}_f\} \\ &= W(1 - r\Delta s) \cdot V(r\Delta s) \end{aligned} \quad (4.68)$$

where $W(x) = \exp\{-ix\mathcal{H}_0\}$, and $V(x) = \exp\{-ix\mathcal{H}_f\}$. The evolution reduces to a sequence of unitary operations,

$$\begin{aligned} U'(s = 1) &= \cdots U'_r U'_{r-1} \cdots U'_2 U'_1 = & (4.69) \\ &= (\cdots V \cdot V \cdot V \cdot V \cdot V \cdots) (\cdots V \cdot V \cdot W \cdot V \cdot V \cdots) \cdots \\ &(\cdots V \cdot W \cdot V \cdot W \cdot V \cdots) \cdots (\cdots W \cdot V \cdot W \cdot V \cdot W \cdots) \cdots \\ &(\cdots W \cdot V \cdot W \cdot W \cdots) (\cdots W \cdot W \cdot W \cdot W \cdot W \cdots) \end{aligned}$$

acting on the ground state of \mathcal{H}_0 . It is clearly seen that the frequency of occurrence of W is increasing but the frequency of occurrence of V is decreasing. In the limit of $\Delta s \rightarrow 0$, the sequence in equation (4.69) becomes infinite long length with difference frequency of W 's and V 's. For a finite Δs , the sequence is not infinite and becomes an approximation of the adiabatic evolution. For a mathematically focused survey on the annealing processes (quantum and stochastic) see e.g. [118].

4.6 Low-depth quantum circuits

4.6.1 A combinatorial quantum circuit area law

Our construction of universal variational quantum computation has not considered whether a restricted form of ansatz is capable of universal quantum computation at some arbitrary depth as Lloyd [119] and others [120] have. Instead,

the objective function to be minimised is defined in terms of the unitary gates arising in the target circuit to be simulated. What ansatz states are then required to simulate a given target circuit?

This question appears to be difficult and not much is currently known. In the case of QAOA it was recently shown by myself and coauthors that the ability of an ansatz to approximate the ground state energy of a satisfiability instance worsens with increasing problem density (the ratio of constraints to variables) [98]. These related results however do not immediately apply to our interests here.

Towards our goals, we have included a derivation showing that reasonable depth circuits can saturate bipartite entanglement—the depth of these circuits scales with the number of qubits and also depends on the interaction geometry present in a given quantum processor. This result establishes a first relationship between an objective circuit (to be simulated) and a given ansatz state. Consider the following.

An ebit is a unit of entanglement contained in a maximally entangled two-qubit (Bell) state. A quantum state with q ebits of entanglement (quantified by any entanglement measure) contains the same amount of entanglement (in that measure) as q Bell states.

Lemma 12 (Combinatorial Quantum Circuit Area Law—[10]). Let c be the depth of 2-qubit controlled gates in the n -qubit hardware-efficient ansatz. Then the maximum possible number of ebits across any bipartition is

$$E_b = \min\{\lfloor n/2 \rfloor, c\}.$$

In a low-depth circuit, the underlying geometry of the processor heavily dictates c above. For example, for a line of qubits and for a ring, the minimal c required to possibly maximise E_b is $\sim n/2$ and $\sim n/4$ respectively. However, in the case of a grid, the minimal depth scales as $\sim \sqrt{n}/2$.

Hence, if we wish to simulate a quantum algorithm described by a low-depth circuit, having access to a grid architecture could provide an intrinsic advantage. Specifically, our combinatorial quantum circuit area law establishes that an objective circuit generating $k < \lfloor n/2 \rfloor$ ebits across every bipartition, must be simulated by an ansatz of at least minimal required circuit depth $\sim \sqrt{k}$ on a grid.

While this does establish a preliminary relationship, the general case remains unclear at the time of writing. For example, given a quantum circuit with application time t^* which outputs $|\psi\rangle$, what is the minimal $t(\varepsilon) \leq t^*$ for a control sequence (4.3) to provide an ε close 2-norm approximation to $|\psi\rangle$?

Here we will consider some properties of the quantum states that are accessible in NISQ era quantum information processing. Here we provide a bound for the minimal depth circuit (generated from the so called, hardware efficient Ansatz as used in recent experiments [109]) to possibly saturate bipartite entanglement on any bipartition. Understanding the computational power of these circuits represents a central open question in the field of quantum computation today. This appendix seeks to quantify contemporary capacities. We are currently not able to express the success probability as a function of the circuit depth required for an objective function to accept.

Definition 60 (Interaction graph). Consider the Hamiltonian

$$\mathcal{H} = \sum_{ij} J_{ij} A_i A_j + \sum_i b_i B_i + \sum_i c_i C_i.$$

The support matrix S of J_{ij} is defined to have the entries

$$S_{ij} = (J_{ij})^0$$

and is called the *interaction graph* of \mathcal{H} —a symmetric adjacency matrix. (Here we assume that a^0 (written alternatively as $(a)^0$) vanishes for real $a < \varepsilon$ and a^0 goes to unity for $a > \varepsilon$ for some finite (small) real ε cutoff.)

Remark 58. The interaction graph induces a space-time quantum circuit defined by a *tiling* on the multiplex from S .

Definition 61. A *Tiling* is a gate sequence acting on a multiplex network induced by S .

Remark 59. An active edge (node) will specify if neighboring edges (nodes) can be active. As a general rule, non-commuting terms must be active on different layers.

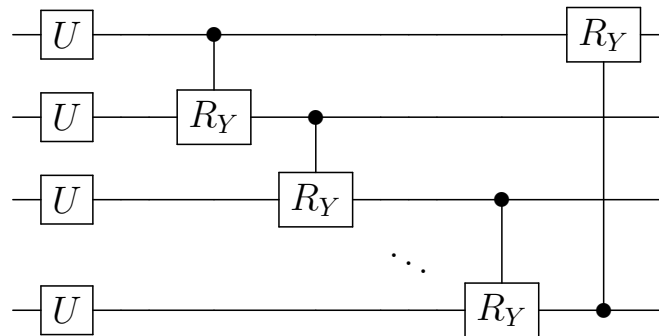
1. Qubits connect network layers by time propagation.
2. Nodes of S in each layer can be acted on by local gates.

3. Edges of S in each layer can be acted on by two-qubit gates.

As an example, consider the following multiplex network.

In the bottom layer of the multiplex graph in Figure 4.9, a sequence of red edges correspond to the application of two-body gates. In the next layer, the red (active) nodes correspond to local rotation gates being applied to all the qubits. Finally, in the top layer the commuting two-body gates are applied. The blue vertical edges represent time passing (going up on the page). The hardware-efficient ansatz is exactly such a tiling.

In terms of example circuits, we typically will be given a short repetitive sequence. For example, here we consider qubits interacting on a ring. A layer of local gates followed by a layer of two-body gates is as follows.



Where the local gates, U are arbitrary and the two-body gates are controlled Y rotations. What is the maximal bipartite entanglement that such a circuit can generate when acting on a product state?

To understand this question, let us consider a pure n -qubit state $|\psi\rangle$.

Definition 62. Bipartite rank is the Schmidt number (the number of non-zero singular values) across any reduced bipartite density state from $|\psi\rangle$ (i.e. $\lfloor n/2 \rfloor$ qubits).

Remark 60. Rank provides an upper-bound on the bipartite entanglement that a quantum state can support—a rank- k state has at most $\log_2(k)$ ebits of entanglement.

Definition 63. An ebit is a unit of entanglement contained in a maximally entangled two-qubit (Bell) state.

Remark 61. A quantum state with q ebits of entanglement (quantified by any entanglement measure) contains the same amount of entanglement (in that measure) as q Bell states.

Remark 62. If a task requires r ebits, it can be done with r or more Bell states, but not with fewer. Maximally entangled states in $\mathbb{C}^d \otimes \mathbb{C}^d$ have $\log_2(d)$ ebits of entanglement.

Now we arrive at what we call a *quantum circuit combinatorial area law*. It is the minimal depth circuit that possibly could saturate the bipartite entanglement with respect to any bipartition.

Lemma 13. Let c be the depth of 2-qubit controlled gates in the n -qubit hardware-efficient ansatz. Then the maximum possible number of ebits across any bipartition is

$$\min\{\lfloor n/2 \rfloor, c\}.$$

Remark 63 (Combinatorial Quantum Circuit Area Law). Minimal possible c saturating specific graphs are given in Table 6.


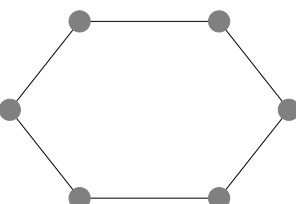
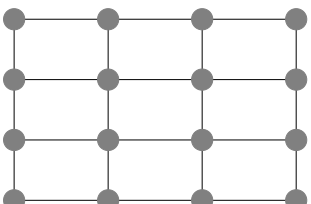
	line	ring	grid
interaction geometry			
saturating depth	$c \sim n/2$	$c \sim n/4$	$c \sim \sqrt{n}/2$

Table 6 — Minimal possible circuit depth c possibly saturating bipartite entanglement with respect to different interaction geometries.

4.7 Reachability deficits

In this section we explore a fundamental limitation discovered in [98] with coauthors. The QAOA algorithms that exploit variational state preparation to find approximate ground states of Hamiltonians encoding combinatorial optimization problems.

In particular we consider the Quantum Approximate Optimization Algorithm or QAOA [96]. As a means to study the performance of QAOA, we turn to constraint satisfiability—a tool with a successful history which was covered in detail in

§ 1 (see particularly § 1.5). Such problems are expressed in terms of N variables and M clauses (or constraints).

Remark 64. Recall from § 1.5, the density of such problem instances is the clause to variable ratio, the clause density $\alpha = M/N$. k -SAT clauses are randomly generated to form instances by uniformly selecting unique k -tuples from the union of a variable set (cardinality $n > k$) and its element wise negation. We consider random instances of the NP-complete decision problem, 3-SAT.

QAOA aims to approximate solutions to optimization version of this problem. Here we consider MAX-3-SAT which is NP-Hard for exact solutions and APX-complete for approximations beyond a certain ratio [121]. In these settings, the algorithm's limiting performance exhibits strong dependence on the problem density. As discovered in [98].

Let N be the number of variables in a SAT instance with M clauses. MAX-SAT solutions are the Boolean strings $\omega = \omega_1, \omega_2, \omega_3, \dots, \omega_N$ that violate the least number of clauses. Techniques discussed in § 1 map SAT instances into Hamiltonians,

$$\mathcal{H}_{\text{SAT}} = \sum_{l=1}^M \mathcal{P}(l), \quad (4.70)$$

where $\mathcal{P}(l)$ are rank-1 projectors acting on the l^{th} clause. It is easy to verify that the ground state energy of \mathcal{H}_{SAT} is representative of the minimum number of violated clauses.

The variational state generated by QAOA can be described as running a p -depth quantum circuit on the state $|+\rangle^{\otimes n}$,

$$|\psi(\boldsymbol{\gamma}, \boldsymbol{\beta})\rangle = \prod_{i=1}^p \mathcal{U}(\gamma_i, \beta_i) |+\rangle^{\otimes n}, \quad (4.71)$$

where

$$\mathcal{U}(\gamma_k, \beta_k) = \exp\{-i\beta_k \mathcal{H}_x\} \cdot \exp\{-i\gamma_k \mathcal{V}\}. \quad (4.72)$$

In order to approximate solutions of MAX-SAT, QAOA with standard settings, $\mathcal{H}_x = \sum_i \sigma_x^{(i)}$ and $\mathcal{V} = \mathcal{H}_{\text{SAT}}$, is used to calculate the energy approximation E_g^{QAOA} , where

$$E_g^{\text{QAOA}} = \min_{\boldsymbol{\gamma}, \boldsymbol{\beta}} \langle \psi(\boldsymbol{\gamma}, \boldsymbol{\beta}) | \mathcal{H}_{\text{SAT}} | \psi(\boldsymbol{\gamma}, \boldsymbol{\beta}) \rangle. \quad (4.73)$$

We numerically studied $f = E_g^{\text{QAOA}} - \min(\mathcal{V})$ as a function of clause density α , for a p -depth QAOA circuit on randomly generated 3-SAT instances (see Figure 4.10). Although increased depth versions achieve better approximations, the limiting performance exhibits a non-trivial dependence on the problem density. Based on this finding we formulate the following:

Definition 64. Let $|\psi\rangle$, be the ansatz states generated from a p -depth QAOA circuit as shown in (4.71). Then

$$f = \min_{\psi \in \mathcal{H}} \langle \psi | \mathcal{V} | \psi \rangle - \min_{\phi \in \mathcal{H}} \langle \phi | \mathcal{V} | \phi \rangle, \quad (4.74)$$

characterises the limiting performance of QAOA. The R.H.S. of equation (4.74) can be expressed as a function, $f(p, \alpha, n)$.

Proposition 20 (Reachability Deficit [98]). For $p \in \mathbb{N}$ and fixed problem size, $\exists \alpha > \alpha_c$ such that f from (4.74) is non-vanishing. This is a reachability deficit.

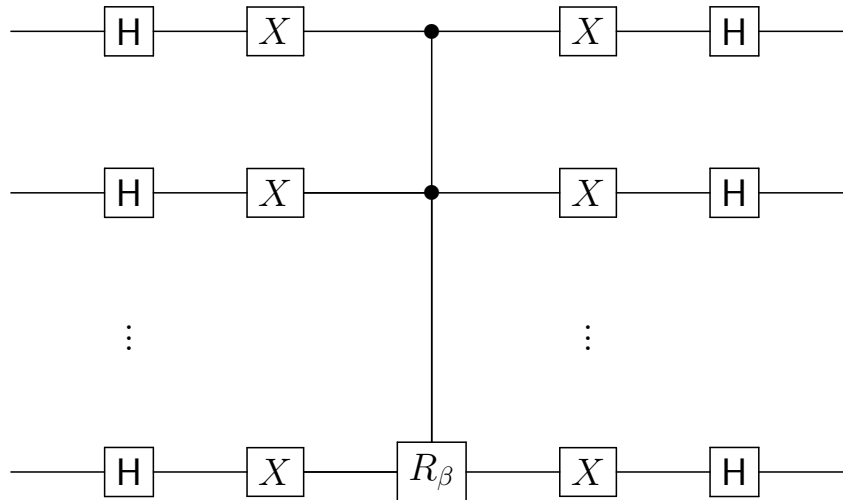


Figure 4.3 — Diffusion circuit used in Grover search and variational Grover search.

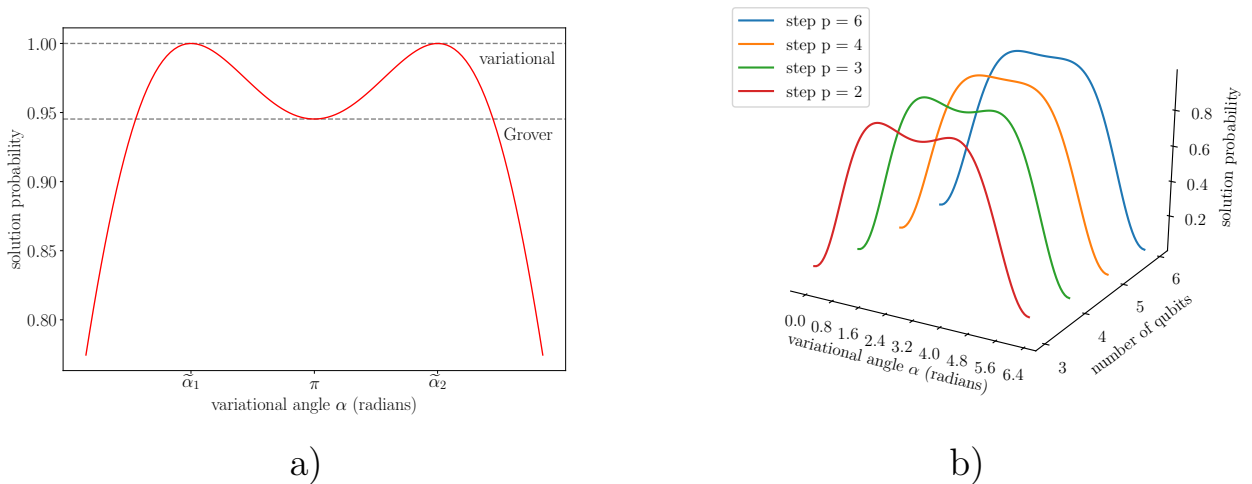


Figure 4.4 — (color online) (left) Grover’s algorithm takes a saddle point between two hills. Variational search recovers the hill peaks. Note that the valley becomes increasingly less pronounced past four qubits, providing negligible range for improvement. (right) Probability as a function of the variational angle for the 3 qubit case. Grover’s algorithm is recovered in the case $\alpha = \pi$, the variational algorithm obtains angles $\tilde{\alpha}_1 = 2.12^{\text{rad}}$ and $\tilde{\alpha}_2 = 2\pi - \tilde{\alpha}_1$. (Figure originally from [110]).

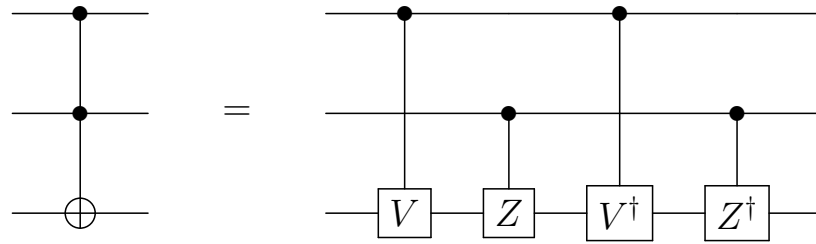


Figure 4.5 — Kitaev decomposition for 2-controlled (Toffoli) gate. The structure of the decomposition appeared in [7], where the gates (V, Z) are chosen here specifically as they satisfy the group commutator relation. [Note that the decomposition introduces a factor of i in front of the controlled X . This requires slight modification of algorithms in applications.]

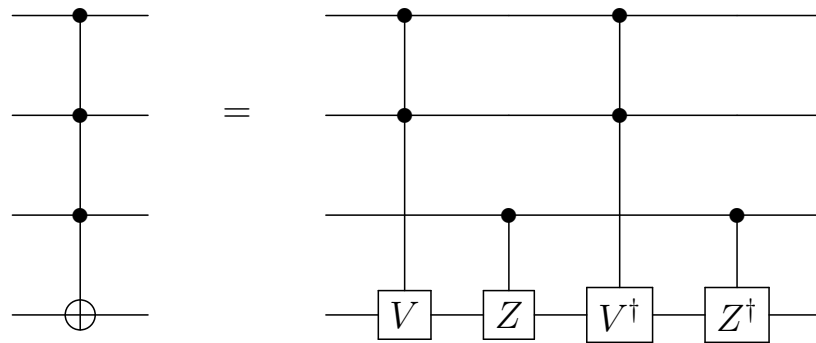


Figure 4.6 — Decomposition for 3-controlled gate. [Note that the decomposition introduces a factor of i in front of the controlled X . This requires slight modification of algorithms in applications.]

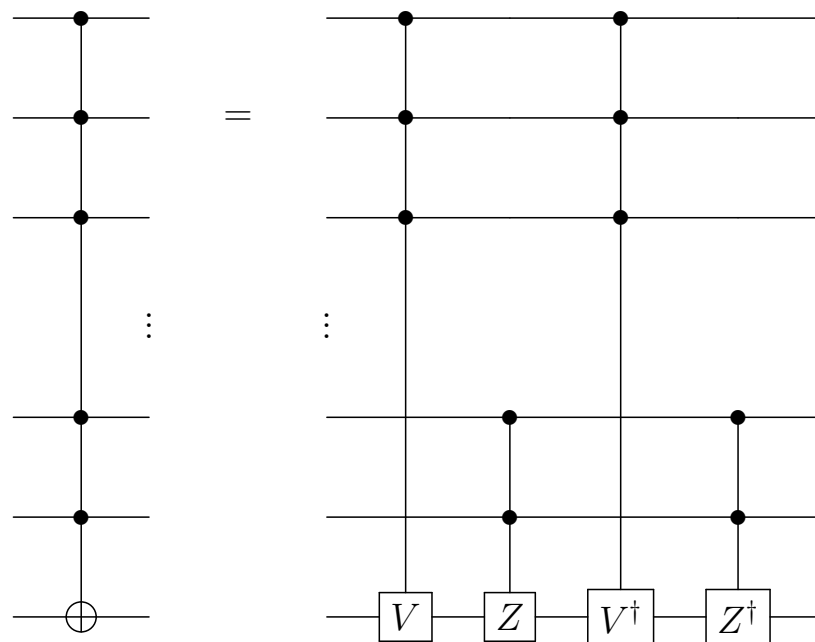


Figure 4.7 — Decomposition for k -controlled gate. [Note that the decomposition introduces a factor of i , yielding a controlled iX . This requires slight modification of algorithms in applications.]

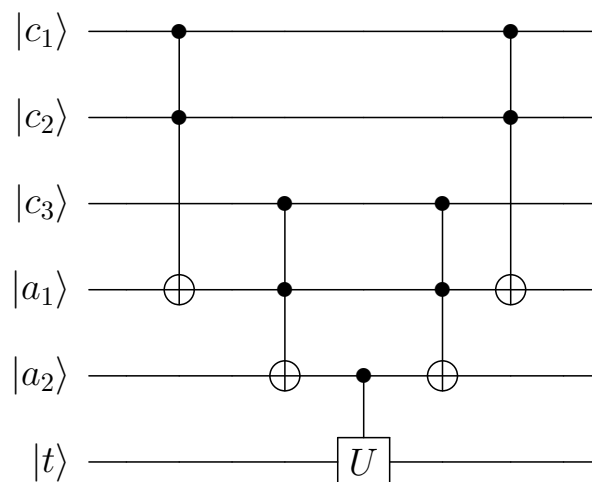


Figure 4.8 — Standard decomposition [6] for 3-CN gate which uses ancillary qubits labeled with states $|a_1\rangle$ and $|a_3\rangle$.

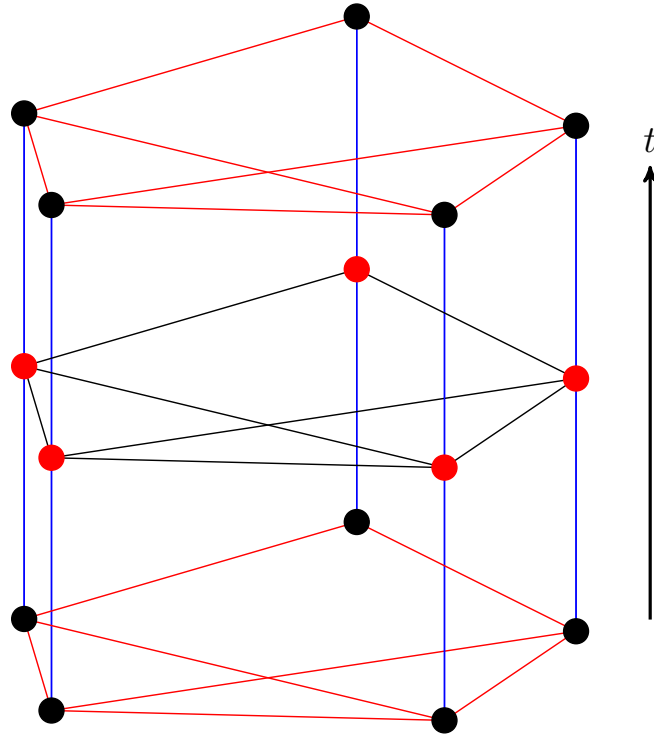


Figure 4.9 — Five qubits evolve as time goes up on the page. At $t = 0$, commuting interaction terms (red edges) are applied between the qubits. At $t = 1$ local gates (red nodes) are applied to each of the qubits.

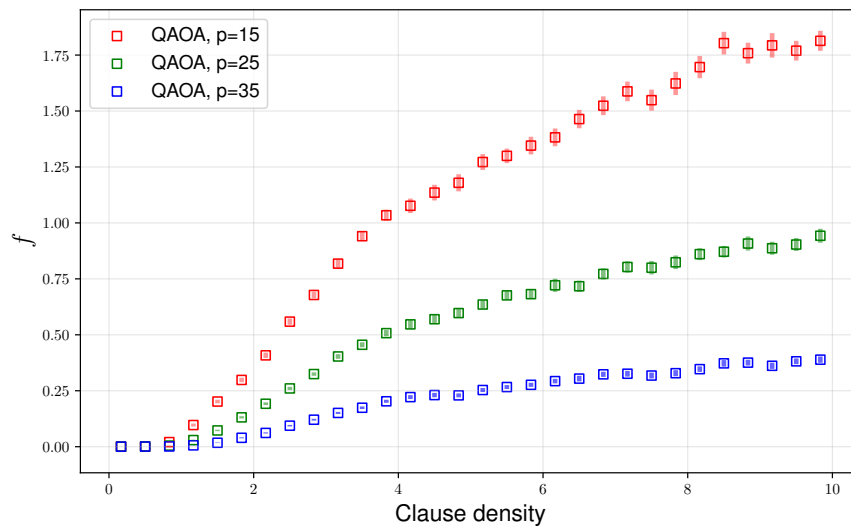


Figure 4.10 — $f = E_g^{\text{QAOA}} - \min(\mathcal{H}_{\text{SAT}})$ vs clause density for 3-SAT for differing QAOA depths. Squares show the average value obtained over 100 randomly generated instances for $n = 6$ with error bars indicating the standard error of mean. Figure taken from [98].

Chapter 5. Universal variational quantum computation

In Chapter 4 we considered variational quantum search and optimization. Here we address a different problem. We wish to simulate the output of an L gate quantum circuit acting on the n -qubit product state $|0\rangle^{\otimes n}$. We have access to p appropriately bounded and tunable parameters to prepare and vary over a family of quantum states. All coefficients herein are assumed to be accurate to not more than $\text{poly}(n)$ decimal places. We will define an objective function that when minimized will produce a state close to the desired quantum circuit output. We will provide a solution to the minimization problem.

5.1 Notions of quantum computational universality

There are different notions of *computational universality* in the literature. A strong notion is algebraic, wherein a system is called universal if its generating Lie algebra is proven to span $\mathfrak{su}(2^n)$ for n qubits. Here we call this *controllability*. An alternative notion is that of *computational universality*, in which a system is proven to emulate a universal set of quantum gates—which implies directly that the system has access to any polynomial time quantum algorithm on n -qubits (the power of quantum algorithms in the class BQP). Evidently these two notions can be related (or even interrelated): by proving that a controllable system can efficiently simulate a universal gate set, a controllable system becomes computationally universal. It is conversely anticipated by the strong Church-Turing-Deutsch principle [3], that a universal system can be made to simulate any controllable system.

The present chapter follows the work I did in [10], where we assume access to control sequences which can create quantum gates such as [43; 122; 123]. Given a quantum circuit of L gates, preparing a state

$$|\psi\rangle = \prod_{l=1}^L U_l |0\rangle^{\otimes n}$$

for unitary gates U_l , we construct a universal objective function that is minimised by $|\psi\rangle$. The objective function is engineered to have certain desirable properties. Importantly, a gapped Hamiltonian and minimisation past some fixed tolerance, ensures sufficient overlap with the desired output state $|\psi\rangle$. Recent work of interest by Lloyd considered an alternative form of universality, which is independent of the objective function being minimised [119].

Specifically, in the case of QAOA the original goal of the algorithm was to alternate and target- and a driver-Hamiltonian to evolve the system close to the target Hamiltonian's ground state—thereby solving an optimization problem instance. Lloyd showed that alternating a driver and target Hamiltonian can also be used to perform universal quantum computation: the times for which the Hamiltonians are applied can be programmed to give computationally universal dynamics [119]. In related work [120], myself with two coauthors extended Lloyd's QAOA universality result [119].

In yet another approach towards computational universality, Hamiltonian minimization has long been considered as a means towards universal quantum computation—in the setting of adiabatic quantum computation [8; 124]. In that case however, such mappings adiabatically prepare quantum states close to quantum circuit outputs. Importantly, unlike in ground state quantum computation, in universal variational quantum computation we need not simulate Hamiltonians explicitly. We instead expand the Hamiltonians in the Pauli basis, and evaluate expected values of these operators term-wise (with tolerance $\sim \varepsilon$ for some $\sim \varepsilon^{-2}$ measurements—see Hoeffding's inequality [125]). Measurement results are then paired with their appropriate coefficients and the objective function is calculated classically. Hence, we translate universal quantum computation to that of (i) state preparation (ii) followed by measurement in a single basis where (iii) the quantum circuit being simulated is used to seed an optimizer to ideally reduce coherence time.

After introducing variational quantum computation as it applies to our setting, we construct an objective function (called a telescoping construction). The number of expected values has no dependence on Clifford gates appearing in the simulated circuit and is efficient for circuits with $\mathcal{O}(\text{poly } \ln n)$ non-Clifford gates, making it amenable for near term demonstrations. We then modify the Feynman–Kitaev clock construction and prove that universal variational quantum computa-

tion is possible by minimising $\mathcal{O}(L^2)$ expected values while introducing not more than $\mathcal{O}(\ln L)$ slack qubits, for a quantum circuit partitioned into L Hermitian blocks.

We conclude by considering how the universal model of variational quantum computation can be utilised in practice. In particular, the given gate sequence prepares a state which will minimise the objective function. In practice, we think of this as providing a starting point for a classical optimizer. Given a T gate sequence, we consider the first $L \leq T$ gates. This L gate circuit represents an optimal control problem where the starting point is the control sequence to prepare the L gates. The goal is to modify this control sequence (shorten it) using a variational feedback loop. We iterate this scenario, increasing L up to T . Hence, the universality results proven here also represent a means towards optimal control which does not suffer from the exponential overheads of classically simulating quantum systems.

5.2 Maximizing projection onto a circuit

We will now explicitly construct an elementary Hermitian penalty function that is non-negative, with a non-degenerate lowest (0) eigenstate. Minimisation of this penalty function prepares the output of a quantum circuit. We state this in Lemma 14.

Lemma 14 (Telescoping Lemma—[10]). Consider $\prod_l U_l |0\rangle^{\otimes n}$ a L -gate quantum circuit preparing state $|\psi\rangle$ on n -qubits and containing not more than $\mathcal{O}(\text{poly } \ln n)$ non-Clifford gates. Then there exists a Hamiltonian $\mathcal{H} \geq 0$ on n -qubits with $\text{poly}(L, n)$ cardinality, a (L, n) -independent gap Δ and non-degenerate ground eigenvector $|\phi\rangle \propto \prod_l U_l |0\rangle^{\otimes n}$. In particular, a variational sequence exists causing the Hamiltonian to accept $|\phi\rangle$ viz., $0 \leq \langle \phi | \mathcal{H} | \phi \rangle < \Delta$ then Theorem 13 implies stability (Theorem 13).

Proof sketch (Telescoping Lemma 14). First we show existence of the penalty function. Construct Hermitian $\mathcal{H} \in \mathcal{L}(\mathbb{C}_2^{\otimes n})$ with $\mathcal{H} \geq 0$ such that there exists a non-degenerate $|\psi\rangle \in \mathbb{C}_2^{\otimes n}$ with the property that $\mathcal{H}|\psi\rangle = 0$. We will view the Hamiltonian \mathcal{H} as a penalty function preparing the initial state and restrict

\mathcal{H} to have bounded cardinality (poly(n) non-vanishing terms in the Pauli-basis). Define P_ϕ as a sum of projectors onto product states, i.e.

$$P_\phi = \sum_{i=1}^n |1\rangle \langle 1|^{(i)} = \frac{n}{2} \left(\mathbb{1} - \frac{1}{n} \sum_{i=1}^n Z^{(i)} \right) \quad (5.1)$$

and consider (5.1) as the initial Hamiltonian, preparing state $|0\rangle^{\otimes n}$. We will act on (5.1) with a sequence of gates $\prod_{l=1}^L U_l$ corresponding to the circuit being simulated as

$$h(k) = \left(\prod_{l=1}^{k \leq L} U_l \right) P_\phi \left(\prod_{l=1}^{k \leq L} U_l \right)^\dagger \geq 0 \quad (5.2)$$

which preserves the spectrum. From the properties of P_ϕ it hence follows that $h(k)$ is non-negative and non-degenerate $\forall k \leq L$. We now consider the action of the gates (5.2) on (5.1).

At $k = 0$ from (5.1) there are n expected values to be minimized plus a global energy shift that will play a multiplicative role as the circuit depth increases. To consider $k = 1$ we first expand a universal gate set expressed in the linear extension of the Pauli basis.

Interestingly, the coefficients $\mathcal{J}_{\alpha\beta\dots\gamma}^{ab\dots c}$ of the gates will not serve as direct input(s) to the quantum hardware; these coefficients play a direct role in the classical step where the coefficients weight the sum to be minimized. Let us then consider single qubit gates, in general form viz.,

$$e^{-i\mathbf{a}\cdot\boldsymbol{\sigma}\theta} = \mathbb{1} \cos(\theta) - i\mathbf{a}\cdot\boldsymbol{\sigma} \sin(\theta) \quad (5.3)$$

where \mathbf{a} is a unit vector and $\mathbf{a}\cdot\boldsymbol{\sigma} = \sum_{i=1}^3 a_i \sigma_i$. So each single qubit gate increases the number of expected values by a factor of at most 4^2 . At first glance, this appears prohibitive yet there are two factors to consider. The first is the following Lemma (15).

Lemma 15 (Clifford Gate Cardinality Invariance). Let \mathcal{C} be the set of all Clifford circuits on n qubits, and let \mathcal{P} be the set of all elements of the Pauli group on n qubits. Let $C \in \mathcal{C}$ and $P \in \mathcal{P}$ then it can be shown that

$$CPC^\dagger \in \mathcal{P}$$

or in other words

$$C (\sigma_\alpha^a \sigma_\beta^b \cdots \sigma_\gamma^c) C^\dagger = \sigma_{\alpha'}^{a'} \sigma_{\beta'}^{b'} \cdots \sigma_{\gamma'}^{c'}$$

and so Clifford circuits act by conjugation on tensor products of Pauli operators to produce tensor products of Pauli operators.

For some U a Clifford gate, Lemma 15 shows that the cardinality is invariant. Non-Clifford gates increase the cardinality by factors $\mathcal{O}(e^n)$ and so must be logarithmically bounded from above. Hence, telescopes bound the number of expected values by restricting to circuit's with

$$k \sim \mathcal{O}(\text{poly } \ln n)$$

general single qubit gates. Clifford gates do however modify the locality of terms appearing in the expected values—this is highly prohibitive in adiabatic quantum computation yet arises here as local measurements.

A final argument supporting the utility of telescopes is that the initial state is restricted primarily by the initial Hamiltonian having only a polynomial number of non-vanishing coefficients in the Pauli basis. In practice—using today's hardware—it should be possible to prepare an ε -close 2-norm approximation to any product state

$$\bigotimes_{k=1}^n (\cos \theta_k |0\rangle + e^{i\phi_k} \sin \theta_k |1\rangle)$$

which is realised by modifying the projectors in (5.1) with a product of single qubit maps $\bigotimes_{k=1}^n U_k$. Other more complicated states are also possible.

Finally to finish the proof of Lemma 14, the variational sequence is given by the description of the gate sequence itself. Hence a state can be prepared causing the Hamiltonian to accept and stability applies (Lemma 13).

To explore telescopes in practice, let us then explicitly consider the quantum algorithm for state overlap (a.k.a., *swap test* see e.g. [126]). This algorithm has an analogous structure to phase estimation, a universal quantum primitive which form the backbone of error-corrected quantum algorithms.

Example 34. We are given two d -qubit states $|\rho\rangle$ and $|\tau\rangle$ which will be non-degenerate and minimal eigenvalue states of some initial Hamiltonian(s) on $n + 1$ qubits

$$h(0) |+, \rho, \tau\rangle = 0 \tag{5.4}$$

corresponding to the minimization of $\text{poly}(n/2) + 1$ expected values where the first qubit (superscript 1 below) adds one term and is measured in the X -basis. The controlled swap gate takes the form

$$[U_{\text{swap}}]_m^1 = \frac{1}{2} (\mathbf{1}^1 + Z^1) \otimes \mathbf{1}^m + \frac{1}{2} (\mathbf{1}^1 - Z^1) \otimes \mathcal{S}^m \quad (5.5)$$

where $m = (i, j)$ indexes a qubit pair and the exchange operator of a pair of qubit states is $\mathcal{S} = \mathbf{1} + \boldsymbol{\sigma} \cdot \boldsymbol{\sigma}$. For the case of $d = 1$ we arrive at the simplest (3-qubit) experimental demonstration. At the minimum ($= 0$), the expected value of the first qubit being in logical zero is $\frac{1}{2} + \frac{1}{2} |\langle \rho | \tau \rangle|^2$. The final Hadamard gate on the control qubit is considered in the measurement step.

Telescopes offer some versatility yet fail to directly prove universality in their own right. The crux lies in the fact that we are only allowed some polynomial in $\ln n$ non-Clifford gates (which opens an avenue for classical simulation, see [127; 128]). Interestingly however, we considered the initial Hamiltonian in (5.1) as a specific sum over projectors. We instead could bound the cardinality by some polynomial in n . Such a construction will now be established. It retroactively proves universality of telescopes and in fact uses telescopes in its construction. However true this might be, the spirit is indeed lost. Telescopes are a tool which gives some handle on what we can do without adding additional slack qubits. The universal construction then follows.

5.3 Maximizing projection onto the history state

We will now prove the following theorem (14) which establishes universality of the variational model of quantum computation.

Theorem 14 (Universal Objective Function—[10]). Consider a quantum circuit of L gates on n -qubits producing state $\prod_l U_l |0\rangle^{\otimes n}$. Then there exists an objective function (Hamiltonian, \mathcal{H}) with non-degenerate ground state, cardinality $\mathcal{O}(L^2)$ and spectral gap $\Delta \geq \mathcal{O}(L^{-2})$ acting on $n + \mathcal{O}(\ln L)$ qubits such that acceptance implies efficient preparation of the state $\prod_l U_l |0\rangle^{\otimes n}$. Moreover, a variational sequence exists causing the objective function to accept.

To construct an objective function satisfying Theorem 14, we modify the Feynman-Kitaev clock construction [2; 7]. Coincidentally (and tangential to our objectives here), this construction is also used in certain definitions of the complexity class quantum-Merlin-Arthur (QMA), the quantum analog of NP, through the QMA-complete problem k-LOCAL HAMILTONIAN [7].

Feynman developed a time-independent Hamiltonian that induces unitary dynamics to simulate a sequence of gates [2]. Consider

$$\begin{aligned}\tilde{\mathcal{H}}_t &= U_t \otimes |t\rangle\langle t-1| + U_t^\dagger \otimes |t-1\rangle\langle t| \\ \tilde{\mathcal{H}}_{\text{prop}} &= \sum_{t=1}^L \tilde{\mathcal{H}}_t\end{aligned}\tag{5.6}$$

where the Hamiltonian (5.6) acts on a clock register (right) with orthogonal clock states 0 to L and an initial state $|\xi\rangle$ (left). Observation of the clock in state $|L\rangle$ after some time $s = s_*$ produces

$$\mathbb{1} \otimes \langle L| e^{-i \cdot s \cdot \tilde{\mathcal{H}}_{\text{prop}}} |\xi\rangle \otimes |0\rangle = U_L \cdots U_1 |\xi\rangle.\tag{5.7}$$

The Hamiltonian $\mathcal{H}_{\text{prop}}$ in (5.6) can be modified as (5.8) so as to have the history state (5.9) as its ground state

$$-U_t \otimes |t\rangle\langle t-1| - U_t^\dagger \otimes |t-1\rangle\langle t| + |t\rangle\langle t| + |t-1\rangle\langle t-1| = 2 \cdot \mathcal{H}_t \geq 0\tag{5.8}$$

where \mathcal{H}_t is a projector. Then $\mathcal{H}_{\text{prop}} = \sum_{t=1}^L \mathcal{H}_t$ has the history state as its ground state as

$$|\psi_{\text{hist}}\rangle = \frac{1}{\sqrt{L+1}} \sum_{t=0}^L U_t \cdots U_1 |\xi\rangle \otimes |t\rangle\tag{5.9}$$

for any input state $|\xi\rangle$ where $0 = \langle \psi_{\text{hist}} | \mathcal{H}_{\text{prop}} | \psi_{\text{hist}} \rangle$. This forms the building blocks of our objective function. We will hence establish Theorem 14 by a series of lemma.

Lemma 16 (Lifting the degeneracy). Adding the tensor product of a projector with a telescope

$$\mathcal{H}_{\text{in}} = V \left(\sum_{i=1}^n P_1^{(i)} \right) V^\dagger \otimes P_0\tag{5.10}$$

lifts the degeneracy of the ground space of $\mathcal{H}_{\text{prop}}$ and the history state with fixed input as

$$\frac{1}{\sqrt{L+1}} \sum_{t=0}^L \prod_{l=1}^t U_l(V|0\rangle^{\otimes n}) \otimes |t\rangle \quad (5.11)$$

is the non-degenerate ground state of $J \cdot \mathcal{H}_{\text{in}} + K \cdot \mathcal{H}_{\text{prop}}$ for real $J, K > 0$.

Lemma 16. The lowest energy subspace of $\mathcal{H}_{\text{prop}}$ is spanned by $|\psi_{\text{hist}}\rangle$ which has degeneracy given by freedom in choosing any input state $|\xi\rangle$. To fix the input, consider a tensor product with a telescope

$$\mathcal{H}_{\text{in}} = V \left(\sum_{i=1}^n P_1^{(i)} \right) V^\dagger \otimes P_0 \quad (5.12)$$

for $P_1 = |1\rangle\langle 1| = \mathbb{1} - P_0$ acting on the qubit labeled in the subscript (i) on the right hand side and on the clock space (left). It is readily seen that \mathcal{H}_{in} has unit gap and

$$\ker\{\mathcal{H}_{\text{in}}\} = \text{span}\{|\zeta\rangle \otimes |c\rangle, V|0\rangle^{\otimes n} \otimes |0\rangle \mid 0 < c \in \mathbb{N}_+ \leq L, |\zeta\rangle \in \mathbb{C}_2^{\otimes n}\} \quad (5.13)$$

Now for positive J, K

$$\arg \min\{J \cdot \mathcal{H}_{\text{in}} + K \cdot \mathcal{H}_{\text{prop}}\} \propto \frac{1}{\sqrt{L+1}} \sum_{t=0}^L \prod_{l=1}^t U_l(V|0\rangle^{\otimes n}) \otimes |t\rangle \quad (5.14)$$

□

Lemma 17 (Existence of a gap). For appropriate non-negative J and K , the operator $J \cdot \mathcal{H}_{\text{in}} + K \cdot \mathcal{H}_{\text{prop}}$ is gapped with a non-degenerate ground state and hence, Theorem 13 applies with

$$\Delta \geq \max \left\{ J, \frac{K\pi^2}{2(L+1)^2} \right\}. \quad (5.15)$$

Lemma 17. $\mathcal{H}_{\text{prop}}$ is diagonalized by the following unitary transform

$$W = \sum_{t=0}^L U_t \cdots U_1 \otimes |t\rangle\langle t| \quad (5.16)$$

then $W\mathcal{H}_{\text{prop}}W^\dagger$ acts as identity on the register space (left) and induces a quantum walk on a 1D line on the clock space (right). Hence the eigenvalues are known to be $\lambda_k = 1 - \cos\left(\frac{\pi k}{1+L}\right)$ for integer $0 \leq k \leq L$. From the standard inequality, $1 - \cos(x) \leq x^2/2$, we find that $\mathcal{H}_{\text{prop}}$ has a gap lower bounded as

$$\lambda_0 = 0 \leq \frac{\pi^2}{2(L+1)^2} \leq \lambda_1 \quad (5.17)$$

From Weyl's inequalities, it follows that $J \cdot \mathcal{H}_{\text{in}} + K \cdot \mathcal{H}_{\text{prop}}$ is gapped as

$$\lambda_0 = 0 < \max\{\lambda_1(J \cdot \mathcal{H}_{\text{in}}), \lambda_1(K \cdot \mathcal{H}_{\text{prop}})\} \quad (5.18)$$

$$\leq \lambda_1(J \cdot \mathcal{H}_{\text{in}} + K \cdot \mathcal{H}_{\text{prop}}) \quad (5.19)$$

$$\leq \min\{\lambda_{n-1}(J \cdot \mathcal{H}_{\text{in}}), \lambda_{n-1}(K \cdot \mathcal{H}_{\text{prop}})\} \quad (5.20)$$

with a non-degenerate ground state and hence, Theorem 13 applies with

$$\Delta \geq \max\left\{J, \frac{K\pi^2}{2(L+1)^2}\right\} \quad (5.21)$$

□

Lemma 18 ($\mathcal{H}_{\text{prop}}$ admits a log space embedding). The clock space of $\mathcal{H}_{\text{prop}}$ embeds into $\mathcal{O}(\ln L)$ slack qubits, leaving the ground space of $J \cdot \mathcal{H}_{\text{in}} + K \cdot \mathcal{H}_{\text{prop}}$ and the gap invariant.

Lemma 18. An L -gate circuit requires at most $k = \lceil \ln_2 L \rceil$ clock qubits. Consider a projector P onto the orthogonal complement of a basis state given by bit string $\mathbf{x} = x_1x_2 \dots x_k$. Then

$$P_{\mathbf{x}} = |\bar{\mathbf{x}}\rangle \langle \bar{\mathbf{x}}| = \bigotimes_{i=1}^{\lceil \ln_2 L \rceil} \frac{1}{2} (\mathbb{1} + (-1)^{x_i} Z_i) \quad (5.22)$$

where $\bar{\mathbf{x}}$ is the bitwise logical complement of \mathbf{x} . □

Lemma 19. (Existence and Acceptance). The objective function $J \cdot \mathcal{H}_{\text{in}} + K \cdot \mathcal{H}_{\text{prop}}$ satisfies Theorem 14. The gate sequence $\prod_l U_l |0\rangle^{\otimes n}$ is accepted by the objective function from Lemma 19 thereby satisfying Theorem 14.

Proof. (Lemma 19) Sketch. This term (5.22) contributes L terms and hence so does each of the four terms in \mathcal{H}_t from (5.8). Hence, the entire sum contributes

$3 \cdot L^2$ expected values, where we assume $U = U^\dagger$ and that L is upper bounded by some family of circuits requiring $O(\text{poly } n)$ gates. The input penalty \mathcal{H}_{in} contributes n terms and for an L -gate circuit on n -qubits we arrive at a total of $\mathcal{O}(\text{poly } L^2)$ expected values and $\mathcal{O}(\lceil \ln_2 L \rceil)$ slack qubits. Adding identity gates to the circuit can boost output probabilities, causing the objective function to accept for a state prepared by the given quantum circuit. \square

We are faced with considering self-inverse gates. Such gates (U) have a spectrum $\text{Spec}(U) \subseteq \{\pm 1\}$, are bijective to idempotent projectors ($P^2 = P = P^\dagger$), viz. $U = \mathbb{1} - 2P$ and if V is a self-inverse quantum gate, so is the unitary conjugate $\tilde{V} = GVG^\dagger$ under arbitrary G . Shi showed that a set comprising the controlled not gate (a.k.a. Feynman gate) plus any one-qubit gate whose square does not preserve the computational basis is universal [43]. Consider Hermitian

$$R(\theta) = X \cdot \sin(\theta) + Z \cdot \cos(\theta), \quad (5.23)$$

then

$$e^{i\theta Y} = R(\pi/2) \cdot R(\theta). \quad (5.24)$$

Hence, a unitary Y rotation is recovered by a product of two Hermitian operators. A unitary X rotation is likewise recovered by the composition (5.24) when considering Hermitian $Y \cdot \sin(\theta) - Z \cdot \cos(\theta)$. The universality of self-inverse gates is then established, with constant overhead. Hence and to conclude, the method introduces not more than $\mathcal{O}(L^2)$ expected values while requiring not more than $\mathcal{O}(\ln L)$ slack qubits, for an L gate quantum circuit.

5.4 Discussion

We have established that variational methods can approximate any quantum state produced by a sequence of quantum gates and hence that variational quantum computation admits a universal model. It appears evident that this method will yield shorter control sequences compared to the control sequence of the original quantum circuit—that is the entire point. Indeed, the control sequence implementing the gate sequence being simulated serves as an upper-bound

showing that a sequence exists to minimize the expected values. These expected values are the fleeting resource which must be simultaneously minimized to find a shorter control sequence which prepares the desired output state of a given quantum circuit.

Although error correction would allow the circuit model to replace methods developed here, the techniques we develop in universal variational quantum computation should augment possibilities in the NISQ setting, particularly with the advent of error suppression techniques [129; 130]. Importantly, variational quantum computation forms a universal model in its own right and is not (in principle) limited in application scope.

An interesting feature of the model of universal variational quantum computation is how many-body Hamiltonian terms are realized as part of the measurement process. This is in contrast with leading alternative models of universal quantum computation.

In the gate model, many-body interactions must be simulated by sequences of two-body gates. The adiabatic model applies perturbative gadgets to approximate many-body interactions with two-body interactions [8; 124]. The variational model of universal quantum computation simulates many body interactions by local measurements. Moreover the coefficients weighting many-body terms need not be implemented into the hardware directly; this weight is compensated for in the classical-iteration process which in turns controls the quantum state being produced.

Many states cause a considered objective function to accept. Hence the presented model is somewhat inherently agnostic to how the states are prepared. This enables experimentalists to now vary the accessible control parameters to minimize an external and iteratively calculated objective function. Though the absolute limitations of this approach in the absence of error correction are not known, a realizable method of error suppression could get us closer to implementation of the traditional text-book quantum algorithms such as Shor's factorisation algorithm.

Chapter 6. Gadget Hamiltonians

We considered in detail in § 2 how to use gates to realize many-body Hamiltonian terms. Here we consider a different situation. One which does not assume access to pulses (unitary gates). In this setting, which is relevant to a host of physical systems, we must turn to alternative methods to realize k -body interactions. This section follows [24; 124].

Although adiabatic quantum computation is known to be a universal model of quantum computation [8; 124; 131; 132] and hence, in principle equivalent to the circuit model, the mappings between an adiabatic process and an arbitrary quantum circuit require significant overhead. Currently the approaches to universal adiabatic quantum computation require implementing multiple higher order and non-commuting interactions by means of perturbative gadgets [124].

Early work by Kitaev *et al.* [7] established that an otherwise arbitrary Hamiltonian restricted to have at most 5-body interactions has a ground state energy problem which is complete for the quantum analog of the complexity class NP (QMA-COMPLETE). Reducing the locality of the Hamiltonians from 5-body down to 2-body remained an open problem for a number of years. In their 2004 proof that 2-LOCAL HAMILTONIAN is QMA-COMPLETE, Kempe, Kitaev and Regev formalized the idea of a perturbative gadget, which finally accomplished this task [133]. Oliveira and Terhal further reduced the problem, showing completeness when otherwise arbitrary 2-body Hamiltonians were restricted to act on a square lattice [131]. The form of the simplest QMA-COMPLETE Hamiltonian is reduced to physically relevant models in [124] (see also [134]), e.g.

$$\mathcal{H} = \sum_i h_i Z_i + \sum_{i<j} J_{ij} Z_i Z_j + \sum_{i<j} K_{ij} X_i X_j. \quad (6.1)$$

Although this model contains only physically accessible terms, programming problems into a universal adiabatic quantum computer [124] or an adiabatic quantum simulator [65] involves several types of k -body interactions (for bounded k). To reduce from k -body interactions to 2-body is accomplished through the application of gadgets. Hamiltonian gadgets were introduced as theorem-proving tools in the context of quantum complexity theory yet their experimental realization

currently offers the only path towards universal adiabatic quantum computation. In terms of experimental constraints, an important parameter in the construction of these gadgets is a large spectral gap introduced into the slack space as part of a penalty Hamiltonian.

6.1 Hamiltonian complexity

What is the simplest Hamiltonians that allow universal adiabatic quantum computation? For this we turn to the complexity class quantum-Merlin-Arthur (QMA), the quantum analog of NP, and consider the QMA-complete problem k -LOCAL HAMILTONIAN [7]. One solves k -LOCAL HAMILTONIAN by determining if there exists an eigenstate with energy above a given value or below another—with a promise that one of these situations is the case—when the system has at most k -local interactions. A YES instance is shown by providing a witness eigenstate with energy below the lowest promised value.

The problem 5-LOCAL HAMILTONIAN was shown to be QMA-complete by Kitaev [7]. To accomplish this, Kitaev modified the autonomous quantum computer proposed by Feynman [2]. This modification later inspired a proof of the polynomial equivalence between quantum circuits and adiabatic evolutions by Aharonov et al. [8]. Kempe, Kitaev and Regev subsequently proved QMA-completeness of 2-LOCAL HAMILTONIAN [133]. Oliveira and Terhal then showed that universality remains even when the 2-local Hamiltonians act on particles in a subgraph of the 2D square lattice [131]. Any QMA-complete Hamiltonian may realize universal adiabatic quantum computation, and so these results are also of interest for the implementation of quantum computation.

Since 1-LOCAL HAMILTONIAN is efficiently solvable, an open question is to determine which combinations of 2-local interactions allow one to build QMA-complete Hamiltonians. Furthermore, the problem of finding the minimum set of interactions required to build a universal adiabatic quantum computer is of practical, as well as theoretical, interest: every type of 2-local interaction requires a separate type of physical interaction. To address this question we prove the following theorems:

Theorem 15 (ZZXX Hamiltonian is QMA-complete [124]). *The decision problem 2-LOCAL ZZXX HAMILTONIAN is QMA-complete, with the ZZXX Hamiltonian given as:*

$$\mathcal{H}_{ZZXX} = \sum_i h_i Z_i + \sum_i l_i X_i + \sum_{i,j} J_{ij} Z_i Z_j + \sum_{i,j} K_{ij} X_i X_j. \quad (6.2)$$

Theorem 16 (ZX Hamiltonian is QMA-complete [124]). *The decision problem 2-LOCAL ZX HAMILTONIAN is QMA-complete, with the ZX Hamiltonian given as:*

$$\mathcal{H}_{ZX} = \sum_i h_i Z_i + \sum_i l_i X_i + \sum_{i<j} J_{ij} Z_i X_j + \sum_{i<j} K_{ij} X_i Z_j. \quad (6.3)$$

6.2 Local Hamiltonian is QMA-complete

The translation from quantum circuits to adiabatic evolutions began when Kitaev [7] replaced the time-dependence of gate model quantum algorithms with spatial degrees of freedom using the non-degenerate ground state of a positive semidefinite Hamiltonian:

$$0 = \mathcal{H} |\psi_{\text{hist}}\rangle = (\mathcal{H}_{\text{in}} + \mathcal{H}_{\text{clock}} + \mathcal{H}_{\text{clockinit}} + \mathcal{H}_{\text{prop}}) |\psi_{\text{hist}}\rangle. \quad (6.4)$$

To describe this, let T be the number of gates in the quantum circuit with gate sequence $U_T \cdots U_2 U_1$ and let n be the number of logical qubits acted on by the circuit. Denote the circuit's classical input by $|x\rangle$ and its output by $|\psi_{\text{out}}\rangle$. The *history state* representing the circuit's entire time evolution is:

$$\begin{aligned} |\psi_{\text{hist}}\rangle = \frac{1}{\sqrt{T+1}} & \left[|x\rangle \otimes |0\rangle^{\otimes T} + U_1 |x\rangle \otimes |1\rangle |0\rangle^{\otimes T-1} + \right. \\ & + U_2 U_1 |x\rangle \otimes |11\rangle |0\rangle^{\otimes T-2} + \\ & + \dots + \\ & \left. + U_T \cdots U_2 U_1 |x\rangle \otimes |1\rangle^{\otimes T} \right], \end{aligned} \quad (6.5)$$

where we have indexed distinct time steps by a T qubit unary clock. In the following, tensor product symbols separate operators acting on logical qubits (left) and clock qubits (right).

\mathcal{H}_{in} acts on all n logical qubits and the first clock qubit. By annihilating time-zero clock states coupled with classical input x , \mathcal{H}_{in} ensures that valid input state ($|x\rangle \otimes |0\dots 0\rangle$) is in the low energy eigenspace:

$$\mathcal{H}_{\text{in}} = \sum_{i=1}^n (\mathbb{1} - |x_i\rangle \langle x_i|) \otimes |0\rangle \langle 0|_1 = \left(\frac{1}{4}\right) \sum_{i=1}^n (\mathbb{1} - (-1)^{x_i} Z_i) \otimes (\mathbb{1} + Z_1). \quad (6.6)$$

$\mathcal{H}_{\text{clock}}$ is an operator on clock qubits ensuring that valid unary clock states $|00\dots 0\rangle$, $|10\dots 0\rangle$, $|110\dots 0\rangle$ etc., span the low energy eigenspace:

$$\mathcal{H}_{\text{clock}} = \sum_{t=1}^{T-1} |01\rangle \langle 01|_{(t,t+1)} = \frac{1}{4} \left[(T-1)\mathbb{1} + Z_1 - Z_T - \sum_{t=1}^{T-1} Z_t Z_{(t+1)} \right], \quad (6.7)$$

where the superscript $(t,t+1)$ indicates the clock qubits acted on by the projection. This Hamiltonian has a simple physical interpretation as a line of ferromagnetically coupled spins with twisted boundary conditions, so that the ground state is spanned by all states with a single domain wall. The term $\mathcal{H}_{\text{clockint}}$ applies a penalty $|1\rangle \langle 1|_{t=1}$ to the first qubit to ensure that the clock is in state $|0\rangle^{\otimes T}$ — at time $t = 0$.

$\mathcal{H}_{\text{prop}}$ acts both on logical and clock qubits. It ensures that the ground state is the history state corresponding to the given circuit. $\mathcal{H}_{\text{prop}}$ is a sum of T terms, $\mathcal{H}_{\text{prop}} = \sum_{t=1}^T \mathcal{H}_{\text{prop},t}$, where each term checks that the propagation from time $t-1$ to t is correct. For $2 \leq t \leq T-1$, $\mathcal{H}_{\text{prop},t}$ is defined as:

$$\mathcal{H}_{\text{prop},t} \stackrel{\text{def}}{=} \mathbb{1} \otimes |t-1\rangle \langle t-1| - U_t \otimes |t\rangle \langle t-1| - U_t^\dagger \otimes |t-1\rangle \langle t| + \mathbb{1} \otimes |t\rangle \langle t|, \quad (6.8)$$

where operators $|t\rangle \langle t-1| = |110\rangle \langle 100|_{(t-1,t,t+1)}$ etc., act on clock qubits $t-1$, t , and $t+1$ and where the operator U_t is the t^{th} gate in the circuit. For the boundary cases ($t = 1, T$), one writes $\mathcal{H}_{\text{prop},t}$ by omitting a clock qubit ($t-1$ and $t+1$ respectively).

We have now explained all the terms in the Hamiltonian from (6.4)—a key building block used to prove the QMA-completeness of 5-LOCAL HAMILTONIAN [7]. The construction reviewed in the present section was also used in a

proof of the polynomial equivalence between quantum circuits and adiabatic evolutions [8]. Which physical systems can implement the Hamiltonian model of computation from (6.4)? Ideally, we wish to find a simple Hamiltonian that is in principle realizable using current, or near-future technology. The ground states of many physical systems are real-valued, such as the ground states of the Hamiltonians from (6.2) and (6.3). So a logical first step in our program is to show the QMA-completeness of general real-valued local Hamiltonians.

6.2.1 Real Hamiltonian is QMA-complete

One can show that 5-LOCAL REAL HAMILTONIAN is already QMA-complete—leaving the proofs in [7] otherwise intact and changing only the gates used in the circuits. \mathcal{H}_{in} from (6.6) and $\mathcal{H}_{\text{clock}}$ from (6.7) are already real-valued and at most 2-local. Now consider the terms in $\mathcal{H}_{\text{prop}}$ from (6.8) for the case of *self-inverse* elementary gates $U_t = U_t^\dagger$:

$$\mathcal{H}_{\text{prop},t} = \frac{1}{4}(\mathbb{1} - Z_{(t-1)})(\mathbb{1} + Z_{(t+1)}) - \frac{U}{4}(\mathbb{1} - Z_{(t-1)})X_t(\mathbb{1} + Z_{(t+1)}) \quad (6.9)$$

For the boundary cases ($t = 1, T$), define:

$$\begin{aligned} \mathcal{H}_{\text{prop},1} &= \frac{1}{2}(\mathbb{1} + Z_2) - U_1 \otimes \frac{1}{2}(X_1 + X_1 Z_2) \\ \mathcal{H}_{\text{prop},T} &= \frac{1}{2}(\mathbb{1} - Z_{(T-1)}) - U_T \otimes \frac{1}{2}(X_T - Z_{(T-1)}X_T). \end{aligned} \quad (6.10)$$

The terms from (6.9) and (6.10) acting on the clock space are already real-valued and at most 3-local. As an explicit example of the gates U_t , let us define a universal real-valued and self-inverse 2-qubit gate as in (6.11).

$$R_{ij}(\phi) = \frac{1}{2}(\mathbb{1} + Z_i) + \frac{1}{2}(\mathbb{1} - Z_i) \otimes (\sin(\phi)X_j + \cos(\phi)Z_j). \quad (6.11)$$

The gate sequence $R_{ij}(\phi)R_{ij}(\pi/2)$ recovers the universal gate from [135]. This is a continuous set of elementary gates parameterized by the angle ϕ . Discrete sets of self inverse gates which are universal are also readily constructed. For example,

Shi showed that a set comprising the **CNOT** plus any one-qubit gate whose square does not preserve the computational basis is universal [43]. We immediately see that a universal set of self-inverse gates cannot contain only the **CNOT** and a single one-qubit gate. However, the set $\{\mathbf{CNOT}, X, \cos \psi X + \sin \psi Z\}$ is universal for any *single* value of ψ which is not a multiple of $\pi/4$.

A reduction from 5-LOCAL to 2-LOCAL HAMILTONIAN was accomplished by the use of *gadgets* that reduced 3-local Hamiltonian terms to 2-local terms [133]. From the results in [133] (see also [131]) and the QMA-completeness of 5-LOCAL REAL HAMILTONIAN, it now follows that 2-LOCAL REAL HAMILTONIAN is QMA-complete and universal for adiabatic quantum computation. We note that the real product $Y_i \otimes Y_j$, or tensor powers thereof, are not necessary in any part of our construction, and so Hamiltonians composed of the following pairwise products of real-valued Pauli matrices are QMA-complete and universal for adiabatic quantum computation:

$$\begin{aligned} &\{\mathbf{1} \otimes \mathbf{1}, \mathbf{1} \otimes X, \mathbf{1} \otimes Z, X \otimes \mathbf{1}, \\ &Z \otimes \mathbf{1}, X \otimes Z, Z \otimes X, X \otimes X, Z \otimes Z\}. \end{aligned} \tag{6.12}$$

To prove our Theorems (15) and (16), we will next show that one can approximate all the terms from (6.12) using either the ZX or ZZXX Hamiltonians—the Hamiltonians from (6.2) and (6.3) respectively. We do this using perturbation theory [131; 133] to construct gadget Hamiltonians that approximate the operators $Z_i X_j$ and $X_j Z_i$ with terms from the ZZXX Hamiltonian as well as the operators $Z_i Z_j$ and $X_i X_j$ with terms from the ZX Hamiltonian.

Remark 65 (Experimental Gadget Realizations [136–138]). While recent progress in the experimental implementation of adiabatic quantum processors [139–141] suggests the ability to perform sophisticated adiabatic quantum computing experiments, the perturbative gadgets require very large values of Δ . This places high demands on experimental control precision by requiring that devices enforce very large couplings between slack qubits while still being able to resolve couplings from the original problem—even though those fields may be orders of magnitude smaller than Δ . Accordingly, if perturbative gadgets are to be used, it is necessary to find gadgets which can efficiently approximate their target Hamiltonians with significantly lower values of Δ . See for example the work in [136–138].

Example 35. (Two-Qubit Experimental Proposal: Towards Adiabatic Universality). Consider a quantum state promised to be of the following form where $f(x)$ is unknown

$$|\psi_{\text{in}}\rangle \propto \sum_{x \in \{0,1\}^n} (-1)^{f(x)} |x\rangle. \quad (6.13)$$

Here n -variable Boolean function $f(x)$ is promised to be either *constant* or *balanced*¹. The universal building blocks to demonstrate ground state quantum computation by adiabatic evolution can be demonstrated by performing the Deutsch-Jozsa algorithm on two-qubits. This demonstration is closely related to other two-qubit variants, such as phase estimation—see § 2.4.

The Deutsch-Jozsa algorithm decides the promise, given $|\psi_{\text{in}}\rangle$, by means of a Fourier transform over the group \mathbb{Z}_2 . Demonstrating this Hamiltonian would demonstrate all the universal building blocks from [124].

Consider the function $f(x_1)$ yielding state

$$|\psi_{\text{in}}\rangle \propto (-1)^{f(0)} |0\rangle + (-1)^{f(1)} |1\rangle. \quad (6.14)$$

In the following circuit, denote the outcome of observable $|1\rangle\langle 1|$ by m , where m decides the Deutsch-Jozsa promise:

$$(-1)^{f(0)} |0\rangle + (-1)^{f(1)} |1\rangle \xrightarrow{H} \boxed{\text{---} \overline{m}}$$

If $m = 0$ ($m = 1$), $f(x_1)$ is constant (balanced). Now the circuit's history,

$$|\psi_{\text{hist}}\rangle \propto |\psi_{\text{in}}\rangle \otimes |0\rangle + H \cdot |\psi_{\text{in}}\rangle \otimes |1\rangle, \quad (6.15)$$

be the ground state of $\mathcal{H}_{\text{in}} + \mathcal{H}_{\text{prop}}$, where:

$$\begin{aligned} \mathcal{H}_{\text{in}} &= \frac{1}{4} \left(\mathbb{1} + (-1)^{f(0)+f(1)} X_l \right) \otimes (\mathbb{1} + Z_c), \\ \mathcal{H}_{\text{prop}} &= \frac{1}{2} \left(\mathbb{1} - \frac{1}{\sqrt{2}} Z_l \otimes X_c - \frac{1}{\sqrt{2}} X_l \otimes X_c \right). \end{aligned}$$

\mathcal{H}_{in} plays the role of an oracle Hamiltonian provided to us without knowledge of the function. The computation requires a 2-qubit effective subspace (logical qubit

¹A balanced Boolean function outputs 1 (and 0) for exactly half of all input strings, while a constant function always outputs the same value 1 or 0.

l and clock qubit c) combined with dual ancillary qubits implementing respective ZX or ZZXX gadgets. The adiabatic path Hamiltonian,

$$\mathcal{H}(s) = (1 - s)\mathcal{H}_{\text{in}} + s(\mathcal{H}_{\text{in}} + \mathcal{H}_{\text{prop}})$$

for monotonic $s \in [0,1]$, has $|\psi_{\text{hist}}\rangle$ as the $s = 1$ ground state. The experiment is repeated until clock qubit c is measured in $|1\rangle$ —thereby projectively measuring qubit l , such that $m = H \cdot |\psi_{\text{in}}\rangle$.

Example 36. (Experimental Proposal: Realization of Ground State Quantum Gates). Realization of universal ground state quantum computation requires the realization of quantum gates implemented as Hamiltonian operators. In this direction, realization of the gates appearing in (6.11)—see also (6.11)—would represent a step towards a significant milestone.

A 4-qubit quantum Fourier transform (QFT) suffices for many applications of recursive phase estimation of the ground state energy of molecules. The QFT circuit requires both controlled and single qubit $R_k \stackrel{\text{def}}{=} |0\rangle\langle 0| + e^{2\pi i/2^k} |1\rangle\langle 1|$ gates as well as single qubit Hadamard gates. Here we outline a real-valued mapping of the QFT.

In what follows, normalization constants are often omitted. Consider the state of n -qubits $|\psi\rangle = \sum_{x \in \{0,1\}^n} \alpha_x |x\rangle$. Let $\alpha_x = a_x + b_x i$ and define a real-valued wave function $|\tilde{\psi}\rangle$ to represent $|\psi\rangle$ using an extra qubit that indexes the real and imaginary parts of the wavefunction:

$$|\tilde{\psi}\rangle = \sum_{x \in \{0,1\}^n} a_x |x\rangle \otimes |0\rangle + \sum_{x \in \{0,1\}^n} b_x |x\rangle \otimes |1\rangle. \quad (6.16)$$

For example, an arbitrary pure single-qubit state

$$|\psi\rangle = \cos(\theta) |0\rangle + e^{i\phi} \sin(\theta) |1\rangle \quad (6.17)$$

is written as:

$$|\tilde{\psi}\rangle = \cos(\theta) |0\rangle \otimes |0\rangle + \cos(\phi) \sin(\theta) |1\rangle \otimes |0\rangle + \sin(\phi) \sin(\theta) |1\rangle \otimes |1\rangle. \quad (6.18)$$

One now replaces each complex gate U operating on k qubits by its *real valued version*, denoted as \tilde{U} and operating on $k+1$ qubits. Let $\Re\{U\}$ ($\Im\{U\}$) denote

the real (imaginary) part of the operator U and define the real-valued version of any complex gate as:

$$\tilde{U} = \Re\{U\} \otimes \mathbb{1} + \Im\{U\} \otimes \Re\{-i\sigma_y\}. \quad (6.19)$$

The Hadamard gates needed in the QFT are real-valued. The real-valued version of the R_k gate now acts on an extra qubit:

$$\tilde{R}_k = |0\rangle\langle 0| \otimes \mathbb{1} + \cos(2\pi/2^k) |1\rangle\langle 1| \otimes \mathbb{1} + \sin(2\pi/2^k) |1\rangle\langle 1| \otimes (|1\rangle\langle 0| - |0\rangle\langle 1|) \quad (6.20)$$

and can be constructed from the gate sequence $R_{ij}(2\pi/2^k)R_{ij}(\pi/2)$. Similarly, the required controlled \tilde{R}_k gates are concatenations of 3-qubit rotation gates:

$$\begin{aligned} R_{ijk}(\phi) = & \frac{1}{4}(3 \cdot \mathbb{1} + Z_i + Z_j - Z_i \otimes Z_j) + \\ & + \frac{1}{4}(\mathbb{1} - Z_i) \otimes (\mathbb{1} - Z_j) \otimes (\sin(\phi)Z_k + \cos(\phi)Z_k). \end{aligned} \quad (6.21)$$

To construct the QFT, add an extra qubit initialized in $|0\rangle$ and replace each gate with its real-valued version. Write the Hamiltonian describing the 2-local terms from (6.6) and (6.7) as well as the 6-local terms from (6.9). The terms in (6.9) can be reduced to 4-local without perturbation theory [142] (see also [143]). Parallel application of the gadget in [133] followed by application of ZX (ZZXX) gadgets completes the reduction.

Definition 65 (Gadget Overview). A perturbative gadget consists of

1. an slack system acted on by Hamiltonian \mathcal{H} , characterized by the spectral gap Δ between its ground state subspace and excited state subspace,
2. and a perturbation V which acts on both the slack and the system.

Definition 66 (Perturbation Overview). V perturbs the ground state subspace of \mathcal{H} such that the perturbed low-lying spectrum of the gadget Hamiltonian $\tilde{\mathcal{H}} = \mathcal{H} + V$ captures the spectrum of the target Hamiltonian, $\mathcal{H}_{\text{target}}$, up to error ε .

Remark 66 (Reduction Gadgets [133]). The purpose of a gadget is dependent on the form of the desired target Hamiltonian $\mathcal{H}_{\text{target}}$. For example, if the target Hamiltonian is k -local with $k \geq 3$ while the gadget Hamiltonian is 2-local, the gadget serves as a tool for reducing locality.

Remark 67 (Creation Gadgets [124]). Also if the target Hamiltonian involves interactions that are difficult to implement experimentally and the gadget Hamiltonian contains only interactions that are physically accessible, the gadget becomes a generator of physically inaccessible terms from accessible ones. For example the gadget which we introduce in § 6.6 emulates YY interactions from ZZ and XX interactions so might fall into this use category.

Remark 68 (Exact, Non-Perturbative Gadgets [12]). Exact, non-perturbative, gadgets [12] are commonly used for embedding classical optimization problems into adiabatic quantum computations. These optimization algorithms require diagonal many-body Hamiltonians where one needs a Hamiltonian of form $\mathcal{H} = \mathbb{1} - |s\rangle\langle s|$ with s being a binary string.

Apart from the physical relevance to quantum computation, gadgets have been central to many results in quantum complexity theory [49; 124; 134; 144]. Hamiltonian gadgets were employed to help characterize the complexity of density functional theory [145] and are required components in current proposals related to error correction on an adiabatic quantum computer [146] and the adiabatic and ground state quantum simulator [65].

Remark 69 (Kempe, Kitaev and Regev [133]). The first use of perturbative gadgets [133] relied on a 2-body gadget Hamiltonian to simulate a 3-body Hamiltonian of the form $\mathcal{H}_{\text{targ}} = \mathcal{H}_{\text{else}} + \alpha \cdot A \otimes B \otimes C$ with three auxiliary spins in the slack space. Here $\mathcal{H}_{\text{else}}$ is an arbitrary Hamiltonian that does not operate on the auxiliary spins. Further, A , B and C are unit-norm operators and α is the desired coupling. For such a system, it is shown that it suffices to construct V with $\|V\| < \Delta/2$ to guarantee that the perturbative self-energy expansion approximates $\mathcal{H}_{\text{targ}}$ up to error ε [131; 133; 144]. Because the gadget Hamiltonian is constructed such that in the perturbative expansion (with respect to the low energy subspace), only virtual excitations that flip all 3 slack bits would have non-trivial contributions in the 1st through 3rd order terms.

Remark 70 (Jordan and Farhi [147]). In [147] Jordan and Farhi generalized the construction in [133] to a general k -body to 2-body reduction using a perturbative expansion that appears to date to 1958 due to Bloch.² They showed that one can

²Sur la théorie des perturbations des états liés, *Nuclear Physics*, 6:329–347, 1958

approximate the low-energy subspace of a Hamiltonian containing r distinct k -local terms using a 2-local Hamiltonian.

Remark 71 (Oliveira and Terhal [131]). Two important gadgets were introduced by Oliveira and Terhal [131] in their proof that 2-LOCAL HAMILTONIAN ON SQUARE LATTICE is QMA-COMPLETE. In particular, they introduced an alternative 3- to 2-body gadget which uses only one additional spin for each 3-body term as well as a “subdivision gadget” that reduces a k -body term to a $(\lceil k/2 \rceil + 1)$ -body term using only one additional spin [131].

These gadgets (listed in the three remarks above), which we improved in the work [24], find their use as the de facto standard whenever the use of gadgets is necessitated. For instance, the gadgets from [131] were used by Bravyi, DiVincenzo, Loss and Terhal [144] to show that one can combine the use of subdivision and 3- to 2-body gadgets to recursively reduce a k -body Hamiltonian to 2-body, which is useful for simulating quantum many-body Hamiltonians.

6.3 Exact ZZZ-gadget from Z, ZZ

Non-perturbative, exact or classical gadgets, as introduced in [12], will be considered along with their limitations and interrelations with perturbative gadgets. This section employs heavily the techniques we developed from § 1. Similar ideas originating from [12] and [13] have been experimentally demonstrated in [148]—see also [149].

Suppose we need to simulate a diagonal target Hamiltonian

$$\mathcal{H}_{\text{targ}} = \mathcal{H}_{\text{else}} + \alpha \bigotimes_{i=1}^k \sigma_i. \quad (6.22)$$

Here all operators σ_i share the same basis and $\mathcal{H}_{\text{else}}$ commutes with $\bigotimes_{i=1}^k \sigma_i$.

Remark 72 (Perturbative Approach to ZZZ). The perturbative approach requires a 5th order gadget to simulate a 3-body term $Z_1 Z_2 Z_3$. The gap however scales as $\Delta = \Theta(\varepsilon^{-5})$ renders it challenging to realize using current experimental resources.

Remark 73 (Penalty Function Approach to ZZZ). Unlike their perturbative counterparts, non-perturbative gadgets do not require a large penalty on the slack spins, which render them more realistic to implement experimentally [12; 13; 150].

Remark 74. The idea of a non-perturbative 3-body reduction gadget comes originally from two insights which relate the spectra of diagonal Hamiltonians to Boolean algebra [12].

1. The first insight is that the spectrum of $\mathcal{H}_{\text{targ}} = Z_1 Z_2 Z_3$ has a unique correspondence with the truth table of the logic operation

$$f(s_1, s_2, s_3) = s_1 \oplus s_2 \oplus s_3, \quad s_i \in \{0, 1\}. \quad (6.23)$$

The ground state subspace of $\mathcal{H}_{\text{targ}}$ corresponds to all states with $s_1 \oplus s_2 \oplus s_3 = 0$ and the first excited subspace corresponds to $s_1 \oplus s_2 \oplus s_3 = 1$.

2. The second insight is that the Boolean function XOR $s = s_1 \oplus s_2$ cannot be mapped to the ground state subspace of a 3-spin diagonal Hamiltonian using only 2-body interactions while AND $s = s_1 \wedge s_2$ can be implemented with 2-body interactions [12; 13].

Thus, we see that if we can express $f(s_1, s_2, s_3)$ as a function of only 1- or 2-variable AND clauses with auxiliary variables, then the spectrum of $Z_1 Z_2 Z_3$ can be directly mapped to a diagonal Hamiltonian consisting of only 2-body interactions.

Remark 75 (k -body exact gadget). This idea can be generalized to simulate a k -body diagonal target term $\bigotimes_{i=1}^k Z_i$ [12; 150]. Since the spectrum of the k -body term can be mapped to Boolean expression

$$f(s_1, \dots, s_k) = \bigoplus_{i=1}^k s_i, \quad (6.24)$$

we can introduce $k - 3$ auxiliary variables y_1, y_2, \dots, y_s such that $y_1 = s_1 \oplus s_2$ and

$$y_j = y_{j-1} \oplus s_{j+1}, \quad \text{with } j = 2, \dots, k - 3. \quad (6.25)$$

Then $f(s_1, \dots, s_k)$ becomes a sum of 3-variable XOR terms up to $k - 3$ constraints. Each of the 3-variable XORs can then be reduced to 2-body using gadget described above.

Example 37. Non-perturbative gadgets [12] do not require large gaps and they capture the target term exactly. Given these advantages, we ask if these gadgets can replace perturbative gadgets. To answer this, consider two non-commuting Hamiltonians $\mathcal{H}_Z = Z_1 Z_2 Z_3$ and $\mathcal{H}_X = X_1 X_2 X_3$. Introduce slack spins w and w' for reducing $\mathcal{H}_Z + \mathcal{H}_X$ to 2-body respectively. For each eigenstate $|j\rangle$ such that

$$(\mathcal{H}_Z + \mathcal{H}_X)|j\rangle = \beta_j |j\rangle, \quad (6.26)$$

let $\tilde{\mathcal{H}}_Z$ and $\tilde{\mathcal{H}}_X$ be the non-perturbative gadgets generated for \mathcal{H}_Z and \mathcal{H}_X respectively, we are faced with the question whether the following is true for all j :

$$\min_{\psi, \phi} \langle \psi | \langle \phi | \langle j | (\tilde{\mathcal{H}}_Z + \tilde{\mathcal{H}}_X) | j \rangle | \phi \rangle | \psi \rangle = \beta_j \quad (6.27)$$

where $|\phi\rangle$ and $|\psi\rangle$ denote the states of slack qubits w and w' respectively. We claim that (6.27) is impossible to hold for all j . This would violate the gadget theorem because \mathcal{H}_Z and \mathcal{H}_X induces transitions in each other's slack spaces that cause the perturbation series to no longer converge. However, the condition of the gadget theorem is only sufficient. In order to show that non-perturbative gadgets cannot simulate a sum of non-commuting target terms, a counter-example is easy to find. Therefore, for a general k -body target Hamiltonian, one still needs perturbative methods for simulating it using 2-body interactions.

6.4 Perturbation theory

Definition 67. In our notation the spin-1/2 Pauli operators will be represented as $\{X, Y, Z\}$ with subscript indicating which spin-1/2 particle (qubit) it acts on. For example X_2 is a Pauli operator $X = |0\rangle\langle 1| + |1\rangle\langle 0|$ acting on the qubit labelled as 2.

Remark 76. In the literature there are different formulations of the perturbation theory that are adopted when constructing and analyzing the gadgets. This adds to the challenge faced in comparing the physical resources required among the various proposed constructions. For example, Jordan and Farhi [147] use a formulation due to Bloch, while Bravyi et al. use a formulation based on the

Schrieffer-Wolff transformation [144]. Here we employ the formulation used in [131; 133]. For a small survey on various formulations of perturbation theory, refer to [151].

A gadget Hamiltonian

$$\tilde{\mathcal{H}} = \mathcal{H} + V \quad (6.28)$$

consists of a penalty Hamiltonian \mathcal{H} , which applies an energy gap onto an slack space, and a perturbation V . To explain in further detail how the low-lying sector of the gadget Hamiltonian $\tilde{\mathcal{H}}$ approximates the entire spectrum of a certain target Hamiltonian $\mathcal{H}_{\text{targ}}$ with error ε , we set up the following notations:

1. Let λ_j and $|\psi_j\rangle$ be the j^{th} eigenvalue and eigenvector of \mathcal{H} and similarly define $\tilde{\lambda}_j$ and $|\tilde{\psi}_j\rangle$ as those of $\tilde{\mathcal{H}}$, assuming all the eigenvalues are labelled in a weakly increasing order ($\lambda_1 \leq \lambda_2 \leq \dots$, same for $\tilde{\lambda}_j$).
2. Using a cutoff value λ_* , let

$$\mathcal{L}_- = \text{span}\{|\psi_j\rangle | \forall j : \lambda_j \leq \lambda_*\} \quad (6.29)$$

be the low energy subspace and

$$\mathcal{L}_+ = \text{span}\{|\psi_j\rangle | \forall j : \lambda_j > \lambda_*\} \quad (6.30)$$

be the high energy subspace.

3. Let Π_- and Π_+ be the orthogonal projectors onto the subspaces \mathcal{L}_- and \mathcal{L}_+ respectively.
4. For an operator O we define the partitions of O into the subspaces as $O_- = \Pi_- O \Pi_-$, $O_+ = \Pi_+ O \Pi_+$, $O_{-+} = \Pi_- O \Pi_+$ and $O_{+-} = \Pi_+ O \Pi_-$.

With the definitions above, one can turn to perturbation theory to approximate $\tilde{\mathcal{H}}_-$ using \mathcal{H} and V . We now consider the operator-valued resolvent

$$\tilde{G}(z) = (z\mathbb{1} - \tilde{\mathcal{H}})^{-1}. \quad (6.31)$$

Similarly one would define

$$G(z) = (z\mathbb{1} - \mathcal{H})^{-1}. \quad (6.32)$$

Note that

$$\tilde{G}^{-1}(z) - G^{-1}(z) = -V \quad (6.33)$$

so that this allows an expansion in powers of V as

$$\begin{aligned} \tilde{G} &= (G^{-1} - V)^{-1} = G(\mathbf{1} - VG)^{-1} = \\ &= G + GVG + GVGVG + GVGVGVG + \dots \end{aligned} \quad (6.34)$$

It is then standard to define the self-energy

$$\Sigma_-(z) = z\mathbf{1} - (\tilde{G}_-(z))^{-1}. \quad (6.35)$$

The self-energy is important because the spectrum of $\Sigma_-(z)$ gives an approximation to the spectrum of $\tilde{\mathcal{H}}_-$ since by definition

$$\tilde{\mathcal{H}}_- = z\mathbf{1} - \Pi_-(\tilde{G}^{-1}(z))\Pi_- \quad (6.36)$$

while

$$\Sigma_-(z) = z\mathbf{1} - (\Pi_-\tilde{G}(z)\Pi_-)^{-1}. \quad (6.37)$$

Remark 77. As is explained by Oliveira and Terhal [131], loosely speaking, if $\Sigma_-(z)$ is roughly constant in some range of z (defined below in Theorem 17) then $\Sigma_-(z)$ is playing the role of $\tilde{\mathcal{H}}_-$.

The gadget theorem was formalized in [133] and improved in [131] where the following theorem is proven (as in [131] we state the case where \mathcal{H} has zero as its lowest eigenvalue and a spectral gap of Δ).

Definition 68. We use operator norm $\|\cdot\|$ which is defined as

$$\|M\| \equiv \max_{|\psi\rangle \in \mathcal{M}} |\langle \psi | M | \psi \rangle| \quad (6.38)$$

for an operator M acting on a vectors in the Hilbert space \mathcal{M} .

Theorem 17 (Gadget Theorem [131; 133]). Let

$$\|V\| \leq \Delta/2$$

where Δ is the spectral gap of \mathcal{H} and let the low and high spectrum of \mathcal{H} be separated by a cutoff

$$\lambda_* = \Delta/2.$$

Now let there be an effective Hamiltonian \mathcal{H}_{eff} with a spectrum contained in $[a, b]$. If for some real constant $\varepsilon > 0$ and

$$\forall z \in [a - \varepsilon, b + \varepsilon]$$

with

$$a < b < \Delta/2 - \varepsilon,$$

the self-energy $\Sigma_-(z)$ has the property that

$$\|\Sigma_-(z) - \mathcal{H}_{\text{eff}}\| \leq \varepsilon,$$

then each eigenvalue $\tilde{\lambda}_j$ of $\tilde{\mathcal{H}}_-$ differs to the j^{th} eigenvalue of \mathcal{H}_{eff} , λ_j , by at most ε . In other words

$$|\tilde{\lambda}_j - \lambda_j| \leq \varepsilon, \quad \forall j.$$

To apply Theorem 17, a series expansion for $\Sigma_-(z)$ is truncated at low order for which \mathcal{H}_{eff} is approximated. The 2-body terms in \mathcal{H} and V by construction can give rise to higher order terms in \mathcal{H}_{eff} . For this reason it is possible to engineer \mathcal{H}_{eff} from $\Sigma_-(z)$ to approximate $\mathcal{H}_{\text{targ}}$ up to error ε in the range of z considered in Theorem 17 by introducing auxiliary spins and a suitable selection of 2-body \mathcal{H} and V . Using the series expansion of \tilde{G} in (6.34), the self-energy

$$\Sigma_-(z) = z\mathbf{1} - \tilde{G}_-^{-1}(z) \tag{6.39}$$

can be expanded as (for further details see [133])

$$\Sigma_-(z) = H_- + V_- + V_{-+}G_+(z)V_{+-} + V_{-+}G_+(z)V_+G_+(z)V_{+-} + \dots \tag{6.40}$$

The terms of 2nd order and higher in this expansion give rise to the effective many-body interactions.

6.5 Subdivision gadget

Summary. The subdivision gadget is introduced by Oliveira and Terhal [131] in their proof that 2-LOCAL HAMILTONIAN ON SQUARE LATTICE is QMA-COMplete. Here we show an improved lower bound for the spectral gap Δ needed on the slack of the gadget. A subdivision gadget simulates a many-body target Hamiltonian $\mathcal{H}_{\text{targ}} = \mathcal{H}_{\text{else}} + \alpha \cdot A \otimes B$ ($\mathcal{H}_{\text{else}}$ is a Hamiltonian of arbitrary norm, $\|A\| = 1$ and $\|B\| = 1$) by introducing an slack spin w and applying onto it a penalty Hamiltonian $\mathcal{H} = \Delta|1\rangle\langle 1|_w$ so that its ground state subspace $\mathcal{L}_- = \text{span}\{|0\rangle_w\}$ and its excited subspace $\mathcal{L}_+ = \text{span}\{|1\rangle_w\}$ are separated by energy gap Δ . In addition to the penalty Hamiltonian \mathcal{H} , we add a perturbation V of the form

$$V = \mathcal{H}_{\text{else}} + |\alpha||0\rangle\langle 0|_w + \sqrt{\frac{|\alpha|\Delta}{2}}(\text{sgn}(\alpha)A - B) \otimes X_w. \quad (6.41)$$

Hence if the target term $A \otimes B$ is k -local, the gadget Hamiltonian $\tilde{\mathcal{H}} = \mathcal{H} + V$ is at most $(\lceil k/2 \rceil + 1)$ -local, accomplishing the locality reduction. Assume $\mathcal{H}_{\text{targ}}$ acts on n qubits. Prior work [131] shows that $\Delta = \Theta(\varepsilon^{-2})$ is a sufficient condition for the lowest 2^n levels of the gadget Hamiltonian $\tilde{\mathcal{H}}$ to be ε -close to the corresponding spectrum of $\mathcal{H}_{\text{targ}}$. However, by bounding the infinite series of error terms in the perturbative expansion, we are able to obtain a tighter lower bound for Δ for error ε . Hence we arrive at our first result (details will be presented later in this section), that it suffices to let

$$\Delta \geq \left(\frac{2|\alpha|}{\varepsilon} + 1 \right) (2\|\mathcal{H}_{\text{else}}\| + |\alpha| + \varepsilon). \quad (6.42)$$

In Figure 6.2 we show numerics indicating the minimum Δ required as a function of α and ε . In Figure 6.2a the numerical results and the analytical lower bound in (6.42) show that for our subdivision gadgets, Δ can scale as favorably as $\Theta(\varepsilon^{-1})$. For the subdivision gadget presented in [131], Δ scales as $\Theta(\varepsilon^{-2})$. Though much less than the original assignment in [131], the lower bound of Δ in (6.42), still satisfies the condition of Theorem 17. In Figure 6.2 we numerically find the minimum value of such Δ that yields a spectral error of exactly ε .

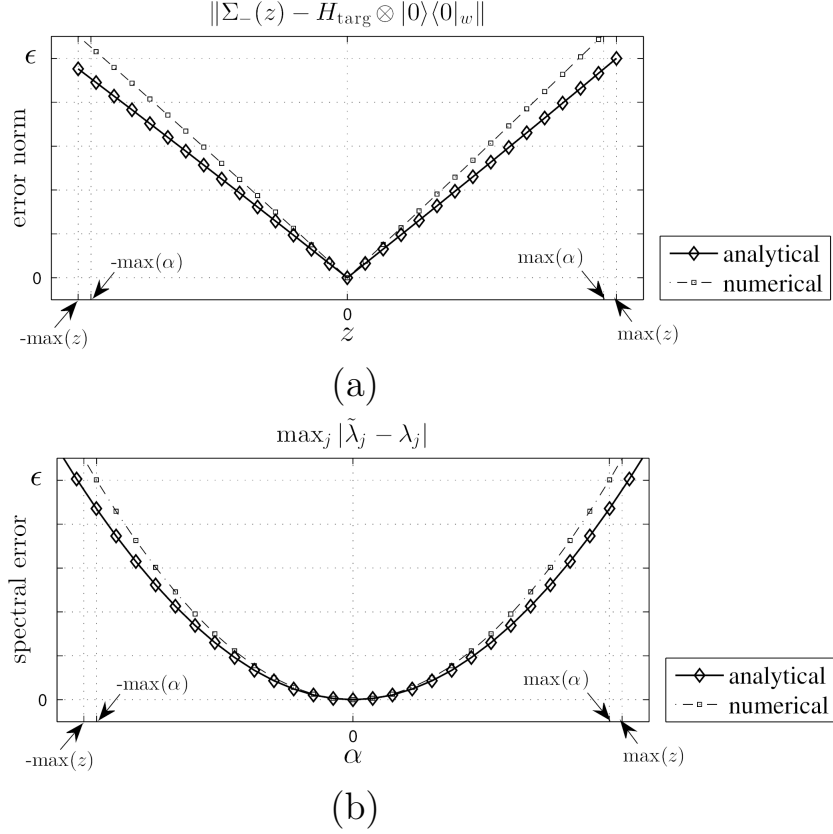


Figure 6.1 — Numerical illustration of gadget theorem using a subdivision gadget. Here we use a subdivision gadget to approximate $\mathcal{H}_{\text{targ}} = \mathcal{H}_{\text{else}} + \alpha Z_1 Z_2$ with $\|\mathcal{H}_{\text{else}}\| = 0$ and $\alpha \in [-1, 1]$. $\epsilon = 0.05$. “analytical” stands for the case where the value of Δ is calculated using (6.49) when $|\alpha| = 1$. “numerical” represents the case where Δ takes the value that yield the spectral error to be ϵ . In (a) we let $\alpha = 1$. $z \in [-\max z, \max z]$ with $\max z = \|\mathcal{H}_{\text{else}}\| + \max \alpha + \epsilon$. The operator $\Sigma_-(z)$ is computed up to the 3rd order. Subplot (b) shows for every value of α in its range, the maximum difference between the eigenvalues $\tilde{\lambda}_j$ in the low-lying spectrum of $\tilde{\mathcal{H}}$ and the corresponding eigenvalues λ_j in the spectrum of $\mathcal{H}_{\text{targ}} \otimes |0\rangle\langle 0|_w$. (These plots are from [24]).

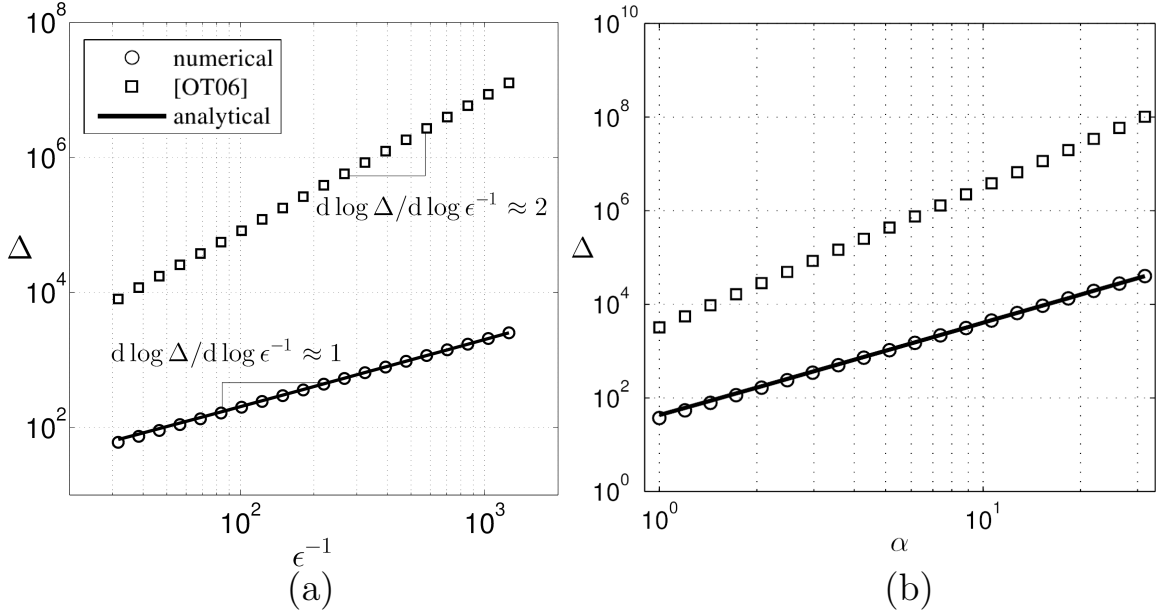


Figure 6.2 — Comparison between our subdivision gadget with that of Oliveira and Terhal [131]. The data labelled as “numerical” represent the Δ values obtained from the numerical search such that the spectral error between $\mathcal{H}_{\text{targ}}$ and $\tilde{\mathcal{H}}_-$ is ϵ . The data obtained from the calculation using (6.42) are labelled as “analytical”. “[OT06]” refers to values of Δ calculated according to the assignment by Oliveira and Terhal [131]. In this example we consider $\mathcal{H}_{\text{targ}} = \mathcal{H}_{\text{else}} + \alpha Z_1 Z_2$. (a) Gap scaling with respect to ϵ^{-1} . Here $\|\mathcal{H}_{\text{else}}\| = 0$ and $\alpha = 1$. (b) The gap Δ as a function of the desired coupling α . Here $\|\mathcal{H}_{\text{else}}\| = 0$, $\epsilon = 0.05$.

Analysis. The currently known subdivision gadgets in the literature assume that the gap in the penalty Hamiltonian Δ scales as $\Theta(\varepsilon^{-2})$ (see for example [131; 144]). Here we employ a method which uses infinite series to find the upper bound to the norm of the high order terms in the perturbative expansion. We find that in fact $\Delta = \Theta(\varepsilon^{-1})$ is sufficient for the error to be within ε .

The key aspect of developing the gadget is that given $\mathcal{H} = \Delta|1\rangle\langle 1|_w$, we need to determine a perturbation V to perturb the low energy subspace

$$\mathcal{L}_- = \text{span}\{|\psi\rangle \otimes |0\rangle_w, |\psi\rangle \text{ is any state of the system excluding the slack spin } w\}$$

such that the low energy subspace of the gadget Hamiltonian $\tilde{\mathcal{H}} = \mathcal{H} + V$ approximates the spectrum of the entire operator $\mathcal{H}_{\text{targ}} \otimes |0\rangle\langle 0|_w$ up to error ε . Here we will define V and work backwards to show that it satisfies Theorem 17. We let

$$V = \mathcal{H}_{\text{else}} + \frac{1}{\Delta}(\kappa^2 A^2 + \lambda^2 B^2) \otimes |0\rangle\langle 0|_w + (\kappa A + \lambda B) \otimes X_w \quad (6.43)$$

where κ, λ are constants which will be determined such that the dominant contribution to the perturbative expansion which approximates $\tilde{\mathcal{H}}_-$ gives rise to the target Hamiltonian $\mathcal{H}_{\text{targ}} = \mathcal{H}_{\text{else}} + \alpha \cdot A \otimes B$. In (6.43) and the remainder of the section, by slight abuse of notation, we use $\kappa A + \lambda B$ to represent $\kappa(A \otimes \mathbb{1}_{\mathcal{B}}) + \lambda(\mathbb{1}_{\mathcal{A}} \otimes B)$ for economy. Here $\mathbb{1}_{\mathcal{A}}$ and $\mathbb{1}_{\mathcal{B}}$ are identity operators acting on the subspaces \mathcal{A} and \mathcal{B} respectively. The partitions of V in the subspaces are

$$\begin{aligned} V_+ &= \mathcal{H}_{\text{else}} \otimes |1\rangle\langle 1|_w, & V_- &= \left(\mathcal{H}_{\text{else}} + \frac{1}{\Delta}(\kappa^2 A^2 + \lambda^2 B^2) \mathbb{1} \right) \otimes |0\rangle\langle 0|_w, \\ V_{-+} &= (\kappa A + \lambda B) \otimes |0\rangle\langle 1|_w, & V_{+-} &= (\kappa A + \lambda B) \otimes |1\rangle\langle 0|_w. \end{aligned} \quad (6.44)$$

We would like to approximate the target Hamiltonian $\mathcal{H}_{\text{targ}}$ and so expand the self-energy in (6.40) up to 2nd order. Note that $\mathcal{H}_- = 0$ and $G_+(z) = (z - \Delta)^{-1}|1\rangle\langle 1|_w$.

Therefore the self energy $\Sigma_-(z)$ can be expanded as

$$\begin{aligned}
\Sigma_-(z) &= V_- + \frac{1}{z - \Delta} V_{-+} V_{+-} + \sum_{k=1}^{\infty} \frac{V_{-+} V_+^k V_{+-}}{(z - \Delta)^{k+1}} = \\
&= \underbrace{\left(\mathcal{H}_{\text{else}} - \frac{2\kappa\lambda}{\Delta} A \otimes B \right)}_{\mathcal{H}_{\text{eff}}} \otimes |0\rangle\langle 0|_w + \\
&\quad + \underbrace{\frac{z}{\Delta(z - \Delta)} (\kappa A + \lambda B)^2 \otimes |0\rangle\langle 0|_w + \sum_{k=1}^{\infty} \frac{V_{-+} V_+^k V_{+-}}{(z - \Delta)^{k+1}}}_{\text{error term}}.
\end{aligned} \tag{6.45}$$

By selecting $\kappa = \text{sgn}(\alpha)(|\alpha|\Delta/2)^{1/2}$ and $\lambda = -(|\alpha|\Delta/2)^{1/2}$, the leading order term in $\Sigma_-(z)$ becomes $\mathcal{H}_{\text{eff}} = \mathcal{H}_{\text{targ}} \otimes |0\rangle\langle 0|_w$. We must now show that the condition of Theorem 17 is satisfied i.e. for a small real number $\varepsilon > 0$, $\|\Sigma_-(z) - \mathcal{H}_{\text{eff}}\| \leq \varepsilon, \forall z \in [\min z, \max z]$ where $\max z = \|\mathcal{H}_{\text{else}}\| + |\alpha| + \varepsilon = -\min z$. Essentially this amounts to choosing a value of Δ to cause the error term in (6.45) to be $\leq \varepsilon$. In order to derive a tighter lower bound for Δ , we bound the norm of the error term in (6.45) by letting $z \mapsto \max z$ and from the triangle inequality for operator norms:

$$\begin{aligned}
\left\| \frac{z}{\Delta(z - \Delta)} (\kappa A + \lambda B)^2 \otimes |0\rangle\langle 0|_w \right\| &\leq \frac{\max z}{\Delta(\Delta - \max z)} \cdot 4\kappa^2 = \frac{2|\alpha| \max z}{\Delta - \max z} \tag{6.46} \\
\left\| \sum_{k=1}^{\infty} \frac{V_{-+} V_+^k V_{+-}}{(z - \Delta)^{k+1}} \right\| &\leq \sum_{k=1}^{\infty} \frac{\|V_{-+}\| \cdot \|V_+\|^k \cdot \|V_{+-}\|}{(\Delta - \max z)^{k+1}} \leq \\
&\leq \sum_{k=1}^{\infty} \frac{2|\kappa| \cdot \|\mathcal{H}_{\text{else}}\|^k \cdot 2|\kappa|}{(\Delta - \max z)^{k+1}} = \\
&= \sum_{k=1}^{\infty} \frac{2|\alpha|\Delta \|\mathcal{H}_{\text{else}}\|^k}{(\Delta - \max z)^{k+1}}.
\end{aligned}$$

Using $\mathcal{H}_{\text{eff}} = \mathcal{H}_{\text{targ}} \otimes |0\rangle\langle 0|_w$, from (6.45) we see that

$$\|\Sigma_-(z) - \mathcal{H}_{\text{targ}} \otimes |0\rangle\langle 0|_w\| \leq \frac{2|\alpha| \max z}{\Delta - \max z} + \sum_{k=1}^{\infty} \frac{2|\alpha|\Delta \|\mathcal{H}_{\text{else}}\|^k}{(\Delta - \max z)^{k+1}} = \quad (6.47)$$

$$= \frac{2|\alpha| \max z}{\Delta - \max z} + \frac{2|\alpha|\Delta}{\Delta - \max z} \cdot \frac{\|\mathcal{H}_{\text{else}}\|}{\Delta - \max z - \|\mathcal{H}_{\text{else}}\|}. \quad (6.48)$$

Here going from (6.47) to (6.48) we have assumed the convergence of the infinite series in (6.47), which adds the reasonable constraint that

$$\Delta > |\alpha| + \varepsilon + 2\|\mathcal{H}_{\text{else}}\|.$$

To ensure that

$$\|\Sigma_-(z) - \mathcal{H}_{\text{targ}} \otimes |0\rangle\langle 0|_w\| \leq \varepsilon$$

it is sufficient to let expression (6.48) be $\leq \varepsilon$, which implies that

$$\Delta \geq \left(\frac{2|\alpha|}{\varepsilon} + 1 \right) (|\alpha| + \varepsilon + 2\|\mathcal{H}_{\text{else}}\|) \quad (6.49)$$

which is $\Theta(\varepsilon^{-1})$, a tighter bound than $\Theta(\varepsilon^{-2})$ in the literature [131; 133; 144]. This bound is illustrated with a numerical example (Figure 6.1). From the data labelled as “analytical” in Figure 6.1a we see that the error norm $\|\Sigma_-(z) - \mathcal{H}_{\text{eff}}\|$ is within ε for all z considered in the range, which satisfies the condition of the theorem for the chosen example. In Figure 6.1b, the data labelled “analytical” show that the spectral difference between $\tilde{\mathcal{H}}_-$ and $\mathcal{H}_{\text{eff}} = \mathcal{H}_{\text{targ}} \otimes |0\rangle\langle 0|_w$ is indeed within ε as the theorem promises. Furthermore, note that the condition of Theorem 17 is only sufficient, which justifies why in Figure 6.1b for α values at $\max \alpha$ and $\min \alpha$ the spectral error is strictly below ε . This indicates that an even smaller Δ , although below the bound we found in (6.49) to satisfy the theorem, could still yield the spectral error within ε for all α values in the range. The smallest value Δ can take would be one such that the spectral error is exactly ε when α is at its extrema. We numerically find this Δ (up to numerical error which is less than $10^{-5}\varepsilon$) and as demonstrated in Figure 6.1b, the data labelled “numerical” shows that the spectral error is indeed ε at $\max(\alpha)$ and $\min(\alpha)$, yet in Figure 6.1a the data labelled “numerical” shows that for some z in the range the condition of the

Theorem 17,

$$\|\Sigma_-(z) - \mathcal{H}_{\text{targ}} \otimes |0\rangle\langle 0|_w\| \leq \varepsilon, \quad (6.50)$$

no longer holds. In Figure 6.1 we assume that ε is kept constant. In Figure 6.2a we compute both analytical and numerical Δ values for different values of ε .

6.6 YY-gadget

Summary. The gadgets which we have presented so far are intended to reduce the locality of the target Hamiltonian. Here we present another type of gadget, called “creation” gadgets [124], which simulate the type of effective couplings that are not present in the gadget Hamiltonian. Many creation gadgets proposed so far are modifications of existing reduction gadgets. For example, the ZZXX gadget in [124], which is intended to simulate $Z_i X_j$ terms using Hamiltonians of the form

$$\mathcal{H}_{ZZXX} = \sum_i \Delta_i X_i + \sum_i h_i Z_i + \sum_{i,j} J_{ij} Z_i Z_j + \sum_{i,j} K_{ij} X_i X_j, \quad (6.51)$$

is essentially a 3- to 2-body gadget with the target term $A \otimes B \otimes C$ being such that the operators A , B and C are X , Z and identity respectively. Therefore the analyses on 3- to 2- body reduction gadgets that we have presented for finding the lower bound for the gap Δ are also applicable to this ZZXX creation gadget.

Note that YY terms can be easily realized via bases rotation if single-qubit Y terms are present in the Hamiltonian in (6.51). Otherwise it is not *a priori* clear how to realize YY terms using \mathcal{H}_{ZZXX} in (6.51). We will now present the first YY gadget which starts with a universal Hamiltonian of the form (6.51) and simulates the target Hamiltonian $\mathcal{H}_{\text{targ}} = \mathcal{H}_{\text{else}} + \alpha Y_i Y_j$. The basic idea is to use the identity $X_i Z_i = i Y_i$ and induce a term of the form $X_i Z_i Z_j X_j = Y_i Y_j$ at the 4th order. Introduce slack qubit w and apply a penalty $\mathcal{H} = \Delta |1\rangle\langle 1|_w$. With a perturbation V we could perform the same perturbative expansion as previously. Given that the 4th order perturbation is $V_{-+} V_{+} V_{+} V_{+-}$ up to a scaling constant, we could let single X_i and X_j be coupled with X_w , which causes both X_i and X_j to appear in V_{-+} and V_{+-} . Furthermore, we couple single Z_i and Z_j terms with Z_w . Then $\frac{1}{2}(\mathbb{1} + Z_w)$ projects single Z_i and Z_j onto the + subspace and causes

them to appear in V_+ . For $\mathcal{H}_{\text{targ}} = \mathcal{H}_{\text{else}} + \alpha Y_1 Y_2$, the full expressions for the gadget Hamiltonian is the following: the penalty Hamiltonian $\mathcal{H} = \Delta |1\rangle\langle 1|_w$ acts on the slack qubit. The perturbation $V = V_0 + V_1 + V_2$ where V_0 , V_1 , and V_2 are defined as

$$\begin{aligned} V_0 &= \mathcal{H}_{\text{else}} + \mu(Z_1 + Z_2) \otimes |1\rangle\langle 1|_w + \mu(X_1 - \text{sgn}(\alpha)X_2) \otimes X_w \\ V_1 &= \frac{2\mu^2}{\Delta} (\mathbf{1} \otimes |0\rangle\langle 0|_w + X_1 X_2) \\ V_2 &= -\frac{2\mu^4}{\Delta^3} Z_1 Z_2. \end{aligned} \tag{6.52}$$

with $\mu = (|\alpha|\Delta^3/4)^{1/4}$. For a specified error tolerance ε , we have constructed a YY gadget Hamiltonian of gap scaling $\Delta = O(\varepsilon^{-4})$ and the low-lying spectrum of the gadget Hamiltonian captures the spectrum of $\mathcal{H}_{\text{targ}} \otimes |0\rangle\langle 0|_w$ up to error ε .

The YY gadget implies that a wider class of Hamiltonians such as

$$\mathcal{H}_{ZZYY} = \sum_i h_i X_i + \sum_i l_i Z_i + \sum_{i,j} J_{ij} Z_i Z_j + \sum_{i,j} K_{ij} Y_i Y_j \tag{6.53}$$

and

$$\mathcal{H}_{XXYY} = \sum_i h_i X_i + \sum_i l_i Z_i + \sum_{i,j} J_{ij} X_i X_j + \sum_{i,j} K_{ij} Y_i Y_j \tag{6.54}$$

can be simulated using the Hamiltonian of the form in (6.51). Therefore using the Hamiltonian in (6.51) one can in principle simulate any finite-norm real valued Hamiltonian on qubits. Although by the QMA-completeness of \mathcal{H}_{ZZXX} one could already simulate such Hamiltonian via suitable embedding, our YY gadget provides a more direct alternative for the simulation.

Analysis. The results in [124] shows that Hamiltonians of the form in (6.51) supports universal adiabatic quantum computation and finding the ground state of such a Hamiltonian is QMA-COMplete. This form of Hamiltonian is also interesting because of its relevance to experimental implementation [139]. Here we show that with a Hamiltonian of the form in (6.51) we could simulate a target Hamiltonian $\mathcal{H}_{\text{targ}} = \mathcal{H}_{\text{else}} + \alpha Y_1 Y_2$. Introduce an slack w and define the penalty

Hamiltonian as $\mathcal{H} = \Delta|1\rangle\langle 1|_w$. Let the perturbation $V = V_0 + V_1 + V_2$ be

$$\begin{aligned} V_0 &= \mathcal{H}_{\text{else}} + \kappa(Z_1 + Z_2) \otimes |1\rangle\langle 1|_w + \kappa(X_1 - \text{sgn}(\alpha)X_2) \otimes X_w \\ V_1 &= 2\kappa^2\Delta^{-1}[|0\rangle\langle 0|_w - \text{sgn}(\alpha)X_1X_2] \\ V_2 &= -4\kappa^4\Delta^{-3}Z_1Z_2. \end{aligned} \quad (6.55)$$

Then the gadget Hamiltonian $\tilde{\mathcal{H}} = \mathcal{H} + V$ is of the form in (6.51). Here we choose the parameter $\kappa = (|\alpha|\Delta^3/4)^{1/4}$. In order to show that the low lying spectrum of $\tilde{\mathcal{H}}$ captures that of the target Hamiltonian, define $\mathcal{L}_- = \text{span}\{|\psi\rangle \text{ such that } \tilde{\mathcal{H}}|\psi\rangle = \lambda|\psi\rangle, \lambda < \Delta/2\}$ as the low energy subspace of $\tilde{\mathcal{H}}$ and $\mathcal{L}_+ = \mathbb{1} - \mathcal{L}_-$. Define Π_- and Π_+ as the projectors onto \mathcal{L}_- and \mathcal{L}_+ respectively.

With these notations in place, here we show that the spectrum of $\tilde{\mathcal{H}}_- = \Pi_- \tilde{\mathcal{H}} \Pi_-$ approximates the spectrum of $\mathcal{H}_{\text{target}} \otimes |0\rangle\langle 0|_w$ with error ε . To begin with, the projections of V into the subspaces \mathcal{L}_- and \mathcal{L}_+ can be written as

$$\begin{aligned} V_- &= \left(\mathcal{H}_{\text{else}} + \underbrace{\frac{\kappa^2}{\Delta}(X_1 - \text{sgn}(\alpha)X_2)^2}_{(a)} - \underbrace{\frac{4\kappa^4}{\Delta^3}Z_1Z_2}_{(b)} \right) \otimes |0\rangle\langle 0|_w \\ V_+ &= \left(\mathcal{H}_{\text{else}} + \kappa(Z_1 + Z_2) - \frac{2\kappa^2}{\Delta}\text{sgn}(\alpha)X_1X_2 - \frac{4\kappa^4}{\Delta^3}Z_1Z_2 \right) \otimes |1\rangle\langle 1|_w \\ V_{-+} &= \kappa(X_1 - \text{sgn}(\alpha)X_2) \otimes |0\rangle\langle 1|_w \\ V_{+-} &= \kappa(X_1 - \text{sgn}(\alpha)X_2) \otimes |1\rangle\langle 0|_w \end{aligned} \quad (6.56)$$

Given the penalty Hamiltonian \mathcal{H} , we have the operator valued resolvent $G(z) = (z\mathbb{1} - \mathcal{H})^{-1}$ that satisfies $G_+(z) = \Pi_+ G(z) \Pi_+ = (z - \Delta)^{-1}|1\rangle\langle 1|_w$. Then the low lying sector of the gadget Hamiltonian $\tilde{\mathcal{H}}$ can be approximated by the perturbative expansion (6.40). For our purposes we will consider terms up to the 4th order:

$$\begin{aligned} \Sigma_-(z) &= V_- + \frac{1}{z - \Delta}V_{-+}V_{+-} + \frac{1}{(z - \Delta)^2}V_{-+}V_+V_{+-} + \\ &+ \frac{1}{(z - \Delta)^3}V_{-+}V_+V_+V_{+-} + \sum_{k=3}^{\infty} \frac{V_{-+}V_+^kV_{+-}}{(z - \Delta)^{k+1}}. \end{aligned} \quad (6.57)$$

Now we explain the perturbative terms that arise at each order. The 1st order is the same as V_- in (6.56). The 2nd order term gives

$$\frac{1}{z - \Delta} V_{-+} V_{+-} = \underbrace{\frac{1}{z - \Delta} \cdot \kappa^2 (X_1 - \text{agn}(\alpha) X_2)^2}_{(c)} \otimes |0\rangle\langle 0|_w. \quad (6.58)$$

At the 3rd order, we have

$$\begin{aligned} \frac{1}{(z - \Delta)^2} V_{-+} V_+ V_{+-} &= \\ &= \left(\frac{1}{(z - \Delta)^2} \cdot \kappa^2 (X_1 - \text{agn}(\alpha) X_2) \mathcal{H}_{\text{else}} (X_1 - \text{sgn}(\alpha) X_2) \times \right. \\ &\quad \left. \cdot \underbrace{\frac{1}{(z - \Delta)^2} \frac{4\kappa^4}{\Delta} (X_1 X_2 - \text{sgn}(\alpha) \mathbb{1})}_{(d)} \right) \otimes |0\rangle\langle 0|_w + O(\Delta^{-1/4}). \end{aligned} \quad (6.59)$$

The 4th order contains the desired YY term:

$$\begin{aligned} \frac{1}{(z - \Delta)^3} V_{-+} V_+ V_+ V_{+-} &= \\ &= \left(\underbrace{\frac{1}{(z - \Delta)^3} \cdot 2\kappa^4 (X_1 - \text{sgn}(\alpha) X_2)^2}_{(e)} - \underbrace{\frac{1}{(z - \Delta)^3} 4\kappa^4 Z_1 Z_2}_{(f)} + \right. \\ &\quad \left. + \frac{4\kappa^4 \text{sgn}(\alpha)}{(z - \Delta)^3} Y_1 Y_2 \right) \otimes |0\rangle\langle 0|_w + O(\|\mathcal{H}_{\text{else}}\| \cdot \Delta^{-3/4}) + \\ &\quad + O(\|\mathcal{H}_{\text{else}}\|^2 \cdot \Delta^{-1/2}) \end{aligned} \quad (6.60)$$

Note that with the choice of $\kappa = (|\alpha| \Delta^3 / 4)^{1/4}$, all terms of 5th order and higher are of norm $O(\Delta^{-1/4})$. In the 1st order through 4th order perturbations the unwanted terms are labelled as (a) through (f) in (6.56), (6.58), (6.59), and (6.60). Note how they compensate in pairs: the sum of (a) and (c) is $O(\Delta^{-1/4})$. The same holds for (d) and (e), (b) and (f). Then the self energy is then

$$\Sigma_-(z) = (\mathcal{H}_{\text{else}} + \alpha Y_1 Y_2) \otimes |0\rangle\langle 0|_w + O(\Delta^{-1/4}). \quad (6.61)$$

Let $\Delta = \Theta(\varepsilon^{-4})$, then by the Gadget Theorem (17), the low-lying sector of the gadget Hamiltonian $\tilde{\mathcal{H}}_-$ captures the spectrum of $\mathcal{H}_{\text{targ}} \otimes |0\rangle\langle 0|_w$ up to error ε .

The fact that the gadget relies on 4th order perturbation renders the gap scaling relatively larger than it is in the case of subdivision or 3- to 2-body reduction gadgets. However, this does not diminish its usefulness in all applications.

Chapter 7. Conclusion and Open Problems

I believe the presented results, as they were carefully selected, form the foundation of the modern theory of quantum information processing. While many aspects of the topic have been well developed, the ending point of this story is just a beginning of what I think will prove to be an even deeper and perhaps an even more exciting direction in this changing field: from the variational NISQ-era and beyond.

I now plan to address the following open questions. Perhaps I can hope that readers of this thesis will also work on these questions. I hope that the materials presented here will serve these purposes, or otherwise serve your research. Some of the questions I am now considering include:

To understand the power of low-depth circuits, particularly the approximate trainability of circuits (e.g. with respect to the hardware efficient ansatz [109] or the checkerboard ansatz).

1. It was recently shown in [152] that variational circuits can approximate t -designs. In general, how well short circuits can approximate t -designs remains open. (see related results in [107])
2. A systematic analysis of the epsilon neighborhood of a variational family with respect to ansatz depth is still lacking.
3. Furthermore, a theory to avoid barren plateaus appears to be distant yet possibly can follow from recent findings. The development of such a theory is of tantamount importance.

To develop a means of active error mitigation for the variational model of quantum computation. While post-processing error decoders [153] have been developed recently, as have compilation of error control codes into ansatz states see e.g. [154; 155], novel approaches to variational error mitigation are emerging [156; 157] yet still lacking development.

1. Does the circuit to variational mapping [10] to approximate the output of general quantum circuits offer a means towards active error correction in variational algorithms?

2. As variational algorithms rely on local measurements, can information gained in this process influence consequential measurement basis choices and operations to correct errors?
3. Furthermore, the impacts of noise on variational algorithms (while studied in some detail) represents largely an unknown domain. For example, recently QAOA experiments by Google were limited to depth 3 ansatz levels due to noise levels.
4. To study existing variational quantum algorithms and to determine, in physical and mathematical terms, their inherent limitations and potential advantages for tasks such as machine learning [158] and quantum simulation.

To understand variable concentrations. E.g. It was recently proven in [104] for the Sherrington-Kirkpatrick model, how generally to variable concentrations extend with respect to the algorithmic 3SAT phase transition?

Hall of Fame

I thank all of my coauthors who are often mentioned in the main body of the text but sometimes they are not. Sergey Filippov kindly agreed to offer his advise as I needed it many times, especially when trying to figure out Russian thesis regulations. The Russian Quantum Center, courtesy in particular of Alex Fedorov and Ruslan Yunusov, kindly agreed to review my work as did M. V. Lomonosov Moscow State University Quantum Technology Center.

I hope this thesis will be readable by graduate students and serve as an introduction to many modern concepts.

I humbly tip my hat to the following readers. These brave souls found and reported typos, errors or omissions, improving this monograph for all future readers.

Ernesto Campos

Alex Fedorov

Andrey Kardashin

Vladimir Korepin

Albert Nasibulin

Sergey Rykovanov

Beat Toedtli

Alexey Uvarov

Alexander Vlasov

I also gratefully acknowledge Aly Nasrallah and Przemysław Scherwentke for assisting with \LaTeX typesetting. Finally, I thank Andrey Kardashin, Dina Fedotova and Ksenia Samburskaya for assisting in understanding the myriad of rules in both the document format and the defense process.

List of abbreviations

AND — Logical conjunction. Logic gate.

AQC — Adiabatic quantum computation.

cbit, c-Bit — A deterministic bit able to store logical zero or otherwise logical one.

CN, k -CN, CNOT — A controlled NOT activated when the AND of all k controls is logical 1.

CNF — Conjunctive Normal Form. A formula is in conjunctive normal form if it is an AND of ORs. It is often called a *product of sums*.

DNF — Disjunctive Normal Form. A formula is in disjunctive normal form is a Boolean-logical formula consisting of an OR of ANDs. It is often called a *sum of products*.

k -body/ k -local Hamiltonian — A Hermitian operator acting on a finite number of qubits where each term acts non-trivially on at most k -qubits.

ML — Machine Learning.

pbit, p-bit — A *probabilistic* bit able to store expected values of recovering logical zero and logical one.

NAND — Logical Negation of AND. Logic gate.

NOR — Logical Negation of OR. Logic gate.

NOT — Logical Negation. Inverter. Represented by Pauli matrix X .

NISQ — Noisy Intermediate Scale Quantum Technology.

OR — Logical Disjunction. Logic gate.

SAT — Boolean Satisfiability Problem (see also 2-, 3- and k -SAT).

T.D.S.E. — Time Dependent Schrödinger's Equation.

T.I.S.E. — Time Independent Schrödinger's Equation.

QAOA — Quantum Approximate Optimization Algorithm.

QAOA — Quantum Alternating Operator Ansatz.

QFT — Quantum Fourier Transform.

QMA — Complexity Class Quantum Merlin Author (analog of NP).

QML — Quantum Machine Learning.

S.E. — Schrödinger's Equation.

VQE — Variational Quantum Eigensolver (Quantum Algorithm).

XOR — Logical Exclusive OR. Logic gate.

2-, 3- and k -SAT — Boolean Satisfiability Problem with specified variables per clause.

List of symbols

\S	section or chapter
$\stackrel{\text{def}}{=}$	defined as
\in	belongs to (a set)
\notin	does not belong to (a set)
\cap	intersection of sets
\cup	union of sets
\emptyset, \varnothing	empty set
\mathbb{B}	the single space of booleans $\{0,1\}$
\mathbb{B}^n	space of n -long boolean numbers $\{0,1\}^n$
\mathbb{N}	set of natural numbers which we assume includes zero ($\mathbb{N} \stackrel{\text{def}}{=} \mathbb{N} \cup \{0\}$)
\mathbb{Z}	set of integer numbers
\mathbb{Q}	set of rational numbers
\mathbb{R}	set of real numbers
\mathbb{R}^+	set of nonnegative real numbers
\mathbb{C}	set of complex numbers
$\mathbb{C}/\{0\}$	set of complex numbers with zero excluded
\mathbb{R}^n	space of column vectors with n real components
\mathbb{C}^n	space of column vectors with n complex components
i	$\sqrt{-1}$
\Re	projection; real part of the complex number
\Im	projection; part of the complex number
$ z $	modulus of complex number z
$T \subset S$	subset T of set S
$S \cap T$	intersection of sets S and T
$S \cup T$	union of sets S and T
$f(S)$	image of set S under mapping f
$f \circ g$	composition of two mappings $(f \circ g)(x) = f(g(x))$
$ x\rangle$	column vector in \mathbb{C}^n
$\langle x $	complex conjugate transpose of $ x\rangle$
$\ \cdot\ $	norm

$\langle x y\rangle$	scalar product (inner product) in \mathbb{C}^n
$\det(A)$	determinant of square matrix A
$\text{Tr}(A)$	trace of square matrix A
$\text{rank}(A)$	rank of matrix A
A^T	transpose of matrix A
\overline{A}	conjugate of matrix A
$\text{span}\{ i\rangle, j\rangle, \dots, k\rangle\}$	vector space formed by linear combinations of $ i\rangle, j\rangle, \dots, k\rangle$
$\text{span}\{A, B, \dots, C\}$	vector space formed by linear combinations of A, B, \dots, C
A^\dagger	conjugate transpose of matrix A
A^{-1}	inverse of matrix A
$\mathbb{1}$	identity matrix
AB	matrix product of $m \times n$ matrix A and $n \times p$ matrix B
$A \bullet B$	Hadamard (entrywise) product of $m \times n$ matrices A and B
$[A, B] \stackrel{\text{def}}{=} AB - BA$	commutator for square matrices A and B
$\{A, B\} \stackrel{\text{def}}{=} AB + BA$	anticommutator for square matrices A and B
$A \otimes B$	Kronecker (a.k.a. tensor) product
$A \oplus B$	direct sum of matrices/operators/spaces
$\mathcal{L}(\mathcal{A}, \mathcal{B})$	the space of linear maps between spaces \mathcal{A} and \mathcal{B}
$\mathcal{L}(\mathcal{A})$	the space of linear maps from \mathcal{A} to itself
δ_{jk}	Kronecker delta with $\delta_{jk} = 1$ for $j = k$ and $\delta_{jk} = 0$ for $j \neq k$
iff	if and only if
$A B$	The predicate A conditioned <i>such that</i> B is true
\mathfrak{u}	A Lie algebra of a unitary group, e.g. $\mathfrak{su}(2)$
\mathbf{U}	A unitary (Lie) group, e.g. $\mathbf{SU}(2)$

Definition 69 (Bell Basis). The standard Bell basis is denoted as follows.

1. $\sqrt{2}|\Phi^+\rangle = |00\rangle + |11\rangle$
2. $\sqrt{2}|\Phi^-\rangle = |00\rangle - |11\rangle$
3. $\sqrt{2}|\Psi^+\rangle = |01\rangle + |10\rangle$
4. $\sqrt{2}|\Psi^-\rangle = |01\rangle - |10\rangle$

Remark 78 (Using \cdot for a product with scalar(s)). Though typically omitted, we sometimes use \cdot to denote multiplication by a scalar.

Remark 79. We will interchange the notation $\sigma_0 \equiv \mathbb{1}$, $\sigma_1 \equiv X$, $\sigma_2 \equiv Y$, $\sigma_3 \equiv Z$.

Definition 70 (Pauli Matrices). We use the Pauli basis (or group; group algebra) defined by the following matrices and relations.

$$X = \begin{pmatrix} 0 & 1 \\ 1 & 0 \end{pmatrix} \quad Y = \begin{pmatrix} 0 & -i \\ i & 0 \end{pmatrix} \quad Z = \begin{pmatrix} 1 & 0 \\ 0 & -1 \end{pmatrix} \quad (7.1)$$

$$XY = iZ \quad (7.2)$$

$$X^2 = Y^2 = Z^2 = \mathbf{1} = -iXYZ \quad (7.3)$$

This group called the Pauli group together with the tensor product contains $4 \cdot 4^n$. This structure arises in angular momentum theory. Some properties are

1. $[O_i, O_j] = 2i\varepsilon^{ijk}O_k$ (Lie product)
2. complex conjugation

$$\forall \omega \in \{1, 2, 3\} \quad O_i O_\omega^* O_i = -O_\omega$$

3. $Tr(O_i O_j) = 2\delta_{ij}$
4. $O_i O_j = \delta_{ij}\mathbf{1} + i\varepsilon^{ijk}O_k$ (geometric product)
5. For $i = j$ $\{O_i, O_j\} = 2\delta_{ij}\mathbf{1}$

Example 38 (Single qubit density operator). A polarisation vector is defined as

$$\mathbf{P} = (p_1, p_2, p_3)$$

where $\forall i \ p_i \in \mathbb{R}$. We also define

$$\mathbf{O} = (O_1, O_2, O_3)$$

where the $O_i \in \{X, Y, Z\}$ A density operator can be written as

$$\rho = \rho^\dagger, \quad \rho \geq 0 \quad \text{Tr } \rho = 1, \quad (7.4)$$

with $\rho : \mathbb{C}^2 \rightarrow \mathbb{C}^2$. The density operator is another way to write a quantum state. This density operator can be written as

$$\rho = \frac{1}{2}\mathbf{1} + \mathbf{O} \cdot \mathbf{P} = \frac{1}{2}\mathbf{1} + \sum_i p_i O_i = \frac{1}{2} + p_1 X + p_2 Y + p_3 Z \quad (7.5)$$

We also define an inner product $(-, -) : (\mathbb{C}^2 \rightarrow \mathbb{C}^2) \times (\mathbb{C}^2 \rightarrow \mathbb{C}^2) \rightarrow \mathbb{C}$

$$(\mathbf{O} \cdot \mathbf{A}, \mathbf{O} \cdot \mathbf{B}) = \text{Tr} [(\mathbf{O} \cdot \mathbf{A})(\mathbf{O} \cdot \mathbf{B})] = \mathbf{A} \cdot \mathbf{B}$$

Remark 80. One readily verifies that $(\mathbf{O} \cdot \mathbf{A}, \mathbf{O} \cdot \mathbf{B}) = \mathbf{A} \cdot \mathbf{B} + i\mathbf{O}(\mathbf{A} \wedge \mathbf{B})$.

Remark 81. One can readily establish that for $\mathbf{A} = \mathbf{B}$ show that $\mathbf{A} \wedge \mathbf{B}$ vanishes. Hence $\lambda(\mathbf{A} \cdot \mathbf{O}) = \pm|A|$ and both roots appear as $\text{Tr} \mathbf{A} \cdot \mathbf{O} = 0$.

Switching Algebra Postulates

Identity Elements

$$x \vee 0 = 0$$

$$x \wedge 1 = x$$

Commutativity

$$x \vee y = y \vee x$$

$$x \wedge y = y \wedge x$$

Complements

$$x \vee \bar{x} = 1$$

$$x \wedge \bar{x} = 0$$

Absorption

$$x \vee (x \wedge y) = x$$

$$x \wedge (x \vee y) = x$$

$$x \vee (\bar{x} \wedge y) = x \vee y$$

$$x \wedge (\bar{x} \vee y) = x \wedge y$$

$$(x \wedge y) \vee (x \wedge \bar{y}) = x$$

$$(x \vee y) \wedge (x \vee \bar{y}) = x$$

Consensus

$$(x \wedge y) \vee (\bar{x} \wedge z) \vee (y \wedge z) = (x \wedge y) \vee (\bar{x} \wedge z) \quad (x \vee y) \wedge (\bar{x} \vee z) \wedge (y \vee z) = (x \vee y) \wedge (\bar{x} \vee z)$$

Associativity

$$(x \vee y) \vee z = x \vee (y \vee z)$$

$$(x \wedge y) \wedge z = x \wedge (y \wedge z)$$

Distributivity

$$x \vee (y \wedge z) = (x \vee y) \wedge (x \vee z)$$

$$x \wedge (y \vee z) = (x \wedge y) \vee (x \wedge z)$$

Idempotency

$$x \vee x = x$$

$$x \wedge x = x$$

Null elements

$$x \vee 1 = 1$$

$$x \wedge 0 = 0$$

Involution

$$\overline{(\overline{x})} = \overline{\overline{x}} = x$$

De Morgan's Laws

$$\neg(x \vee y) = \overline{x} \wedge \overline{y}$$

$$\neg(x \wedge y) = \overline{x} \vee \overline{y}$$

De Morgan's Principle of Duality

Any theorem or postulate in Boolean algebra remains true if:

$$0 \leftrightarrow 1$$

$$\wedge \leftrightarrow \vee$$

XOR algebra

Here we recall the algebraic normal form (ANF) for Boolean polynomials, commonly known as PPRMs, (Positive Polarity Reed Muller Forms).

Definition 71. The XOR-algebra forms a commutative ring with presentation $M = \{\mathbb{B}, \wedge, \oplus\}$ where the following product is called XOR

$$— \oplus — : \mathbb{B} \times \mathbb{B} \mapsto \mathbb{B} : (a,b) \rightarrow a + b - ab \text{ mod } 2 \quad (7.6)$$

and conjunction is given as

$$— \wedge — : \mathbb{B} \times \mathbb{B} \mapsto \mathbb{B} : (a,b) \rightarrow a \cdot b, \quad (7.7)$$

where $a \cdot b$ is regular multiplication over the reals (restricted to 0, 1). One defines left negation $\neg(\text{---})$ in terms of \oplus as $\neg(\text{---}) \equiv$

$$1 \oplus (\text{---}) : \mathbb{B} \mapsto \mathbb{B} : a \rightarrow 1 - a. \quad (7.8)$$

In the XOR-algebra, (i-v) hold.

- (i) $a \oplus 0 = a$,
- (ii) $a \oplus 1 = \neg a$,
- (iii) $a \oplus a = 0$,
- (iv) $a \oplus \neg a = 1$ and
- (v) $a \vee b = a \oplus b \oplus (a \wedge b)$

Hence, 0 is the unit of the operation XOR and 1 is the unit of AND. The 5th rule (v) reduces to $a \vee b = a \oplus b$ whenever $a \wedge b = 0$, which is the case for disjoint (mod 2) sums. The truth table for AND/XOR follows

x_1	x_2	$f(x_1, x_2) = x_1 \wedge x_2$	$f(x_1, x_2) = x_1 \oplus x_2$
0	0	0	0
0	1	0	1
1	0	0	1
1	1	1	0

Definition 72. Any Boolean equation may be uniquely expanded to the fixed polarity Reed-Muller form as

$$f(x_1, x_2, \dots, x_k) = c_0 \oplus c_1 x_1^{\sigma_1} \oplus c_2 x_2^{\sigma_2} \oplus \dots \oplus c_n x_n^{\sigma_n} \oplus c_{n+1} x_1^{\sigma_1} x_n^{\sigma_n} \oplus \dots \oplus c_{2k-1} x_1^{\sigma_1} x_2^{\sigma_2}, \dots, x_k^{\sigma_k}, \quad (7.9)$$

where selection variable $\sigma_i \in \{0, 1\}$, literal $x_i^{\sigma_i}$ represents a variable or its negation and any c term labeled c_0 through c_j is a binary constant 0 or 1. In (7.9) only fixed polarity variables appear such that each is in either uncomplemented or complemented form.

Let us now consider derivation of the form from Definition 72. As illustrative example, we avoid keeping track of indices in the n node case, by considering the case where $n \equiv 2^n = 8$.

Example 39. The vector $\underline{c} = (c_0, c_1, c_2, c_3, c_4, c_5, c_6, c_7)^\top$ represents all possible outputs of any function $f(x_1, x_2, x_3)$ over algebra $\mathbb{Z}_2 \times \mathbb{Z}_2 \times \mathbb{Z}_2$. We wish to

construct a normal form in terms of the vector \underline{c} , where each $c_i \in \{0,1\}$, and therefore \underline{c} is a selection vector that represents the output of the function $f : \mathbb{B} \times \mathbb{B} \times \mathbb{B} \rightarrow \mathbb{B} : (x_1, x_2, x_3) \mapsto f(x_1, x_2, x_3)$. One may expand f as (7.10).

$$\begin{aligned} f(x_1, x_2, x_3) = & (c_0 \cdot \neg x_1 \cdot \neg x_2 \cdot \neg x_3) \vee (c_1 \cdot \neg x_1 \cdot \neg x_2 \cdot x_3) \vee (c_2 \cdot \neg x_1 \cdot x_2 \cdot \neg x_3) \\ & \vee (c_3 \cdot \neg x_1 \cdot x_2 \cdot x_3) \vee (c_4 \cdot x_1 \cdot \neg x_2 \cdot \neg x_3) \vee (c_5 \cdot x_1 \cdot \neg x_2 \cdot x_3) \\ & \vee (c_6 \cdot x_1 \cdot x_2 \cdot \neg x_3) \vee (c_7 \cdot x_1 \cdot x_2 \cdot x_3) \end{aligned} \quad (7.10)$$

Since each disjunctive term is disjoint the logical OR operation may be replaced with the logical XOR operation. By making the substitution $\neg a = a \oplus 1$ for all variables and rearranging terms one arrives at the normal form (7.11).¹

$$\begin{aligned} f(x_1, x_2, x_3) = & \quad (7.11) \\ & c_0 \oplus (c_0 \oplus c_4) \cdot x_1 \oplus (c_0 \oplus c_2) \cdot x_2 \oplus (c_0 \oplus c_1) \cdot x_3 \oplus (c_0 \oplus c_2 \oplus c_4 \oplus c_6) \cdot x_1 \cdot x_2 \\ & \oplus (c_0 \oplus c_1 \oplus c_4 \oplus c_5) \cdot x_1 \cdot x_3 \oplus (c_0 \oplus c_1 \oplus c_2 \oplus c_3) \cdot x_2 \cdot x_3 \\ & \oplus (c_0 \oplus c_1 \oplus c_2 \oplus c_3 \oplus c_4 \oplus c_5 \oplus c_6 \oplus c_7) \cdot x_1 \cdot x_2 \cdot x_3 \end{aligned}$$

The set of algebraically independent polynomials, $\{x_1, x_2, x_3, x_1 \cdot x_2, x_1 \cdot x_3, x_2 \cdot x_3, x_1 \cdot x_2 \cdot x_3\}$ combined with a set of scalars from (7.11) spans the eight dimensional space of the hypercube representing the Algebra. A similar form holds for arbitrary n .

¹For instance, $\neg x_1 \cdot \neg x_2 \cdot \neg x_3 = (1 \oplus x_1) \cdot (1 \oplus x_2) \cdot (1 \oplus x_3) = (1 \oplus x_1 \oplus x_2 \oplus x_2 \cdot x_3) \cdot (1 \oplus x_3) = 1 \oplus x_1 \oplus x_2 \oplus x_3 \oplus x_1 \cdot x_3 \oplus x_2 \cdot x_3 \oplus x_1 \cdot x_2 \cdot x_3$.

Glossary of terms

adiabatic model of quantum computation; A model of quantum computation that relies on the adiabatic theorem to ensure that a physical process will minimize a target Hamiltonian which embeds a problem instance solution in its ground state.

adjoint; The complex conjugate transpose of the operation (inverse of a unitary).

advantage, quantum; For a given problem, the improvement in run time for a quantum computer versus a conventional computer running the best known conventional algorithm.

annealing, quantum/simulated/physical; Annealing algorithms mimic (simulate) the cooling process. Alternatively, physical annealing utilizes a physical process to replace simulated annealing with a physical annealing process. Likewise, quantum annealing utilizes quantum effects to help accelerate the physical annealing process.

ansatz. An ansatz is the establishment of the starting equation(s), the theorem(s), or the value(s) describing a mathematical or physical problem or solution. It is often determined by a so called, educated guess.

bit, classical; A deterministic ideal memory/register storing one binary unit (logical zero or logical one).

bit, probabilistic; A probabilistic bit is a controllable memory/register that is able to store probabilistic values of logical zero and logical one. For example, storing the state $(1 - p) |0\rangle + p |1\rangle$ for probability p , implies that the expected value of recovering $|1\rangle$ ($|0\rangle$) is p ($1 - p$). This is typically ensured through redundancy (i.e. multiple deterministic bits can mimic a probabilistic bit).

Bloch sphere; The Bloch sphere is a geometrical representation of the pure state space of a two-level quantum mechanical system (qubit), named after the physicist Felix Bloch.

coherence, quantum; The (quantum) coherence of a qubit, roughly is the ability to maintain superposition over time. (Not to be confused with optics.)

complement, logical; The logical negation of a Boolean variable, sending x to $\bar{x} = 1 - x$.

costate, dual state, effect; The result of a measurement. The mathematical dual (dagger) of a state vector. A measurement outcome operator. A linear map from the complex numbers to the dual of a vector space. A linear map from a vector space to the complex numbers.

Dirichlet operator; A Hamiltonian that is both self-adjoint and infinitesimal stochastic.

EPR pair, Einstein–Podolsky–Rosen; Also known as a Bell State. An entangled bipartite quantum state. The state is typically written as $\sqrt{2} |\Phi^+\rangle = |00\rangle + |11\rangle$, see e.g. 1.12.

gadget Hamiltonian; A construction(s) to emulate desired Hamiltonian coupling terms.

gate model, quantum; The defacto model of universal quantum computation described by quantum logic gates acting on registers of qubits.

measurement based or one-way model; The measurement based model of quantum computation performs universal quantum computation by local measurements on an initially entangled resource state, usually a *cluster state* or *graph state*.

monotonic function/quantity; To be varying in such a way as to either (i) never decrease or (ii) never increase.

slack space, slack bits, ancillary; Additional bits/qubits used to assist information processing tasks.

spin, classical/quantum; Sometimes called *nuclear spin* or *intrinsic spin* is the quantum version form of angular momentum carried by elementary particles.

supremacy, quantum; An adversarial game consisting of a calculation on a quantum computer that cannot be in practice be performed on any foreseeable conventional computer.

tuple; Delimiter (comma) separated types grouped together by parenthesis.

uniform circuit, polynomial-time; A family of (Boolean) circuits $\{C_n : n \in \mathbb{N}\}$ generated by an algorithm \mathcal{M} , such that

1. \mathcal{M} successfully terminates in polynomial time in n ,
2. $\forall n \in \mathbb{N}$, \mathcal{M} outputs a description of C_n given input $1^{\times n}$.

Bibliography

1. *Feynman R. P.* There's Plenty of Room at the Bottom // Lecture given at the annual American Physical Society meeting at Caltech December 29. — 1959.
2. *Feynman R. P.* Quantum Mechanical Computers // Optics News. — 1985. — Feb. — Vol. 11, no. 2. — Pp. 11–20. — URL: <http://www.osa-opn.org/abstract.cfm?URI=on-11-2-11>.
3. *Deutsch D.* Quantum theory, the Church–Turing principle and the universal quantum computer // Proceedings of the Royal Society of London Series A, Mathematical and Physical Sciences. — 1985. — Vol. 400, no. 1818. — Pp. 97–117.
4. *Feynman R. P.* Quantum mechanical computers // Foundations of Physics. — 1986. — Vol. 16, no. 6. — Pp. 507–531. — URL: <https://doi.org/10.1007/BF01886518>.
5. *Deutsch D.* Quantum computational networks // Proceedings of the Royal Society London Series A, Mathematical and Physical Sciences. — 1989. — Vol. 425, no. 1868. — Pp. 73–90.
6. *Nielsen M. A., Chuang I. L.* Quantum Computation and Quantum Information. — Cambridge University Press, 2000. — URL: <https://doi.org/10.1017/cbo9780511976667>.
7. *Kitaev A. Y., Shen A. H., Vyalyi M. N.* Classical and Quantum Computation. — Boston, MA, USA : American Mathematical Society, 2002.
8. *Aharonov D.* [et al.] Adiabatic quantum computation is equivalent to standard quantum computation // 45th Annual IEEE Symposium on Foundations of Computer Science. — 10/2004. — Pp. 42–51.
9. *Peruzzo A.* [et al.] A variational eigenvalue solver on a photonic quantum processor // Nature Communications. — 2014. — July. — Vol. 5. — P. 4213. — arXiv: 1304.3061 [quant-ph].

10. *Biamonte J.* Universal Variational Quantum Computation // arXiv e-prints. — 2019. — Mar. — arXiv:1903.04500. — arXiv: 1903 . 04500 [quant-ph].
11. *Whitfield J. D., Biamonte J., Aspuru-Guzik A.* Simulation of electronic structure Hamiltonians using quantum computers // Molecular Physics. — 2011. — Mar. — Vol. 109, no. 5. — Pp. 735–750. — URL: <https://doi.org/10.1080/00268976.2011.552441>.
12. *Biamonte J. D.* Nonperturbative k -body to two-body commuting conversion Hamiltonians and embedding problem instances into Ising spins // Physical Review A. — 2008. — May. — Vol. 77, no. 5. — P. 052331. — arXiv: 0801.3800 [quant-ph].
13. *Whitfield J. D., Faccin M., Biamonte J. D.* Ground-state spin logic // EPL (Europhysics Letters). — 2012. — Sept. — Vol. 99. — P. 57004. — arXiv: 1205.1742 [quant-ph].
14. *Kirkpatrick S., Gelatt D. C., Vecchi M. P.* Optimization by simulated annealing // Science. — 1983. — Vol. 220, no. 4598. — Pp. 671–680.
15. *Utsunomiya S., Takata K., Yamamoto Y.* Mapping of Ising models onto injection-locked laser systems // Optics express. — 2011. — Vol. 19, no. 19. — Pp. 18091–18108.
16. *Inagaki T.* [et al.] A coherent Ising machine for 2000-node optimization problems // Science. — 2016. — Vol. 354, no. 6312. — Pp. 603–606.
17. *Pierangeli D., Marcucci G., Conti C.* Large-scale photonic Ising machine by spatial light modulation // Physical Review Letters. — 2019. — Vol. 122, no. 21. — P. 213902.
18. *Marandi A.* [et al.] Network of time-multiplexed optical parametric oscillators as a coherent Ising machine // Nature Photonics. — 2014. — Vol. 8, no. 12. — P. 937.
19. *Nixon M.* [et al.] Observing geometric frustration with thousands of coupled lasers // Physical Review Letters. — 2013. — Vol. 110, no. 18. — P. 184102.
20. *Dung D.* [et al.] Variable potentials for thermalized light and coupled condensates // Nature Photonics. — 2017. — Vol. 11, no. 9. — P. 565.

21. *Kalinin K., Berloff N. G.* Global optimization of spin Hamiltonians with gain-dissipative systems // Scientific Reports. — 2018. — Vol. 8, no. 1. — P. 17791.
22. *Cook S. A.* The Complexity of Theorem-proving Procedures // Proceedings of the Third Annual ACM Symposium on Theory of Computing. — Shaker Heights, Ohio, USA : ACM, 1971. — Pp. 151–158. — (STOC '71). — URL: <http://doi.acm.org/10.1145/800157.805047>.
23. *Trakhtenbrot B.* A Survey of Russian Approaches to Perebor (Brute-Force Searches) Algorithms // IEEE Annals of the History of Computing. — 1984. — Oct. — Vol. 6, no. 4. — Pp. 384–400. — URL: <https://doi.org/10.1109/mahc.1984.10036>.
24. *Cao Y.* [et al.] Hamiltonian gadgets with reduced resource requirements // Physical Review A. — 2015. — Jan. — Vol. 91, no. 1. — URL: <http://dx.doi.org/10.1103/PhysRevA.91.012315>.
25. *Philathong H.* [et al.] Computational Phase Transition Signature in Gibbs Sampling // arXiv e-prints. — 2019. — June. — arXiv:1906.10705. — arXiv: 1906.10705 [quant-ph].
26. *Church A.* An unsolvable problem of elementary number theory // American journal of mathematics. — 1936. — Vol. 58, no. 2. — Pp. 345–363.
27. *Turing A. M.* On computable numbers, with an application to the Entscheidungsproblem // Proceedings of the London Mathematical Society. — 1937. — Vol. 2, no. 1. — Pp. 230–265.
28. *Crawford J. M., Auton L. D.* Experimental results on the crossover point in random 3-SAT // Artificial Intelligence. — 1996. — Mar. — Vol. 81, no. 1–2. — Pp. 31–57. — URL: [https://doi.org/10.1016/0004-3702\(95\)00046-1](https://doi.org/10.1016/0004-3702(95)00046-1).
29. *Friedgut E., Bourgain J.*, [et al.] Sharp thresholds of graph properties, and the k-SAT problem // Journal of the American mathematical Society. — 1999. — Vol. 12, no. 4. — Pp. 1017–1054.
30. *Selman B., Kirkpatrick S.* Critical behavior in the computational cost of satisfiability testing // Artificial Intelligence. — 1996. — Vol. 81, no. 1–2. — Pp. 273–295.

31. *Lucas A.* Ising formulations of many NP problems // *Frontiers in Physics*. — 2014. — Vol. 2. — P. 5.
32. *Berloff N. G.* [et al.] Realizing the classical XY Hamiltonian in polariton simulators // *Nature Materials*. — 2017. — Vol. 16, no. 11. — P. 1120.
33. *Johnson M. W.* [et al.] Quantum annealing with manufactured spins // *Nature*. — 2011. — Vol. 473, no. 7346. — P. 194.
34. *Barends R.* [et al.] Digitized adiabatic quantum computing with a superconducting circuit // *Nature*. — 2016. — Vol. 534, no. 7606. — P. 222.
35. *Harris R.* [et al.] Experimental demonstration of a robust and scalable flux qubit // *Physical Review B*. — 2010. — Vol. 81, no. 13. — P. 134510.
36. *Harris R.* [et al.] Phase transitions in a programmable quantum spin glass simulator // *Science*. — 2018. — Vol. 361, no. 6398. — Pp. 162–165.
37. *King A. D.* [et al.] Observation of topological phenomena in a programmable lattice of 1,800 qubits // *Nature*. — 2018. — Vol. 560, no. 7719. — P. 456.
38. *Baez J., Biamonte J. D.* *Quantum Techniques in Stochastic Mechanics*. — World Scientific Publishing Co. Pte. Ltd, 2018. — P. 276. — URL: <https://doi.org/10.1142/10623>.
39. *Faccin M.* [et al.] Degree Distribution in Quantum Walks on Complex Networks // *Physical Review X*. — 2013. — Oct. — Vol. 3, issue 4. — P. 041007. — URL: <http://link.aps.org/doi/10.1103/PhysRevX.3.041007>.
40. *De Domenico M., Biamonte J.* Spectral Entropies as Information-Theoretic Tools for Complex Network Comparison // *Physical Review X*. — 2016. — Dec. — Vol. 6, no. 4. — URL: <http://dx.doi.org/10.1103/PhysRevX.6.041062>.
41. *Biamonte J., Faccin M., Domenico M. D.* Complex networks from classical to quantum // *Communications Physics*. — 2019. — May. — Vol. 2, no. 1. — URL: <https://doi.org/10.1038/s42005-019-0152-6>.
42. *Wootters W. K., Zurek W. H.* A single quantum cannot be cloned // *Nature*. — 1982. — Oct. — Vol. 299, no. 5886. — Pp. 802–803. — URL: <https://doi.org/10.1038/299802a0>.

43. *Shi Y.* Both Toffoli and controlled-NOT Need Little Help to Do Universal Quantum Computing // Quantum Information & Computation. — Paramus, NJ, 2003. — Jan. — Vol. 3, no. 1. — Pp. 84–92. — URL: <http://dl.acm.org/citation.cfm?id=2011508.2011515>.
44. *Bennett C. H.* [et al.] Strengths and Weaknesses of Quantum Computing // SIAM Journal on Computing. — 1997. — Oct. — Vol. 26, no. 5. — Pp. 1510–1523. — URL: <https://doi.org/10.1137/s0097539796300933>.
45. *Newman M.* Networks: An Introduction. — Oxford University Press, 2010.
46. *Faccin M.* [et al.] Community Detection in Quantum Complex Networks // Physical Review X. — 2014. — Oct. — Vol. 4, no. 4. — URL: <http://dx.doi.org/10.1103/PhysRevX.4.041012>.
47. *Zimborás Z.* [et al.] Quantum Transport Enhancement by Time-Reversal Symmetry Breaking // Scientific Reports. — 2013. — Aug. — Vol. 3, no. 1. — URL: <https://doi.org/10.1038/srep02361>.
48. *Lu D.* [et al.] Chiral quantum walks // Physical Review A. — 2016. — Apr. — Vol. 93, no. 4. — URL: <http://dx.doi.org/10.1103/PhysRevA.93.042302>.
49. *Bravyi S.* [et al.] The Complexity of Stoquastic Local Hamiltonian Problems // Quantum Information & Computation. — Paramus, NJ, 2008. — May. — Vol. 8, no. 5. — Pp. 361–385.
50. *Hormozi L.* [et al.] Nonstoquastic Hamiltonians and quantum annealing of an Ising spin glass // Physical Review B. — 2017. — May. — Vol. 95, no. 18. — URL: <http://dx.doi.org/10.1103/PhysRevB.95.184416>.
51. *Bravyi S., Terhal B.* Complexity of Stoquastic Frustration-Free Hamiltonians // SIAM Journal on Computing. — 2010. — Jan. — Vol. 39, no. 4. — Pp. 1462–1485. — URL: <https://doi.org/10.1137/08072689x>.
52. *Jordan S. P., Gosset D., Love P. J.* Quantum-Merlin-Arthur-complete problems for stoquastic Hamiltonians and Markov matrices // Physical Review A. — 2010. — Mar. — Vol. 81, no. 3. — URL: <https://doi.org/10.1103/physreva.81.032331>.

53. *Biamonte J., Turner J.* Topological classification of time-asymmetry in unitary quantum processes. — 2017. — arXiv: 1703.02542 [quant-ph]. — arXiv:1703.02542.
54. *Albert R., Barabási A.-L.* Statistical mechanics of complex networks // *Reviews of Modern Physics*. — 2002. — Vol. 74. — Pp. 47–97.
55. *Noh J. D., Rieger H.* Random walks on complex networks // *Physical Review Letters*. — 2004. — Vol. 92, no. 11. — P. 118701.
56. *Paparo G. D., Martin-Delgado M. A.* Google in a Quantum Network // *Scientific Report*. — 2012. — Vol. 2. — P. 444.
57. *Garnerone S.* Thermodynamic formalism for dissipative quantum walks // *Physical Review A*. — 2012. — Sept. — Vol. 86, issue 3. — P. 032342. — URL: <http://link.aps.org/doi/10.1103/PhysRevA.86.032342>.
58. *Paparo G.* [et al.] Quantum Google algorithm // *The European Physical Journal Plus*. — 2014. — Vol. 129, no. 7. — URL: <http://dx.doi.org/10.1140/epjp/i2014-14150-y>.
59. *Garnerone S., Zanardi P., Lidar D. A.* Adiabatic Quantum Algorithm for Search Engine Ranking // *Physical Review Letters*. — 2012. — Vol. 108. — P. 230506.
60. *Sánchez-Burillo E.* [et al.] Quantum navigation and ranking in complex networks // *Scientific Reports*. — 2012. — Vol. 2.
61. *Deutsch D., Jozsa R.* Rapid solution of problems by quantum computation // *Proceedings of the Royal Society of London. Series A: Mathematical and Physical Sciences*. — 1992. — Vol. 439, no. 1907. — Pp. 553–558. — URL: <https://doi.org/10.1098/rspa.1992.0167>.
62. *Bernstein E., Vazirani U.* Quantum Complexity Theory // *SIAM Journal on Computing*. — 1997. — Oct. — Vol. 26, no. 5. — Pp. 1411–1473. — URL: <https://doi.org/10.1137/s0097539796300921>.
63. *Simon D. R.* On the Power of Quantum Computation // *SIAM Journal on Computing*. — 1997. — Oct. — Vol. 26, no. 5. — Pp. 1474–1483. — URL: <https://doi.org/10.1137/s0097539796298637>.

64. *Cleve R.* [et al.] Quantum algorithms revisited // Proceedings of the Royal Society of London. Series A: Mathematical, Physical and Engineering Sciences. — 1998. — Jan. — Vol. 454, no. 1969. — Pp. 339–354. — URL: <https://doi.org/10.1098/rspa.1998.0164>.
65. *Biamonte J. D.* [et al.] Adiabatic quantum simulators // AIP Advances. — 2011. — Vol. 1, no. 2. — P. 022126. — URL: <http://dx.doi.org/10.1063/1.3598408>.
66. *Wang Y.* [et al.] Quantum Simulation of Helium Hydride Cation in a Solid-State Spin Register // ACS Nano. — 2015. — Apr. — Vol. 9, no. 8. — Pp. 7769–7774. — URL: <https://doi.org/10.1021/acsnano.5b01651>.
67. *Lanyon B. P.* [et al.] Towards quantum chemistry on a quantum computer // Nature Chemistry. — 2010. — Jan. — Vol. 2, no. 2. — Pp. 106–111. — URL: <https://doi.org/10.1038/nchem.483>.
68. *Penrose R.* Applications of negative dimensional tensors // Combinatorial Mathematics and its Applications (Proc. Conf., Oxford, 1969). — Academic Press, London, 1971. — Pp. 221–244.
69. *Orús R.* A practical introduction to tensor networks: Matrix product states and projected entangled pair states // Annals of Physics. — 2014. — Oct. — Vol. 349. — Pp. 117–158. — arXiv: 1306.2164.
70. *Vidal G.* Entanglement Renormalization: an introduction // Understanding Quantum Phase Transitions / ed. by L. D. Carr. — Taylor & Francis, Boca Raton, 2010.
71. *Verstraete F., Murg V., Cirac J. I.* Matrix product states, projected entangled pair states, and variational renormalization group methods for quantum spin systems // Advances in Physics. — 2008. — Vol. 57. — Pp. 143–224. — arXiv: 0907.2796.
72. *Cirac J. I., Verstraete F.* Renormalization and tensor product states in spin chains and lattices // Journal of Physics A Mathematical and Theoretical. — 2009. — Vol. 42, no. 50. — P. 504004. — arXiv: 0910.1130.
73. *Schollwöck U.* The density-matrix renormalization group in the age of matrix product states // Annals of Physics. — 2011. — Jan. — Vol. 326. — Pp. 96–192. — arXiv: 1008.3477.

74. *Sachdev S.* Viewpoint: Tensor networks—a new tool for old problems // *Physics*. — 2009. — Vol. 2. — P. 90. — arXiv: 1006.0675.
75. *Schollwöck U.* The density-matrix renormalization group: a short introduction // *Philosophical Transactions of the Royal Society of London A: Mathematical, Physical and Engineering Sciences*. — 2011. — Vol. 369, no. 1946. — Pp. 2643–2661. — URL: <http://rsta.royalsocietypublishing.org/content/369/1946/2643>.
76. *Orús R.* Advances on tensor network theory: symmetries, fermions, entanglement, and holography // *European Physical Journal B*. — 2014. — Nov. — Vol. 87. — P. 280. — arXiv: 1407.6552.
77. *Eisert J.* Entanglement and tensor network states // *Modeling and Simulation*. — 2013. — Aug. — Vol. 3. — P. 520. — arXiv: 1308.3318.
78. *Evenbly G., Vidal G.* Tensor Network States and Geometry // *Journal of Statistical Physics*. — 2011. — Nov. — Vol. 145. — Pp. 891–918. — arXiv: 1106.1082.
79. *Bridgeman J. C., Chubb C. T.* Hand-waving and interpretive dance: an introductory course on tensor networks // *Journal of Physics A: Mathematical and Theoretical*. — 2017. — May. — Vol. 50, no. 22. — P. 223001. — URL: <https://doi.org/10.1088%2F1751-8121%2Faa6dc3>.
80. *Cichocki A.* [et al.] Tensor Networks for Dimensionality Reduction and Large-scale Optimization: Part 1 Low-Rank Tensor Decompositions // *Foundations and Trends in Machine Learning*. — 2016. — Vol. 9, no. 4–5. — Pp. 249–429. — eprint: 1609.00893.
81. *Pervishko A. A., Biamonte J.* Pushing Tensor Networks to the Limit // *Physics*. — 2019. — May. — Vol. 12. — URL: <http://dx.doi.org/10.1103/Physics.12.59>.
82. *Cichocki A.* [et al.] Tensor Networks for Dimensionality Reduction and Large-scale Optimization: Part 2 Applications and Future Perspectives // *Foundations and Trends in Machine Learning*. — 2017. — Vol. 9, no. 6. — Pp. 431–673.

83. *Ran S.-J.* [et al.] Lecture Notes of Tensor Network Contractions // arXiv e-prints. — 2017. — Aug. — arXiv:1708.09213. — arXiv: 1708 . 09213 [physics.comp-ph].
84. *Biamonte J., Bergholm V.* Tensor Networks in a Nutshell // arXiv:1708.00006. — 2017.
85. *Biamonte J.* Lectures on Quantum Tensor Networks. — 2019. — arXiv: 1912.10049 [quant-ph]. — 178 pages, arXiv:1912.10049.
86. *Coecke B., Duncan R.* Interacting quantum observables // Proceedings of the 37th International Colloquium on Automata, Languages and Programming (ICALP). — 2008. — (Lecture Notes in Computer Science).
87. *Coecke B., Duncan R.* Interacting quantum observables: categorical algebra and diagrammatics // New Journal of Physics. — 2011. — Vol. 13, no. 4. — P. 043016. — URL: <http://dx.doi.org/10.1088/1367-2630/13/4/043016>.
88. *Lafont Y.* Towards an algebraic theory of Boolean circuits // Journal of Pure & Applied Algebra. — 2003. — Vol. 184, no. 2–3. — Pp. 257–310. — URL: [https://doi.org/10.1016/S0022-4049\(03\)00069-0](https://doi.org/10.1016/S0022-4049(03)00069-0).
89. *Biamonte J. D., Clark S. R., Jaksch D.* Categorical Tensor Network States // AIP Advances. — 2011. — Dec. — Vol. 1, no. 4. — P. 042172. — arXiv: 1012.0531 [quant-ph].
90. *Bergholm V., Biamonte J. D.* Categorical quantum circuits // Journal of Physics A Mathematical General. — 2011. — June. — Vol. 44, no. 24. — P. 245304. — arXiv: 1010.4840 [quant-ph].
91. *Biamonte J., Bergholm V., Lanzagorta M.* Tensor network methods for invariant theory // Journal of Physics A Mathematical General. — 2013. — Nov. — Vol. 46, no. 47. — P. 475301. — arXiv: 1209.0631 [quant-ph].
92. *Denny S. J.* [et al.] Algebraically contractible topological tensor network states // Journal of Physics A Mathematical General. — 2012. — Jan. — Vol. 45, no. 1. — P. 015309. — arXiv: 1108.0888 [quant-ph].
93. *Biamonte J. D., Morton J., Turner J.* Tensor Network Contractions for #SAT // Journal of Statistical Physics. — 2015. — Sept. — Vol. 160, no. 5. — Pp. 1389–1404. — arXiv: 1405.7375 [quant-ph].

94. *Gottesman D.* The Heisenberg representation of quantum computers // Proceedings of the XXII International Colloquium in Group Theoretical Methods in Physics (Hobart, 1998). — Int. Press, Cambridge, MA, 1999. — Pp. 32–43.
95. *Biamonte J.* Charged string tensor networks // Proceedings of the National Academy of Sciences. — 2017. — Vol. 114, no. 10. — P. 2447.
96. *Farhi E., Goldstone J., Gutmann S.* A quantum approximate optimization algorithm. — 2014. — unpublished, arXiv:1411.4028.
97. *McClean J. R.* [et al.] Barren plateaus in quantum neural network training landscapes // Nature Communications. — 2018. — Vol. 9, no. 1. — URL: <http://dx.doi.org/10.1038/s41467-018-07090-4>.
98. *Akshay V.* [et al.] Reachability Deficits in Quantum Approximate Optimization // arXiv e-prints. — 2019. — June. — arXiv:1906.11259. — arXiv: 1906.11259 [quant-ph].
99. *Kirby W. M., Love P. J.* Contextuality Test of the Nonclassicality of Variational Quantum Eigensolvers // Physical Review Letters. — 2019. — Vol. 123, no. 20. — URL: <http://dx.doi.org/10.1103/PhysRevLett.123.200501>.
100. *Cerezo M.* [et al.] Cost-Function-Dependent Barren Plateaus in Shallow Quantum Neural Networks // arXiv e-prints. — 2020. — Jan. — arXiv:2001.00550. — arXiv: 2001.00550 [quant-ph].
101. *Mitarai K.* [et al.] Quantum circuit learning // Physical Review A. — 2018. — Vol. 98, no. 3. — URL: <http://dx.doi.org/10.1103/PhysRevA.98.032309>.
102. *Schuld M.* [et al.] Evaluating analytic gradients on quantum hardware // Physical Review A. — 2019. — Vol. 99, no. 3. — URL: <http://dx.doi.org/10.1103/PhysRevA.99.032331>.
103. *Hastings M. B.* Classical and Quantum Bounded Depth Approximation Algorithms // arXiv e-prints. — 2019. — May. — arXiv:1905.07047. — arXiv: 1905.07047 [quant-ph].

104. *Farhi E.* [et al.] The Quantum Approximate Optimization Algorithm and the Sherrington-Kirkpatrick Model at Infinite Size // arXiv e-prints. — 2019. — Oct. — arXiv:1910.08187. — arXiv: 1910.08187 [quant-ph].
105. *Preskill J.* Quantum Computing in the NISQ era and beyond // Quantum. — 2018. — Aug. — Vol. 2. — P. 79. — URL: <https://doi.org/10.22331/q-2018-08-06-79>.
106. *Zhukov A. A.* [et al.] Algorithmic simulation of far-from-equilibrium dynamics using quantum computer // Quantum Information Processing. — 2018. — Sept. — Vol. 17, no. 9. — P. 223. — arXiv: 1807.10149 [quant-ph].
107. *Uvarov A., Biamonte J., Yudin D.* Variational Quantum Eigensolver for Frustrated Quantum Systems // arXiv e-prints. — 2020. — May. — arXiv:2005.00544. — arXiv: 2005.00544 [quant-ph].
108. *Verdon G., Broughton M., Biamonte J.* A quantum algorithm to train neural networks using low-depth circuits // arXiv e-prints. — 2017. — Dec. — arXiv:1712.05304. — arXiv: 1712.05304 [quant-ph].
109. *Kandala A.* [et al.] Hardware-efficient variational quantum eigensolver for small molecules and quantum magnets // Nature. — 2017. — Sept. — Vol. 549. — Pp. 242–246. — arXiv: 1704.05018 [quant-ph].
110. *Morales M. E. S., Tlyachev T., Biamonte J.* Variational learning of Grover’s quantum search algorithm // Physical Review A. — 2018. — Dec. — Vol. 98, no. 6. — URL: <http://dx.doi.org/10.1103/PhysRevA.98.062333>.
111. *Zhang K., Korepin V. E.* Depth optimization of quantum search algorithms beyond Grover’s algorithm // Physical Review A. — 2020. — Mar. — Vol. 101, no. 3. — P. 032346. — arXiv: 1908.04171 [quant-ph].
112. *Barenco A.* [et al.] Elementary gates for quantum computation // Physical Review A. — 1995. — Nov. — Vol. 52, issue 5. — Pp. 3457–3467. — URL: <https://link.aps.org/doi/10.1103/PhysRevA.52.3457>.
113. *Figgatt C.* [et al.] Complete 3-qubit Grover search on a programmable quantum computer // Nature Communications. — 2017. — Dec. — Vol. 8. — P. 1918. — arXiv: 1703.10535 [quant-ph].

114. *Vidal G., Dawson C. M.* Universal quantum circuit for two-qubit transformations with three controlled-NOT gates // *Physical Review A*. — 2004. — Jan. — Vol. 69, issue 1. — P. 010301. — URL: <https://link.aps.org/doi/10.1103/PhysRevA.69.010301>.
115. *Yu N., Duan R., Ying M.* Five two-qubit gates are necessary for implementing the Toffoli gate // *Physical Review A*. — 2013. — July. — Vol. 88, no. 1. — URL: <https://doi.org/10.1103/physreva.88.010304>.
116. *Kadowaki T., Nishimori H.* Quantum annealing in the transverse Ising model // *Physical Review E*. — 1998. — Vol. 58, no. 5. — P. 5355.
117. *Dam W. van, Mosca M., Vazirani U.* How powerful is adiabatic quantum computation? // *Proceedings 42nd IEEE Symposium on Foundations of Computer Science*. — 2001. — URL: <http://dx.doi.org/10.1109/SFCS.2001.959902>.
118. *Morita S., Nishimori H.* Mathematical foundation of quantum annealing // *Journal of Mathematical Physics*. — 2008. — Dec. — Vol. 49, no. 12. — P. 125210. — URL: <https://doi.org/10.1063/1.2995837>.
119. *Lloyd S.* Quantum approximate optimization is computationally universal. — 12/2018. — arXiv: 1812.11075 [quant-ph]. — unpublished, arXiv:1812.11075.
120. *Morales M. E. S., Biamonte J., Zimborás Z.* On the Universality of the Quantum Approximate Optimization Algorithm // arXiv e-prints. — 2019. — Sept. — arXiv:1909.03123. — arXiv: 1909.03123 [quant-ph].
121. *Håstad J.* Some optimal inapproximability results // *Journal of the ACM*. — 2001. — Vol. 48, no. 4. — Pp. 798–859.
122. *Benjamin S. C., Bose S.* Quantum Computing with an Always-On Heisenberg Interaction // *Physical Review Letters*. — 2003. — June. — Vol. 90, issue 24. — P. 247901. — URL: <https://link.aps.org/doi/10.1103/PhysRevLett.90.247901>.
123. *Benjamin S. C., Bose S.* Quantum computing in arrays coupled by “always-on” interactions // *Physical Review A*. — 2004. — Sept. — Vol. 70, issue 3. — P. 032314. — URL: <https://link.aps.org/doi/10.1103/PhysRevA.70.032314>.

124. *Biamonte J. D., Love P. J.* Realizable Hamiltonians for universal adiabatic quantum computers // *Physical Review A*. — 2008. — July. — Vol. 78. — P. 012352. — arXiv: 0704.1287 [quant-ph].
125. *Hoeffding W.* Probability Inequalities for Sums of Bounded Random Variables // *Journal of the American Statistical Association*. — 1963. — Vol. 58, no. 301. — Pp. 13–30. — eprint: <https://www.tandfonline.com/doi/pdf/10.1080/01621459.1963.10500830>. — URL: <https://www.tandfonline.com/doi/abs/10.1080/01621459.1963.10500830>.
126. *Cincio L.* [et al.] Learning the quantum algorithm for state overlap // *New Journal of Physics*. — 2018. — Nov. — Vol. 20. — P. 113022. — arXiv: 1803.04114 [quant-ph].
127. *Bravyi S., Gosset D.* Improved Classical Simulation of Quantum Circuits Dominated by Clifford Gates // *Physical Review Letters*. — 2016. — June. — Vol. 116, no. 25. — URL: <http://dx.doi.org/10.1103/PhysRevLett.116.250501>.
128. *Bravyi S.* [et al.] Simulation of quantum circuits by low-rank stabilizer decompositions // *Quantum*. — 2019. — Sept. — Vol. 3. — P. 181. — URL: <http://dx.doi.org/10.22331/q-2019-09-02-181>.
129. *McClean J. R.* [et al.] The theory of variational hybrid quantum-classical algorithms // *New Journal of Physics*. — 2016. — Feb. — Vol. 18. — P. 023023. — arXiv: 1509.04279 [quant-ph].
130. *Li Y., Benjamin S. C.* Efficient Variational Quantum Simulator Incorporating Active Error Minimization // *Physical Review X*. — 2017. — June. — Vol. 7, issue 2. — P. 021050. — URL: <https://link.aps.org/doi/10.1103/PhysRevX.7.021050>.
131. *Oliveira R., Terhal B. M.* The Complexity of Quantum Spin Systems on a Two-Dimensional Square Lattice // *Quantum Information & Computation*. — Paramus, NJ, 2008. — Nov. — Vol. 8, no. 10. — Pp. 900–924.
132. *Chase B. A., Landahl A. J.* Universal quantum walks and adiabatic algorithms by 1D Hamiltonians. — 2008. — arXiv: 0802.1207 [quant-ph]. — unpublished, arXiv:0802.1207.

133. *Kempe J., Kitaev A., Regev O.* The Complexity of the Local Hamiltonian Problem // SIAM Journal on Computing. — 2006. — Jan. — Vol. 35, no. 5. — Pp. 1070–1097. — URL: <https://doi.org/10.1137/s0097539704445226>.
134. *Cubitt T., Montanaro A.* Complexity Classification of Local Hamiltonian Problems // SIAM Journal on Computing. — 2016. — Jan. — Vol. 45, no. 2. — Pp. 268–316. — URL: <https://doi.org/10.1137/140998287>.
135. *Rudolph T., Grover L.* A 2 rebit gate universal for quantum computing. — 2002. — arXiv: [quant-ph/0210187](https://arxiv.org/abs/quant-ph/0210187) [quant-ph]. — unpublished, [quant-ph/0210187](https://arxiv.org/abs/quant-ph/0210187).
136. *Menke T.* [et al.] Automated discovery of superconducting circuits and its application to 4-local coupler design. — 2019. — arXiv: [1912.03322](https://arxiv.org/abs/1912.03322) [quant-ph]. — arXiv:1912.03322.
137. *Chancellor N., Zohren S., Warburton P. A.* Circuit design for multi-body interactions in superconducting quantum annealing systems with applications to a scalable architecture // npj Quantum Information. — 2017. — Dec. — Vol. 3. — P. 21. — arXiv: [1603.09521](https://arxiv.org/abs/1603.09521) [quant-ph].
138. *Menke T.* [et al.] A many-body coupler for coherent 4-local interaction of superconducting flux qubits // APS March Meeting Abstracts. Vol. 2019. — 01/2019. — A42.011. — (APS Meeting Abstracts).
139. *Harris R.* [et al.] Sign- and Magnitude-Tunable Coupler for Superconducting Flux Qubits // Physical Review Letters. — 2007. — Apr. — Vol. 98, no. 17. — URL: <https://doi.org/10.1103/physrevlett.98.177001>.
140. *Boixo S.* [et al.] Experimental signature of programmable quantum annealing // Nature Communications. — 2013. — June. — Vol. 4, no. 1. — URL: <https://doi.org/10.1038/ncomms3067>.
141. *Bian Z.* [et al.] Experimental Determination of Ramsey Numbers // Physical Review Letters. — 2013. — Sept. — Vol. 111, no. 13. — URL: <https://doi.org/10.1103/physrevlett.111.130505>.
142. *Nagaj D., Mozes S.* New construction for a QMA complete three-local Hamiltonian // Journal of Mathematical Physics. — 2007. — July. — Vol. 48, no. 7. — P. 072104. — URL: <http://dx.doi.org/10.1063/1.2748377>.

143. *Kempe J., Regev O.* 3-Local Hamiltonian is QMA-complete // Quantum Information and Computation. — 2003. — Vol. 3, no. 3. — P. 0302079.
144. *Bravyi S.* [et al.] Quantum Simulation of Many-Body Hamiltonians Using Perturbation Theory with Bounded-Strength Interactions // Physical Review Letters. — 2008. — Aug. — Vol. 101, no. 7. — URL: <https://doi.org/10.1103/physrevlett.101.070503>.
145. *Schuch N., Verstraete F.* Computational complexity of interacting electrons and fundamental limitations of density functional theory // Nature Physics. — 2009. — Aug. — Vol. 5, no. 10. — Pp. 732–735. — URL: <https://doi.org/10.1038/nphys1370>.
146. *Ganti A., Onunkwo U., Young K.* Family of $[[6k, 2k, 2]]$ codes for practical and scalable adiabatic quantum computation // Physical Review A. — 2014. — Apr. — Vol. 89, no. 4. — URL: <https://doi.org/10.1103/physreva.89.042313>.
147. *Jordan S. P., Farhi E.* Perturbative gadgets at arbitrary orders // Physical Review A. — 2008. — June. — Vol. 77, no. 6. — URL: <https://doi.org/10.1103/physreva.77.062329>.
148. *Melanson D.* [et al.] Tunable three-body coupler for superconducting flux qubits. — 2019. — arXiv: 1909.02091 [quant-ph].
149. *Schöndorf M., Wilhelm F.* Nonpairwise Interactions Induced by Virtual Transitions in Four Coupled Artificial Atoms // Physical Review Applied. — 2019. — Dec. — Vol. 12, no. 6. — URL: <https://doi.org/10.1103/physrevapplied.12.064026>.
150. *Babbush R., O’Gorman B., Aspuru-Guzik A.* Resource efficient gadgets for compiling adiabatic quantum optimization problems // Annalen der Physik. — 2013. — Sept. — Vol. 525, no. 10–11. — Pp. 877–888. — URL: <https://doi.org/10.1002/andp.201300120>.
151. *Bravyi S., DiVincenzo D. P., Loss D.* Schrieffer–Wolff transformation for quantum many-body systems // Annals of Physics. — 2011. — Oct. — Vol. 326, no. 10. — Pp. 2793–2826. — URL: <http://dx.doi.org/10.1016/j.aop.2011.06.004>.

152. *Harrow A., Mehraban S.* Approximate unitary t -designs by short random quantum circuits using nearest-neighbor and long-range gates // arXiv e-prints. — 2018. — Sept. — arXiv:1809.06957. — arXiv: 1809 . 06957 [quant-ph].
153. *McClean J. R.* [et al.] Decoding quantum errors with subspace expansions // Nature Communications. — 2020. — Jan. — Vol. 11, no. 1. — URL: <https://doi.org/10.1038/s41467-020-14341-w>.
154. *Xu X., Benjamin S. C., Yuan X.* Variational circuit compiler for quantum error correction // arXiv e-prints. — 2019. — Nov. — arXiv:1911.05759. — arXiv: 1911.05759 [quant-ph].
155. *Johnson P. D.* [et al.] QVECTOR: an algorithm for device-tailored quantum error correction // arXiv e-prints. — 2017. — Nov. — arXiv:1711.02249. — arXiv: 1711.02249 [quant-ph].
156. *Li Y., Benjamin S. C.* Efficient Variational Quantum Simulator Incorporating Active Error Minimization // Phys. Rev. X. — 2017. — Vol. 7, issue 2. — P. 021050. — URL: <https://link.aps.org/doi/10.1103/PhysRevX.7.021050>.
157. *McArdle S., Yuan X., Benjamin S.* Error-mitigated digital quantum simulation // Physical review letters. — 2019. — Vol. 122, no. 18. — P. 180501.
158. *Biamonte J.* [et al.] Quantum machine learning // Nature. — 2017. — Sept. — Vol. 549. — Pp. 195–202. — arXiv: 1611.09347 [quant-ph].

List of Figures

1.1	Percent of satisfiable instances (left axis) and run-time (right axis) versus clause density, α . We randomly generated 1,000 3-SAT instances with 300 variables with observed $\alpha_c \approx 4.27$. Figure taken from [25].	28
1.2	Ground state occupancy of the thermal states corresponding to Hamiltonians embedding 3-SAT instances across the algorithmic phase transition for 26 spins with $\beta = 1, 2, 3$. Figure taken from [25].	31
2.1	Stochastic probability versus time generated by the graph Laplacian (2.18) with initial state $ 0\rangle$. The final state is the equal probabilistic mixture of $ 0\rangle$ and $ 1\rangle$	38
2.2	Quantum probability versus time generated by the graph Laplacian (2.18) with initial state $ 0\rangle$ exhibits strong oscillations.	39
2.3	Example of a simple graph, used herein to compare quantum versus stochastic walks.	44
2.4	Known mappings between quantum and stochastic generators. Here $G = (V, E)$ is a graph with adjacency matrix A , D is a diagonal matrix of node degrees. This yields the graph Laplacian $\mathcal{L} = D - A$, and hence, the stochastic walk generator $\mathcal{L}_S = \mathcal{L}D^{-1}$, from this a similarity transform results in $\mathcal{L}_Q = D^{-\frac{1}{2}}\mathcal{L}D^{-\frac{1}{2}}$, which generates a valid quantum walk and exhibits several interesting connections to the classical case. The mapping $\mathcal{L} \rightarrow \mathcal{L}^\top \mathcal{L}$ preserves the lowest 0 energy ground state, opening the door for adiabatic quantum annealing which solves computational problems by evolving a system into its ground state. (Figure from [41] which was modified from [39]).	62
2.5	A plot of $\frac{1}{2} + \frac{1}{2} \cos \lambda_i t$. The plane wave $\cos \lambda_i t$ has angular frequency λ_i with period $\frac{2\pi}{\lambda_i}$	68

3.1	Lafont’s 2003 model of circuits included the bialgebra (d) and Hopf (g) relations between the building blocks needed to form a controlled-NOT gate—see also ZX calculus [87]. [Redrawn from [88] as it appeared in [89]]. [(a) associativity; (b) gate unit laws; (c) symmetry; (e) copy laws; (f) unit scalar given as a blank on the page.]	70
3.2	Clifford generators drawn as quantum gates.	71
4.1	The suspected relationship of BQP to other classes [6].	89
4.2	Oracle circuit used in Grover search and its variational incarnation.	99
4.3	Diffusion circuit used in Grover search and variational Grover search.	115
4.4	(color online) (left) Grover’s algorithm takes a saddle point between two hills. Variational search recovers the hill peaks. Note that the valley becomes increasingly less pronounced past four qubits, providing negligible range for improvement. (right) Probability as a function of the variational angle for the 3 qubit case. Grover’s algorithm is recovered in the case $\alpha = \pi$, the variational algorithm obtains angles $\tilde{\alpha}_1 = 2.12^{\text{rad}}$ and $\tilde{\alpha}_2 = 2\pi - \tilde{\alpha}_1$. (Figure originally from [110]).	115
4.5	Kitaev decomposition for 2-controlled (Toffoli) gate. The structure of the decomposition appeared in [7], where the gates (V, Z) are chosen here specifically as they satisfy the group commutator relation. [Note that the decomposition introduces a factor of ι in front of the controlled X . This requires slight modification of algorithms in applications.]	116
4.6	Decomposition for 3-controlled gate. [Note that the decomposition introduces a factor of ι in front of the controlled X . This requires slight modification of algorithms in applications.]	116
4.7	Decomposition for k -controlled gate. [Note that the decomposition introduces a factor of ι , yielding a controlled ιX . This requires slight modification of algorithms in applications.] .	117
4.8	Standard decomposition [6] for 3-CN gate which uses ancillary qubits labeled with states $ a_1\rangle$ and $ a_3\rangle$	117

- 4.9 Five qubits evolve as time goes up on the page. At $t = 0$, commuting interaction terms (red edges) are applied between the qubits. At $t = 1$ local gates (red nodes) are applied to each of the qubits. 118
- 4.10 $f = E_g^{\text{QAOA}} - \min(\mathcal{H}_{\text{SAT}})$ vs clause density for 3-SAT for differing QAOA depths. Squares show the average value obtained over 100 randomly generated instances for $n = 6$ with error bars indicating the standard error of mean. Figure taken from [98]. 118
- 6.1 Numerical illustration of gadget theorem using a subdivision gadget. Here we use a subdivision gadget to approximate $\mathcal{H}_{\text{targ}} = \mathcal{H}_{\text{else}} + \alpha Z_1 Z_2$ with $\|\mathcal{H}_{\text{else}}\| = 0$ and $\alpha \in [-1, 1]$. $\varepsilon = 0.05$. “analytical” stands for the case where the value of Δ is calculated using (6.49) when $|\alpha| = 1$. “numerical” represents the case where Δ takes the value that yield the spectral error to be ε . In (a) we let $\alpha = 1$. $z \in [-\max z, \max z]$ with $\max z = \|\mathcal{H}_{\text{else}}\| + \max \alpha + \varepsilon$. The operator $\Sigma_-(z)$ is computed up to the 3rd order. Subplot (b) shows for every value of α in its range, the maximum difference between the eigenvalues $\tilde{\lambda}_j$ in the low-lying spectrum of $\tilde{\mathcal{H}}$ and the corresponding eigenvalues λ_j in the spectrum of $\mathcal{H}_{\text{targ}} \otimes |0\rangle\langle 0|_w$. (These plots are from [24]). 147
- 6.2 Comparison between our subdivision gadget with that of Oliveira and Terhal [131]. The data labelled as “numerical” represent the Δ values obtained from the numerical search such that the spectral error between $\mathcal{H}_{\text{targ}}$ and $\tilde{\mathcal{H}}_-$ is ε . The data obtained from the calculation using (6.42) are labelled as “analytical”. “[OT06]” refers to values of Δ calculated according to the assignment by Oliveira and Terhal [131]. In this example we consider $\mathcal{H}_{\text{targ}} = \mathcal{H}_{\text{else}} + \alpha Z_1 Z_2$. (a) Gap scaling with respect to ε^{-1} . Here $\|\mathcal{H}_{\text{else}}\| = 0$ and $\alpha = 1$. (b) The gap Δ as a function of the desired coupling α . Here $\|\mathcal{H}_{\text{else}}\| = 0$, $\varepsilon = 0.05$ 148

List of Tables

1	Contrasting binary, polarity and matrix embeddings of Boolean bits.	12
2	Constructing penalty Hamiltonians from Boolean (or pseudo-Boolean) functions.	20
3	Summary of deterministic, probabilistic and quantum computation.	32
4	Summary of quantum versus stochastic mechanics reproduced from [38].	43
5	Percentage increase between the highest probability for finding the solution after measurement obtained in Grover and the two-level variational ansatz [110]. Percent given as a function of $N = 2^n$ where n is the number of qubits and at step p_{\max} on which the probability of finding the solution string is maximum. The same table is obtained for the two-level split-operator ansatz with one angle or with $2p$ angles. Both the diffusion and oracle use the same angle. (Table originally from [110]).	99
6	Minimal possible circuit depth c possibly saturating bipartite entanglement with respect to different interaction geometries. . .	112

Alphabetical Index

Boolean Satisfiability,
25, 26, 65

Ising Model, 9, 23, 26,
91, 92

Logic Gates, 14, 15, 72

Phase Estimation, 61

Physical Computing,
26, 105

Quantum Algorithms,
61, 105

Quantum Circuits, 75,
99, 115

Quantum Gates,
40–42, 69, 73–75

Quantum Machine
Learning, 86

Schrödinger's
equation, 33

Tensor Networks, 69

Universal Quantum
Gates, 98

Variational Quantum
Algorithms, 85,
86, 94